# Investigate the Deformation Behavior of Reinforced 7075 Aluminium Metal Matrix Composite through Cold Extrusion Process for Automobile Brake Caliper

Bayush Lemma Batu

A Thesis Submitted to the Department of Mechanical Engineering
School of Mechanical, Chemical and Material Engineering

Presented in Partial Fulfillment of the Requirement for the Degree of Master's in Manufacturing Engineering

Office of Graduate Studies
Adama Science and Technology University

June, 2024

Adama, Ethiopia

**Investigate the Deformation Behavior of Reinforced 7075 Aluminium Metal Matrix Composite through Cold Extrusion Process for Automobile Brake Caliper**

Bayush Lemma Batu

Advisor: Dr. Devendra Kumar Sinha

Co-advisor: Mr. Mengistu Gelaw

A Thesis Submitted To Department Of Mechanical Engineering
School Of Mechanical, Chemical and Material Engineering

Presented in Partial Fulfillment of the Requirement for the Degree of Master's in Manufacturing Engineering

Office of Graduate Studies
Adama Science and Technology University

June, 2024

Adama, Ethiopia

## DECLRATION

I hereby declare that this Master Thesis entitled ‘‘**Investigate the Deformation Behavior of Reinforced 7075 Aluminium Metal Matrix Composite through Cold Extrusion Process for Automobile Brake Caliper**” is my original work . That is, it has not been submitted for the award of any academic degree, diploma or certificate in any other university. All sources of materials that are used for this thesis have been duly acknowledged through citation.

| Bayush Lemma Batu | | |
|---|---|---|
| Name of student | Signature | Date |

.

## RECOMMENDATION

We, the advisors of this thesis, hereby certify that we have read the final version of the thesis entitled **''Investigate the Deformation Behavior of Reinforced 7075 Aluminium Metal Matrix Composite through Cold Extrusion Process for Automobile Brake Caliper**" prepared under our assistance by Bayush Lemma Batu submitted in partial fulfillment of the requirements for the degree of Mater's of Science in Manufacturing Engineering. Therefore, we recommend the submission of the final revised version of the thesis to the department following the applicable procedures.

| Dr. Devendra Kumar Sinha | ______________________ | ______________________ |
|---|---|---|
| Major Advisor | Signature | Date |

| Mr. Mengistu Gelaw | ______________________ | ______________________ |
|---|---|---|
| Co-Advisor | Signature | Date |

## APPROVAL SHEET

We, the advisors of the thesis ‘‘**Investigate the Deformation Behavior of Reinforced 7075 Aluminium Metal Matrix Composite through Cold Extrusion Process for Automobile Brake Caliper**” and developed by Bayush Lemma Batu, hereby certify that the recommendation and suggestions made by the board of examiners are appropriately incorporated into the final version of the thesis.

| | | |
|---|---|---|
| Dr. Devendra Kumar Sinha | ____________________ | ____________________ |
| Major -advisor | Signature | Date |
| Mr. Mengistu Gelaw | ____________________ | ____________________ |
| Co-advisor | Signature | Date |

## APPROVAL BY BOARD OF EXAMINERS

We, the undersigned, members of the Board of Examiners of the thesis by Bayush Lemma Batu, have read and evaluated the thesis entitled ‘‘**Investigate the Deformation Behavior of Reinforced 7075 Aluminium Metal Matrix Composite through Cold Extrusion Process for Automobile Brake Caliper** and examined the candidate during open defense. This is, therefore, to certify that the thesis is accepted for partial fulfillment of the requirement of the degree of Master of Science in Manufacturing Engineering.

| | | |
|---|---|---|
| Chairperson | Signature | Date |
| Internal Examiner | Signature | Date |
| External Examiner | Signature | Date |

Finally, approval and acceptance of the thesis is contingent upon the submission of its final copy to the Office of Postgraduate Studies (OPGS) through the Department Graduate Council (DGC) and School Graduate Committee (SGC).

| | | |
|---|---|---|
| Department Head | Signature | Date |
| School Dean | Signature | Date |
| Office of Postgraduate Studies, Dean | Signature | Date |

## ACKNOWLEDGMENT

First of all I would like to thank God for his granted me with opportunity, countless blessing and knowledge. Then I would like to express my sincere gratitude to my advisors, Dr. Devendra Kumar Sinha for his continuous support and guidance throughout this process. Additionally, I want to thank Mr. Sentayo Legese (HOD), Mr. Mengistu Gelaw, for always being available to provide me with valuable advice whenever I needed it the most. Additionally, Mr .Kanate Sanbaba and Mr. Biruk Sisay from material science department for their technical support and encouragement during experimental work as well my very close friends who shared their helpful ideas and cooperation in completing this thesis: Talile Chirkena, Hanna Tadessa and Sisay Diriba.

Furthermore, I would like to extend my heartfelt thanks to the departments of mechanical engineering, material science engineering, and applied chemistry at ASTU, as well as the mechanical engineering department at AASTU, for granting me access to various resources, facilities, and equipment for conducting machining, testing, and characterization.

Lastly, I would like to express my deep appreciation to all the individuals who have assisted me in any way during the preparation of this paperwork. Your contribution deserves great respect. Thank you all!

## TABLE OF CONTENT

## LIST OF TABLE

## LIST OF FIGURE

## LIST OF ACRONYMS AND ABBREVATION

| | |
|---|---|
| Al MMC | Aluminum Metal Matrix Composite |
| ANOVA | Analysis of Variance |
| ASTM | American Society for Testing and Materials |
| BBD | Box Behnek Design |
| $CeO_2$ | Cerium dioxide |
| DOE | Design of Experiment |
| GA | Genetic Algorithm |
| GRA | Grey Relational Analysis |
| GO | Graphene Oxide |
| HCL | Hydrochloric acid |
| MMC | Metal Matrix Composite |
| MWCNTs | Multi-Walled Carbon Nanotubes |
| RSM | Response Surface Methedology |
| S/N | Signal to Noise Ratio |
| SEM | Scanning Electron Microscopy |
| SiC | Silicon Carbide |
| TiC | Titanium carbide |
| TiO2 | Titanium oxide |
| OM | Optical Microscope |
| WC | Tungsten Carbide |
| XRD | X-ray diffraction |

## ABSTRACT

*The research studied on the comprehensive studies of fabrication and characterization of SiC, CeO2 and GO-7075Al-hybrid composite with improved mechanical and triabological behavior. The two-step approach includes an initial stir casting process SiC, CeO2 and GO hybrid reinforcements, followed by a cold extrusion step to further optimize the material's microstructure and performance. Three different hybrids aluminum composite was fabricated and analyzed with altering the reinforcement ratio 81%Al7075 +10% $CeO_2$+5%SiC+4%GO,81%Al7075+7.5%$CeO_2$+7.5%SiC+4%GO,and81%Al7075+5%$CeO_2$ +10%SiC+4%GO with 650rpm stirring speed for 10 minute through maintaining the stirring temperature of matric 700℃. The optimum string parameter was selected to accomplish a homogeneous distribution of the hybrid reinforcements within the aluminum with homogenous distribution of reinforcement melt. The casted composites show the improvement in mechanical and tribological properties when compare to the pure alloy due to uniform distribution of reinforcement. The 81%Al7075+7.5%$CeO_2$+7.5%SiC+4%GO hybrid composite show highest hardness, compression strength 240.5HV (66.25%improvement ) 490MPa,respectively as well low wear and corrosion rate was recorded. 81%Al7075+7.5%$CeO_2$+7.5%SiC+4%GO composite were chosen using Grey Relational analysis (GRA) method depend on the properties for secondary operation. The plan and design of experiments was performed by Box Behnken method at three factors and levels The DEFORM 3D software was used for the numerical simulation of cold extrusion at varies parameter: extrusion ratio (6, 8, and 10), ram speed (2.5, 3, and 3.5) m/s, and (185,225,265)℃.The surface response methodology in Design expert was used the predicted the box behken method combined damage, extrusion load and effective stress from simulation with input extrusion parameter. The result showed significance and further optimized by genetically algorithm using mat lab. The optimum extrusion ration of 6, ram speed of 2,5m/s and temperature of 265℃ was used to real deform the sample and the post deformation test showed the further improved in properties.*



**Keyword:** Copper Metal Matrix Composite, Casting, Extrusion, Box Behnken Design, Genetically algorithm, Cold extrusion

# CHAPTER ONE

# INTRODUCTION

## 1.1. Background of the Study

The demand of Composites material becomes high when compare to traditional alloys, due to its special property like, low weight with high specific and stiffness property. These special properties and enhancement of the production methods have resulted in fabrication of various kinds of the composites(Karibeeran et al., 2015).Composite material has two parts the one that transfer load applied and the one that provides mechanical strength to the composite which was known us matrix and reinforcement respectively(Sharma et al., 2020).

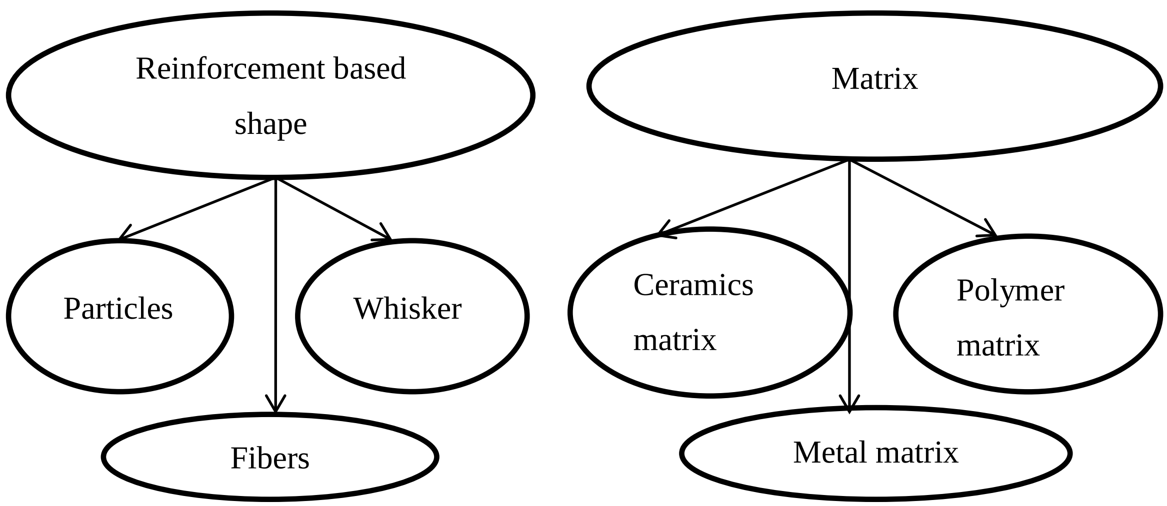


Figure 1.1 Basic form of Reinforcement and Matrix (Sharma et al., 2020)

Metal matrix composites (MMCs) are one of the most widely used type of composite material due to its own high strength to weight ratio together with outstanding mechanical, triabological and chemical behavior. Those properties makes it special candidate for aerospace, automobile, medical, and electronic application. The matrix, reinforcement and the interface between them is the key element that mainly manipulate the behavior of composite materials (Bansal & Upadhyay, 2016).

### 1.1.1. Aluminum metal matrix composite

AMMC is one class of metal matrix composite that consist of Aluminum alloy as matrix. These materials have been drawing attention due to their high strength, superior fatigue, wear and corrosion resistance and good compatibility with various manufacturing processes than MMCs. The growth of aluminum metal matrix composites can be sub sectioned into three stages(Reddy et al., 2019).

- First stage: Aluminum metal matrix material properties enhancement by reinforcing with single hard reinforcement.
- Second stage: Aluminum metal matrix properties enhancement by reinforcing with two or more synthetic ceramic reinforcement.
- Third stage: Aluminum metal matrix properties enhancement by incorporating synthetic ceramic and industrial waste like fly ash red mud etc.

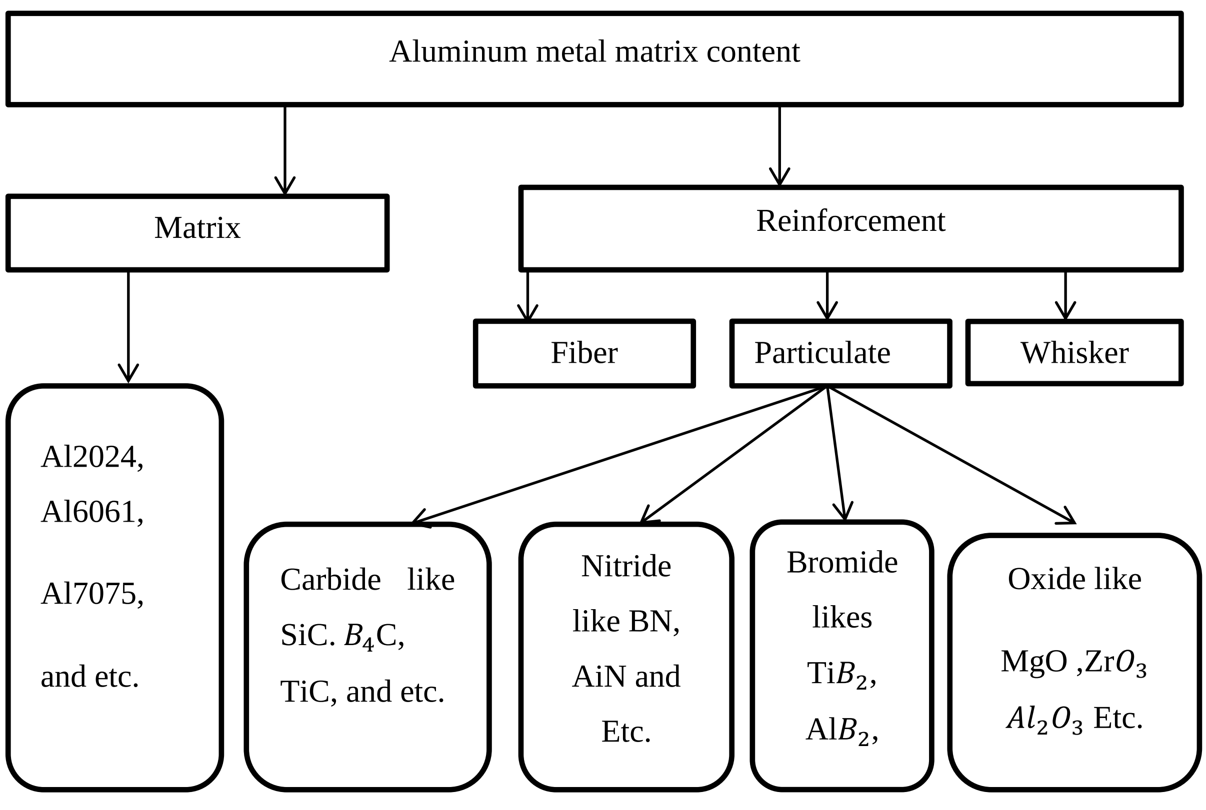


Figure 1.2 The most widely used matrix and reinforcement types in AMMCs

Aluminum matrix composites (AMCs) are currently manufactured by various techniques from the most abridged approach to fabricated near net shaped aluminum based composites is by liquid metallurgy route as it is more economical, and can result in mass production (Mohanachari et al., 2018). The processes performed after the manufacturing of the composite to enhance the strength and modify the micro structure are often referred to as a secondary process. The most common secondary process are  heat treatment and plastic deformation (Abbas et al., 2021).

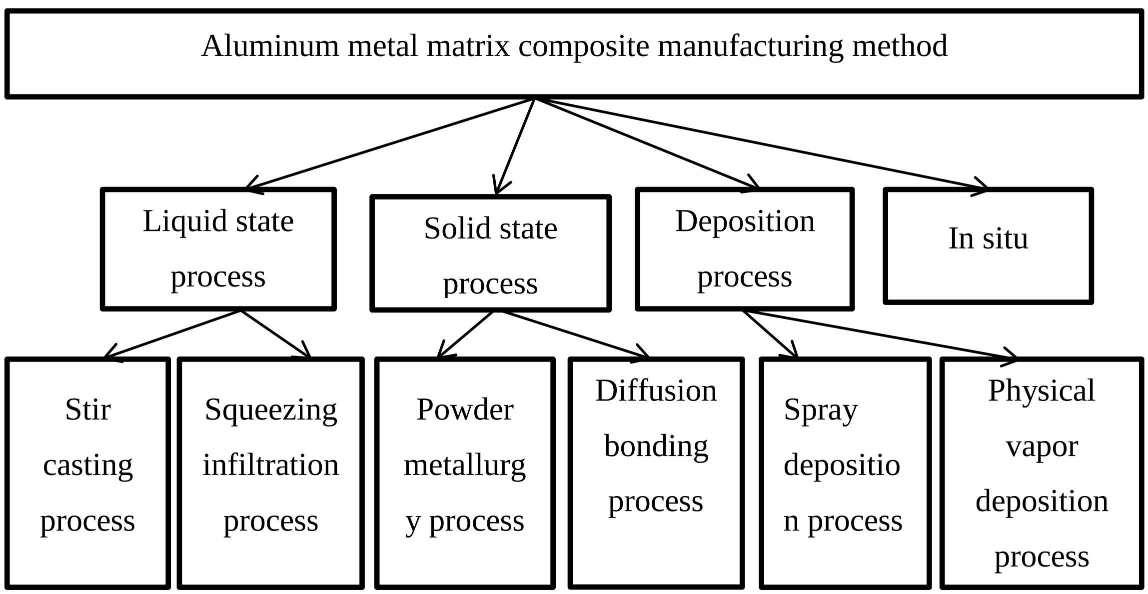


Figure 1.3 Manufacturing methods most of the time used AMMC (Senthil et al. 2021)

In the light of the above, the present research work on the development of AMMCs  by using aluminum alloy (Al7075) as a matrix and, SiC,$CeO_2$ and GO as a reinforcement material as well as analysis the effect of reinforcement ratio and extrusion on the microstructure and mechanical properties AMMCs.  Ceramic has a high melting point, outstanding hardness. Then deformation of material was performed using cold extrusion process to investigate its post deformation behavior.

### 1.1.2. Extrusion process

Extrusion process is one type of forming process used to deform material in to different cross section with better properties. The process starts with putting the billet into the container, which has a cross section area gradually decrease from inlet to outlet, depend on the specification. Then the billet is extruded through die using punch. The material extruded has uniform cross section as the outlet part of the die. This process decreases the diameter and increases the length of material. The process also used to fabricate complex cross section with better strain rate value using complex shaped die. Different class of extrusion is listed below

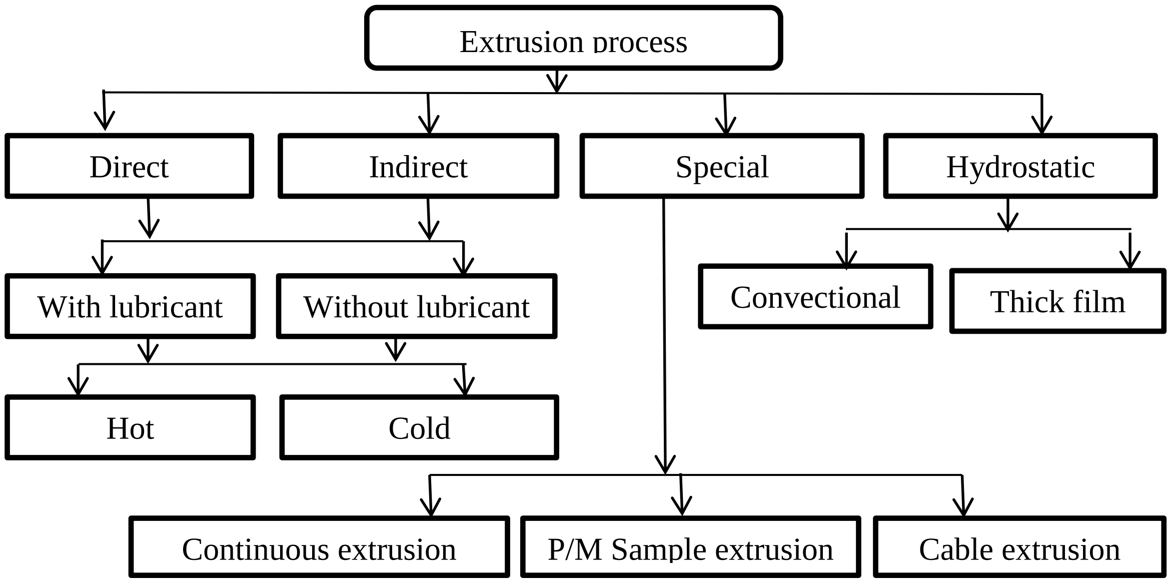


Figure 1.4 Different classes of extrusion process

### 1.2. Application area of aluminum metal matric composite

Aluminum metal matrix composite has wide range application area due its exceptional behavior. This material in aerospace and automotive industry used to fabricate aircraft part such as engine blocks, brake systems landing gear components, pistons, , and structural parts. Their lightweight property, thermal stability  and excellent fatigue resistance make them best for this sector (Nturanabo et al., 2019). Further, lightweight and corrosion resistance nature of material make it  suitable for  marine sector  as well defence and military applications like ship ,boat, and construction offshore structure (Yılmaz, 2019).The design flexibility, lightweight, aesthetic and durability nature of aluminium composite makes it confortable for construction industry parts like building facades, panels interior,  roofing systems ,and etc.

### 1.3. Problem Statement

Aluminum alloy is one of the eminent engineering materials for various applications such as in aerospace, automotive. But still the challenges are being faced by these sectors as far as strength to weight ratio, ductility, wear, and corrosion resistance are concerned. From aluminum alloy, 7075 Al alloy known by its best strength to-weight ratio but it is more vulnerable to stress, corrosion cracking, low formability, low melting point when compared to aluminum other alloys (Callister Jr & Rethwisch, 2020). Those draw back makes 7075 Al alloy not suitable for forming operation as well, corrosion, stress and high temperatures environment. The individual effect of reinforcement SiC, $CeO_2$ and GO in 7075 Al alloy have been studied but the combining effects of these multiple reinforcements are not well studied (Lupulescu et al., 2016).The additions of synthetic ceramic into the matrix result in the decrement of ductility and improvement in the brittleness of the composite materials. As a result of enhancement in brittle nature, the damage value is affected during deformation process (Ramesh et al., 2017). Moreover, the optimization of the cold extrusion process parameters to further improve the properties of these hybrid composites has not been sufficiently studied. Additionally, the difference in density between the particles and the matrix result in enhancement of the weight of composite.

## 1.4. Objectives

### 1.4.1. General Objective

The objective of this research is to Fabricate, Characterize and Test Aluminum based Reinforced Metal Matrix Composites and evaluation of its pre and post deformation behavior at optimum extrusion conditions.

### 1.4.2. Specific Objectives

1. To Develop Reinforced Aluminum Metal Matrix composite at various weight percentages of reinforcement particles.
2. To Evaluate Microstructure, Mechanical, Physical, Tribological Properties of Developed Composite Material.
3. To carry out Numerical Simulation for evaluation of load, effective stresses and damage value for the developed composite material
4. To optimize the input deformation parameters such as extrusion ratio, ram speed and temperature for minimum value of load, effective stresses and damage value.

5. To Evaluate the Post Deformation Characteristics (Density, Hardness, Compression strength and Corrosion resistance) of the developed composite material.

### 1.5. Significant of the study

The research intends to provide considerable significance in the field of material science and engineering. It mainly targeted in providing the following values in mechanical performance of material.

- ✓ To shed light our understanding of how the mechanical performance of Al7075 is influenced by addition of Silicon Carbide (SiC), Cerium Dioxide ($CeO_2$) and Graphene oxide (GO) reinforcement.
- ✓ It assists the engineers to have better understanding of how to optimize the design and component made from this composite.
- ✓ It enables the investigators to identify process parameters, understand the effect of process parameters and refine the process.
- ✓ In real world working condition, it helps the engineers to predict and justify the mechanical performance of the composite.

### 1.6. Expected outcome of the study

In this research work, number of outcomes will be expected such as:

- ✓ Developed lightweight, hard, strong and wear resistant material of Al7075/ SiC , $CeO_2$ and GO composites,
- ✓ Homogeneous particle distribution, uniform mechanical and tribological properties and material having surface finish ,good strength after extrusion,
- ✓ Optimized extrusion process parameters for selected light weight, hard, strong and wear resistant material of Al7075 / SiC, $CeO_2$ and GO composites to improve mechanical and micro structure property.

### 1.7. Scope of the Study

The scope of the research mainly concentrates on the investigation of deformation characteristics of Al7075/SiC, $CeO_2$, and GO reinforced aluminum metal matrix composites fabricated and extruded at selected optimum parameters. The study specifically focuses on the following parts:

- ✓ Deformation and mechanical performance of Al7075 matrix material and SiC, Ce$O_2$ , and GO particles formulate composite.
- ✓ The effects of selected: - process parameters, stir casting fabrication, and cold extrusion on deformation behavior of specific composite.
- ✓ Test deformation behaviors like ultimate strength, ductility, and strain hardening behavior.
- ✓ Characterize and test of pre and post deformation behavior of developed sample.
- ✓ As well as optimization of extrusion parameters for selected light weight, hard, strong and wear resistant material of Al7075/ SiC $CeO_2$ and GO composites.

### 1.8. Research motivation

The motivation behind this research project is the desire to fabricate sample with superior properties and performance. The light weight and high strength application of Aluminium matrix composites makes it the canter of attention. Based on the above motivation, the study aimed to develop aluminium composite by reinforcing 7075Al matrix with SiC, CeO2, and GO, by stir casting techniques. The study also focus to study the combined effects of these multiple reinforcements on the composite's performance.Additionally, the study is further motivated by the benefit of incorporating secondary operations like deformation to improve microstructure, and performance characteristics.

### 1.9. Limitation of the study

- ✓ The research will not address post-processing treatments, such as heat treatment or surface modification, and their effects on the deformation behavior of the composites
- ✓ Stir casting was unavailable at Adama University; thus, installing this machine took a long time.
- ✓ During etching process, the etching chemical attack the grain boundary due to crystallographic orientation and fine and closed packed structure of 7075 Al grain and grain boundary. This makes it difficult to distinguish or reveals the grain boundary

after etching process visually.so it need further study of the material properties to better understand  the behavior of material.

## 1.10. Thesis organization

This study is structured and organized with well-defined plans to achieve specific objectives. The chapters are outlined as follows: In this chapter one, the study provides an introduction encompassing the background, problem statement, research questions, objectives, significance, and limitations of the research. Chapter two focuses on reviewing relevant literature, emphasizing the importance of the study. It explores previous research, highlighting the methods, designs, and identifying the research gaps. Chapter three provides a concise description of the materials and methods employed in the research. It outlines the experimental procedures, including sample preparation, conducting experiments using Stir Casting, and testing and characterization procedures. The primary focus is to investigate the impact of input process parameters (such as the ratio of matrix and reinforcement, stirring time, stirring speed, and stirring temperature) on the mechanical properties, specifically hardness, compression, density, and porosity of the fabricated MMC samples. Additionally, the chapter discusses the utilization of the Taguchi-based GRA multi-objective optimization method to determine the optimal combination of process parameters. It also covers the testing of wear resistance, mechanical properties, and metallurgical analysis (microstructure) of the optimized samples. The results obtained from various tests are interpreted, discussed briefly, and their implications, limitations, and future work are addressed. Chapter four presents a comprehensive discussion of the results obtained from different tests. The results are compared and analyzed in relation to the existing evidence presented in the literature review. The findings are interpreted, highlighting their significance and limitations. Furthermore, the chapter offers insights into potential future research directions. Chapter five concludes the study by summarizing the findings and providing a comparative discussion of the results with the literature review. It offers a concise overview of the study's contributions, implications, and recommendations for further research.

By following this well-structured framework, the study aims to provide a thorough analysis of the subject matter and deliver valuable insights into the fabrication and properties of metal matrix composites.

# CHAPTER TWO

# LITERATURE REVIEW

## 2.1. Introduction of Composite

Composite materials are formed by bringing together one or more materials with their own specific properties and extract out materials with better properties than its individual constituent. In generally a composite consist of three component:-the matrix as major media; the reinforcements as diffused into and strength phase incorporating fiber and particle; and the well interphase area, (Ngo, 2020). Depend on the matrix and reinforcement used, the composite materials classified under two broad categories. Based on matrix used, it is group into Metal Matrix Composites, Polymer Matrix Composites, and Ceramic Matrix Composites. The ability to withstand high temperature, dampness, radiation, zero outgassing at vacuum, thermal and electrical conductivities as well improved mechanical property of Metal Matrix Composites(MMCs) make it best candidate for different application than other (Ramanathan et al., 2019)..

### 2.1.1. Aluminum Metal matrix composite

Aluminium Metal Matrix Composite is a composite which contain aluminium as matrix phase to provide the overall structure and the reinforcement phase to prove strength material embedded within it. The reinforcement used to reinforce the aluminium matrix can in the form of particles, fibres, ad whiskers. The final behaviour of is depend the distribution and alignment of the reinforcement phases within the aluminium matrix (Samal et al., 2020).

## 2.2. Fabrication of reinforced aluminum composite

The two main methods used for manufacturing of aluminum-based composites are stir casting and solid-state technique. The matrix and reinforcement are mixed together for compacting in the powder metallurgy process, and the Result obtained is then sintered to improve its strength. The most traditional and economical process for producing aluminum composites is stir casting (Samal et al., 2020).

### 2.2.1. Stir casting manufacturing process

Stir casting is one of the most common used liquid-state methods utilized for fabrication MMCs. It is preferred due to, simplicity, suitable for large volume production, and cost effective. More ever, the mechanical stirrer is applied through an impeller to distribute the reinforcement into the molten matrix (Lorella Ceschini et al., 2017). Panwar and Chauhan (2018) compared the squeeze casting, compo casting, friction stir processing, and spray casting to stir casting. Gowrishankar et al. (2020) emphasized that stir casting is as an easy and affordable method for creating metal matrix composites with a generally homogeneous distribution of particles.Stir casting is an efficient method for producing aluminum composites, as demonstrated by the uniform distribution of reinforcements and hardness across the whole cross-section. This method has been successfully adopted in fabrication of Al7075-SiC composites reinforced with containing 5% and 7.5% of silicon carbide (Gosavi & 2020).

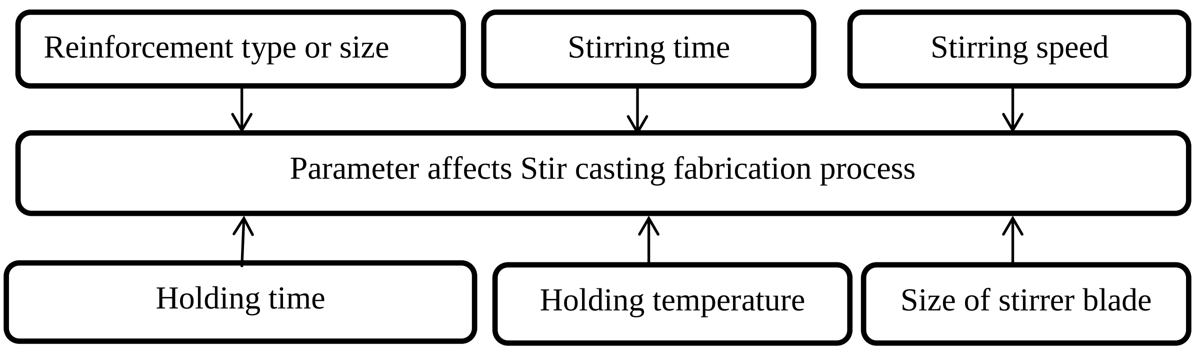


Figure 2.1 Factors affect the fabrication process using stir casting (Samal et al., 2020)

### 2.2.2. Influence of Reinforcement type

The mechanical and physical characteristics of metal matrix composites are the result of the interaction among the soft alloy matrix and the hard, brittle reinforcement. Aluminum metal matrix composites (AMCs) are capable to acquire higher values of stiffness, strength, resistance to wear, corrosion, fatigue and creep, based on the type of reinforcement used and its volume percent in the metal matrix (Gosavi & Jaybhaye, 2021).Venkatesan and Xavior (2017)investigated the mechanical properties of aluminum metal matrix strength with graphene particles in various weight percentages 0.33%, 0.55%, and 0.77%, which was produced by stir casting. Results showed that with the addition of graphene particles, tensile strength of base metal enhanced from 90 MPa to 145 MPa, or 60% more than the base material. Yadav et al. (2018) found that with the addition of multiwall carbon Nanotubes (MWCNTs) to the aluminum SiC composites, compressive strength, wear rate, and coefficient of friction of high bride composite increases. Addition of MWCNTs reinforcement alone causes aggregation; decrease composite's strength, and resistance to wear. SiC is used as an additional reinforcement to enhance the interfacial contact between aluminum and MWCNTs. Mukesh et al. (2019) studied the influence of BN (6%, and 9%) on mechanical properties of the stir casted and extruded Al 6061 composite. The results revealed that with the addition of BN the hardness and tensile strength of both cast and extruded samples were improved. Akbar et al. (2020)compared the mechanical and physical properties of Al6061/sea with Al6061/SiC, and Al6061/$A_2O_3$ high bride composite. The result show that Al6061/sea sand composites have higher density, lower porosity and harder surface than Al6061/$A_2O_3$ and Al6061/SiC composites. (Ramnath et al., 2021) studied the wear behavior of SiC reinforced AMMCs and $A_2O_3$ reinforced AMMCs. The result found that $A_2O_3$ reinforced AMMCs are less resistant to wear than SiC reinforced AMMCs. It has been observed that the AMMC's fracture toughness decreases when the volume fraction $A_2O_3$ of increases Abebe Emiru et al. (2022) fabricated and characterized the effect of reinforcing aluminum alloy with $MoS_2$, SiC, and $B_4C$ –by altering the wt. % (3, 6, 9, and 12%). The result revealed that the samples with double and triple reinforcement had shown less wear loss, due to the solid $MoS_2$ lubricant and the development of $B_2O_3$ layer at the interaction zone.

#### 2.2.2.1. 7075 aluminum metal matrix series

Alumunium7075 is the most widely used 7xxx series alloys because, it has a combination properties like high strength, ductility, and toughness with less density (Sowrabh et al., 2023). (Singh et al., 2021) reviewed different research done the mechanical behavior of Al 7070 and 7075 based materials when incorporation with different type of reinforcement. The comparison result showed that the distribution of the reinforcement in the matrix was moderately homogeneous. The study also revealed that us the weight percentage of particulates reinforcement added into Al 7070 and 7075 base materials increases hardness as well UTS (Ultimate Tensile Strength) of the material also increase when observed relative to the base alloys .Imran and Khan (2019) reviewed the effects of $A_2O_3$, SiC, Gr, $TiO_2$, and bagasse ash on the mechanical and tribological property of Al-7075 metal matrix composite. The reviewed result indicated that the mechanical property like strength, and elastic modulus, of material increases while ductility decreases due to the addition of $A_2O_3$, SiC, $TiO_2$, and bagasse ash reinforcement. Additionally, the hardness and coefficient of friction shows decreases due to due to addition Gr reinforcement. Because Graphene is a very soft material compared to the hard 7075Al alloy matrix. The incorporation of softer Graphene reinforcement within the hard aluminum matrix can lead to an overall decrease in the composite's hardness. Graphene has a very low coefficient of friction. When Graphene is homogeneously distributed in the 7075Al matrix, it can provide a lubricating effect, thereby reducing the coefficient of friction of the composite material

#### 2.2.2.2. Silicon carbide reinforced 7075 aluminum metal matrix composite

One of the most important factors in the performance of an MMC is the compatibility between the ceramic reinforcement and the aluminum matrix. If the reinforcement is not compatible with the matrix, it can lead to a number of problems, including poor mechanical properties, degradation of the matrix, and premature failure of the composite. Silicon carbide (SiC) is a common reinforcement material for MMCs. SiC is a hard, strong, and wear-resistant material that is well-suited for use in high-temperature applications. However, SiC is also a relatively brittle material, and it can be difficult to achieve good compatibility between SiC and aluminum (Surya & Gugulothu, 2022).Imran and Khan (2019) studied the mechanical properties, l properties and corrosion behavior of Al-7075 metal matrix composites when reinforced with SiC reinforcement. The result showed that, improved in mechanical was observed in material. Sonagiri Suresh et al. (2019) investigated on the microstructure of composites; they discovered that the silicon carbide reinforcement is evenly dispersed throughout the matrix of aluminum 7075 in stir-cast Al7075/SiC composites

#### 2.2.2.3. Graphene oxide reinforced 7075 series aluminum metal matrix composite

Narwate and Mohandas (2016)studied the mechanical and tribological Properties of Aluminum Metal Matrix Composite (AMMC) Reinforced with $TiO_2$ (10%) and Graphene Oxide (0.5. 0.75 and 1.0 wt. %) by stir casting methods. The test result revealed that the hardness and tensile strength was improved as the amount graphene oxide added increases.

Highest value of hardness (50HRB) and tensile strength (112.7MP) was recorded for Al7075-10% $TiO_2$1.0%GO fabricated composite. Ashokkumar et al. (2020) investigated the feasibility of Aluminum 7075 Metal Matrix Composite with Graphene Oxide (5 and 10 wt. %) fabricated through stir casting process. The test result reviled that that Al7075 composite with 10 wt. % graphene oxide has optimal a physical and mechanical properties than Al7075 composite with 5 wt. % graphene oxide. (Narwate & Mohandas, 2016) studied the feasibility of Aluminum 7075 Metal Matrix composite reinforced with Graphene Oxide (GO). The study revealed that Al 7075 have high strength, low corrosion resistance, and low weld ability than other common alloys. Because of resistance to stress and strain verses with low weight is highly valuable in automobile, aerospace, and other domestic applications

#### 2.2.2.4. $CeO_2$ reinfoeced 7075 aluminum metal matrix composite

Cerium oxide (CeO2) is a ceramic material with excellent mechanical, electrical, and thermal properties. It has been shown to be a promising reinforcement material for metal matrix composites (MMCs). However, the compatibility of CeO2 with aluminum metal matrices is still need to be investigated .Kumar et al. (2023)investigated corrosion behavior of stir cast hybrid aluminum composite reinforced with $CeO_2$, graphene Nano platelets.the result reviled that addition of $CeO_2$improved the corrosion resistance composite. The optimum combination was found where the weight percentage both $CeO_2$ and graphene Nano platelets was equal (3%, 3%) respectively. The result also showed that the lowest corrosion rate 0.031362 was recorded in the sample contain (3%, 3%) weight percentage of $CeO_2$ and graphene Nano platelets in 94% Al metal matrix at room temperature. The work further showed that, the decrement in corrosion resistance was observed as the temperature increased from.

### 2.2.3. Reinforcement ratio effect

Lokesh et al. (2017) examined the influence of different weight percentage of graphene (0.5%, 1%, 1.5%, and 2.0%) on the hardness of aluminum7075. The result reveled that due to uniform dispersion of graphene particles in the aluminum7075, the samples reinforced with 0.5% graphene have a higher value of hardness number than the samples reinforced with 2% graphene. Composite reinforced with 2% of graphene indicated the lowest value of RHN (Rockwell hardness testing apparatus) due to over-loading of the graphene. Sonagiri Suresh et al. (2019) experimented the Tribological conduct of Al 7075 reinforced with varies weight ratio of 50 nm sized SiC (1.0, 2.0, 3.0 and 4.0%) materials. The composite was fabricated using liquid metallurgy technique. The result indicated that, rate of wear, friction coefficient and weight loss were decrease gradually (1–4 wt. %), reinforced metal compared to the base materials. The micro hardness result exposed that Al 7075/2wt. % composite has greater hardness value compared to Al 7075/4 wt. %and other. With SEM, it was noticed that there were micro- and transverse fractures; light and extreme wear on the worn surface areas as well as wear structure of composite.

Aherwar et al. (2020) examined the mechanical, physical and tribological properties of (4%) $B_4C$ and (0, 4, 8, 12 and 16) % of waste Porcelain reinforced Al7075 hybrid aluminum composite. The result from the analysis showed that, the decrement in density was observed as the weight percentage of porcelain particulates increased. Additionally, the enhancement in mechanical properties was observed due to the formation of ceramic phase. Furthermore, the wear rate and coefficient of friction was reduced with as the porcelain content increased up to a critical value. Finally, the best wear resistance was observed in AA7075/ $B_4$C hybrid composite contain 2% Porcelain. Bhowmik et al. (2020) analyzed the wear behaviors of (0, 3, 6 and 9%) SiC reinforced Al7075 composites fabricated by stir casting. The Pin on Disc tester was used to test the sample wear rate using sliding velocity (1, 2, 3 and 4), constant load (30 N), sliding distance (2000mm).From the result is was observed that as the sliding velocity increases the wear rate increase and COF decreases.it was also observed that minimum material removal was seen in material reinforced with -9Wt. % of SiC.

#### 2.2.4. Stirring speed

Senapati et al. (2020) examined the effect of different stirring speeds on the mechanical behavior of aluminum-silicon alloy reinforced with 10 % weight percentage of fly ash during stir casting. The process was performed by maintaining all other parameters constant and varied stirring speed to 600 and 650 rpm. The result showed that the Composite fabricated with higher stirring speed (650 rpm) had better mechanical property. But after limited stir speed the fabricated composite lose its properties. Ali (2020) discussed the effect of stirring parameters (stirring speed) on the homogeneous distribution of reinforcements, the mechanical properties, and porosities content of the Al- SiC ceramic metal matrix composites during stir casting process. The result of the review showed that, lower speed and stir time causes cluster.

Homogeneous distribution was recorded through increasing stirring speed and stirring time better. The discussion also revealed that more noticeable porosity in microstructures was observed in sample fabricated at higher stirring speed of 700rpm. Mehta and Sutaria (2021)investigated on the effect of stirring process Parameters on the Dispersion of SiC Particles inside Melting Crucible. The effect of stirring speed (300,400,500 rpm) on particle dispersion was studied at optimal value of stirrer position and stirrer geometer. The result showed that, the highest difference in average number densities was recorded at 300rpm velocity as well the upper most inter particle distance was observed at 400rpm and the gas porosities was observed at 500rpm.

#### 2.2.5. Stirring time

According (Chiu et al., 2020) experimented the effect of stirring time during fabrication of reinforced Al-Cu hybrid. The result indicated that reduction in tensile strength and improvement in hardness with increasing duration during reinforcing of of Al-Cu alloys with alumina was observed. Based on the average tensile strength and Vickers hardness results, the 60-second stirring duration resulted in tensile strength of 181.4 MPa and hardness of 53.03 HV. The 180-second stirring duration resulted in tensile strength of 158.3 MPa and hardness of 57.94 HV. Meanwhile, the 300-second stirring duration resulted in tensile strength and hardness of 139.1 MPa and 73.7 HV. In conclusion, stirring duration in stir casting method affected the tensile strength and hardness of Al-Cu alloy reinforced with alumina.

#### 2.2.6. Holding time

Hamed Basuny and El-Sayed (2020) studied the effect of holding time on stir cast fabricated aluminum alloys material behavior. The results of analysis show that the properties casted aluminum was affected by their inclusion content special by the double oxide film defects. These defects not only minimize the mechanical properties but also make the material unreliable. Additionally, the bi film atmosphere might be utilized by reaction with the surrounding melt, which could advance the mechanical behavior of the material.

#### 2.2.7. Melting and pouring temperature

Klemens et al. (2019) studied the effect of melting and pouring temperature on the mechanical properties of Aluminum 7075.The hardness and tensile strength of Al7075 was studied at 770℃ melting temperature and 715, 730, 740, 750 and 770℃ pour temperatures. The result show that the hardness strength increases up to 750℃ then decrease at 770℃ and tensile strength decrease gradually. The study also concluded that too low pouring temperature causes the inlet of the mold cavity to freeze first; this result in improper fill of mold cavity and too high pouring temperature also result in shrinkage and loss of accuracy in the dimensions of the casted sample.

Table 2.1 Hardness and tensile result at different pour temperatures (Klemens et al., 2019)

| Sample | Brinnel (BN) | | | Tensile strength(N/$m^2$) |
|---|---|---|---|---|
| | 1 | 2 | 3 | |
| Cast temperature 715℃ | 55.6 | 55 | 54.7 | 198 |
| Cast temperature 730℃ | 73.6 | 72 | 72.2 | 188 |
| Cast temperature 740℃ | 74.2 | 74.7 | 74 | 169 |
| Cast temperature 750℃ | 78.4 | 79 | 76 | 170 |
| Cast temperature 770℃ | 60.4 | 62 | 60.6 | 150 |

Syahid et al. (2020) analyzed the effect of Pouring Temperature on mechanical strength and microstructures of Al 6061Aluminum Matrix Composite reinforced by 0.1% wt Carbon Nanotube (CNT) with Stir Casting Method. Pouring temperature utilized was 700, 730 and 760℃. The result indicated that the highest hardness (78 HV) and tensile strength (80.97 MPa) value was recorded at 700℃ pouring temperature and the highest impact strength (is 0.128 J/$mm^2$ ) was found at the pouring temperature of 760℃.Thangaraju et al. (2021) investigated the impact of Pouring Temperature (630, 670, and 710℃) on the mechanical properties Al/SiC/Mg/Cu (12 Wt. % SiC, 4Wt. %Mg and 2 Wt. % Cu) Composite fabricated by Stir Casting. The evaluated results indicate that the hardness was higher at 630℃ pouring temperature. This result was obtained due to solidification shrinkage defects and brittle compound formation among the matrix and reinforcement at high pouring temperature (710℃).

#### 2.2.8. Stirrer blade geometer

Ali (2020) reviewed the effect of stirring parameters (Stirrer blade geometer) on the homogeneous distribution of reinforcements, the mechanical properties, and porosities content of the Al- SiC ceramic metal matrix composites during stir casting process. The study stated that 45° and 60° blade angle shows fully particle dispersion and as blade angle increases the dispersion rate also incesases.it is further stated that in most cases 60° form the lowest dispersion time and blade angle as high as 90° and greater consumes high power and cause high level of shearing flow. Mehta and Sutaria (2021)investigated on the effect of stirring process Parameters on the Dispersion of SiC Particles inside Melting Crucible. The effect of blade angle (45°, 60°, 90°) on particle dispersion was studied at optimal value of stirrer position and stirrer speed. The result showed that at blade angle of 45° lowest, 60° lower and 90° higher values of standard deviation number densities was found.

### 2.3. Secondary Process

#### 2.3.1. Extrusion

Extrusion is one of type of deforming process that uses the force generated from hydraulic press to push the cylindrical material through a die to mold the material into required dimension. The compressive and shear pressure applied during the process make stress in the material gradually increase until it reach the point where the material start plastically deformation and make  to flow through the die. There are two types of extrusion, cold extrusion and hot extrusion, cold extrusion provided  mechanical properties enhancement then hot extrusion (Donati et al., 2022). The extrusion process most of the time governed by process parameter such as die angle, ram speed, shape and dimension of the work piece extrusion temperature , extrusion ratio, shape of the product, and coefficient of friction (Kothasiri & Chalamalasetti, 2022).

#### 2.3.2. Extrusion of reinforced aluminum composite

Niteesh Kumar et al. (2017) investigated the properties of multilayer graphene reinforced aluminum metal matrix composites that was fabricated by powder metallurgy then deformed by extrusion. Experimental results revealed that significant increase in mechanical property of composite was observed to consistence distribution of graphene sheets, outstanding interfacial attachment between constituent, and grain modification caused by graphene and extrusion process. The change of ductile fracture to brittle fracture was also observed. Ghanaraja et al. (2017)studied the mechanical and deformation behavior of $Al_2\ O_3$ (0, 3, 6, 9 and 12%) reinforced Al 1100-Mg hybrid, that was fabricated by melt stirring techniques and deformed by 12.25 extrusion ratio. The result showed that the hardness and tensile strength that was reduced beyond 6% of reinforcement was improved through extrusion process. This result was recorded due to reduction in porosity and proper bonding between constituent was achieved by deformation, special in high reinforcement percentage content. Kumar et al. (2021) investigated the influence of extrusion and graphene Nano-platelets content on strain hardening property of GNPs (from 0 to 2 wt. %) reinforced aluminum composite that was fabricated by powder metallurgy process and further deformed through extrusion. The examination performed through SEM, EDS and XRD shows that the incorporation of graphene Nano–platelets into the aluminum matrix. The sample with 1.5 wt. % GNPs has two times greater values of axial stress, hydrostatic stress, and hoop stress, than other after extruded.

#### 2.3.2.1. Effect of extrusion ratio

Han et al. (2017) examined the influence of extrusion rations on behavior of casted Al-Si alloys. The billets were extruded with 4:1 and 10:1extrusion ratio to prevent distortion. The microstructures and phase morphologies examined through optical Microscope revealed that the sample extruded at high extrusion ratio show high density, better tensile and yield strength than the one casted due to reduction in size of particle. Sathishkumar et al. (2017) FE analysis was conducted for sic reinforced aluminum composite using extrusion ratio(4:1, 8:1, 15:1), and work piece temperature(350 °C ,400°C,450°C) parameters. The result indicted that as extrusion ratio increase both the strain rate and strain rate were increased.

#### 2.3.2.2.Weight percentage effect on the extrusion

Zaiemyekeh et al. (2019)investigated was performed to analysis the effect of weight percentage of Nano particle $Al_2O_3$ reinforcement on quasi-static and high strain_rate behaviors of aluminum based composite during deformation. The result indicted that the usage of optimum weight percentage of the Nano particle reinforcement increases the strength and energy absorption potential of the composite material in variety range of strain rates of deformation but excessive addition decreases the properties. (Mukesh et al. (2021) studied on the effect of weight percentage of reinforcement (0.5%, 1.5%, 3%, 4.5%, 6, 7.5%, and 9 wt. %) BN on Al6061 aluminum-based composites fabricated by stir casting and followed by extrusion. The result showed that in both extruded and heat-treated composites sample, the uniform distribution of reinforcement and enhancement in toughness and tensile strength were observed as the weight of reinforcement (Boron nitride) BN increases.

#### 2.3.2.3. Extrusion temperature

Sathishkumar et al. (2017)FE analysis was conducted for SiC reinforced aluminum composite using extrusion ratio(4:1, 8:1, 15:1), and work piece temperature(350 °C ,400°C,450°C) parameters. The result showed that as the temperature increase the strain and strain rate was decreased. Pakdel et al. (2018) investigated the extrude ability, microstructural evolution, and mechanical and fracture behavior of 10 wt. % $B_4C$ reinforced 6063 aluminum composite fabricated by combination of spark plasma sintering and stir casting and deformed by hot extrusion. From result it possible to observe that higher extrusion ratio, punch speed and temperature direct to surface cracking of the sample. However, from the fracture surface of sample it was observed that at lower temperatures and extrusion ratios the sample went to brittle fracture due to the presence of particle clusters and shrinkage voids in their microstructure. Reddy et al. (2019) studied on (5%, 10 %, and 15%) Al-Cu-Li reinforced aluminum metal matrix composite fabricated powder metallurgy followed by hot extrusion. From test result it was observed that Young's modulus, ultimate compression strength, ultimate tensile strength, yield strength and elongation of fabricated composite was increase by 186%, 53%, 42%, 47%, 41%, and 48%, respectively. Shao et al. (2020) investigated the effect of (420 ºC, 450 ºC, 500 ºC) extrusion temperature on the evolution of GNPs in 0.6wt. % graphene Nano platelets reinforced 6061Al composite fabricated by infiltration process and followed by hot extrusion. Through the process GNPs agglomeration was reduced by extrusion. The result showed that the sample extruded at 420 ºC result in non-significant dispersion and some agglomeration of large-sized GNPs however the agglomeration was remove when the sample was extruded at 450 ºC and waved structure, exfoliation and twist of GNPs were observed. While in sample extruded at 500 ºC interlayer sliding of the reinforcement GNPs and interfacial reaction product like $Al_4C_3$ were observed due to excessively temperature. Additionally, the result showed that the highest yield strength and ultimate tensile strength of 389 MPa and 500 MPa where recorded for sample extruded at 450°C with 16.8% and 40.1% percent of increment.

##### 2.3.2.4. Effect of ram speed and die type

Punch speed and extrusion force have direct proportional relation, such as higher punch speed result in higher stress and complex strain rates. Because of the above reason ram speed must be consider as the parameter that have the greater effect of the process(Kothasiri & Chalamalasetti, 2022).Vijay Kumar et al. (2019) Instigated the effect of die angle (12°,15° and 25° )on the mechanical behavior of cold extruded Nano SiC reinforced Al 6065 alloys .the result showed that the extruded load decrease ,and the hardness and surface roughness increase as the die angle increases.

### 2.4. Finite Element Analysis

Finite Element Analysis (FEA) is a widely used numerical simulation methods utilized to investigate the properties and performance of complex systems. This method break down the complex system into smaller and manageable element knows as finite element, and then investigated the properties of individual element to understand the behavior of the all system.(Loh et al., 2016) analyzed the load and effective stress used to extrude 6061Al alloys by finite element analysis. Taguchi's L16 design was used to run the trail and the impact of input parameter on the response was studied by ANOVA. Additionally, the Taguchi optimization approach was utilized to generate a set the optimum process parameter based on greatest S/N ratio for square shape in MINI TAB software. The result showed that the optimum point for minimum load and effective stress.

### 2.5. Literature summary

The previous studies have examined the importance of individual reinforcements, such as silicon carbide (SiC), graphene oxide (GO) ,and cerium di oxide ($CeO_2$) , in 7075 alloys was studied (Surya & Gugulothu, 2022). In the above studies the improved in mechanical properties, wear resistance, and thermal management capabilities of the composites was observed as well the addition, GO solid lubricant reinforcement shown to improve wear resistance material (Ashokkumar et al., 2020). Whereas, the synergistic effects of reinforcements SiC, ($CeO_2$), and (GO), in Al alloy matrix was not well-studied and need to be further studied. Stir casting is a commonly employed AMMCs manufacturing process , however they suffer from certain disadvantages like agglomeration, Wettability issues, Porosity formation , and Segregation of reinforcement which pose as challenges in production (Ramanathan et al., 2019).During this manufacturing process achieving Uniform distribution of reinforcement particles is a significant issue even with micron-sized particles used. To achieve homogeneous distribution of the reinforcement in most fabrication process adjustment of viscosity of the melt, stir time stirrer speed and particle size was done (Gosavi & 2020). Additionally, non-uniform distribution of particles in matrix can be caused by the difference in density between the matrix and the reinforcement since the particles may settle down or either floats. Especially, in the case of Nano-sized reinforcement particle carefully controlling of agglomeration during manufacturing process is mandatory. Another second issue observed during stir casting fabrication is issue concerning about the wettability between the liquid Al matrix and solid reinforcement particles because the factor that affect the bonding between them can also affect the mechanical properties of the MMCs. The other third issue that was seen during the production of MMCs is porosity, which seriously affects the strength (Aherwar et al., 2020). The other critical issue was erosion occurs on the stainless steel stirrer blade especially during the fabrication process of $Al_2O_3$ or SiC reinforced AMMCs reinforced. In most works, a high-temperature grease was applied manually to prevent the stirrer from metal erosion as well as molten Al from sticking to the stirrer Ali (2020). Another challenge that was seen through the process was the problem of adjusting the write reinforcement mixing rate. Reinforcement may react with the matrix material and can form undesirable phases could also be an issue. In most research the aluminum reinforced with two different type of reinforcement has better mechanical property than the one reinforced with one type reinforcement, taking into account the proper control environment and parameter also need. Moreover, the optimization of the manufacturing process parameters, especially the one in extrusion step is important in improving the mechanical and tribological properties of the hybrid 7075 Al alloy MMCs (Donati et al., 2022). However, limited research has been conducted on the optimization of the cold extrusion process for such composite materials.

## 2.6. Research Gap

It has been observed from the literature review that sufficient researches have been carried out on synthesis, characterization and testing of Aluminum metal matrix composites applicable to various applications but very few work has been carried out including the post deformation behavior of casted Aluminum metal matrix composites. The investigation of the deformation and damage behavior of particle reinforced aluminum composites under different loading conditions was studied and the evaluation of formability and prediction of fracture behavior was performed using Finite element analysis (FEA) (Gatea et al., 2023). The response of AMMCs undergo large plastic deformations on complex strain stress flow behaviors was also studied(Li et al., 2024). Additionally, The deformation behavior of multi reinforced aluminum composite was studied also studied (Balokhonov et al., 2022).The presented research on the post-deformation behavior of cast AMCs has some limitations that need to be addressed. The limitation include the lack of wide-ranging studies on the material's response to different deformation modes, beyond the initial tensile and compressive behavior(Kumar et al., 2024) . Additionally, the understanding of the relationship between microstructural evolution and the resulting mechanical properties after deformation is still limited (Zhang et al., 2014). Developing accurate predictive models that can catch the complex behavior of cast AMCs under different loading conditions remains a significant challenge (Adak et al., 2023) .The deformation behavior of casted Aluminum metal matrix composites on optimum extrusion conditions has been rarely studied (Gatea et al., 2023). Most of the work reported in the literature has been found on Aluminum alloys, such as Al 357, Al 359, Al 2618, Al 2214, Al 6063 and Al 6061. However, limited work has been reported on the use of Al 7075 as a matrix material with more than one different reinforcement materials. The 7075 Al matrix is important than other grade of aluminum matrix because it has high strength to weight ration and heat treatable. These properties make it excellent candidate in Aerospace and Military applications after it is reinforced with other strength material. The performance and applications most of the billets fabricated by a stir casting method is the problems of porosity, agglomeration of ceramic particle, gas entrapment and coarse grain size formed inside the material during the fabrication process. The lower ductility of as-cast composites limits their performance and applications. Because of the above reason the further investigation will be needed.

# CHAPTER THREE

# MATERIALS AND METHODOLOGY

## 3.1. Introduction

The research perfumed on Investigated the fabrication and deformation behavior of during Aluminum Metal Matrix Composites and optimization of process parameters through Evolutionary Algorithm. The numerical and experimentally deformation behavior of reinforced Aluminum metal matrix composite with different weight percentage of $CeO_2$ SiC and Graphene Oxide, Nano particles was performed. The material selected was matrix (7075 aluminum alloy) and reinforcement $CeO_2$ ,SiC, and that yields the needed properties and small amount of Graphene Oxide was used for self-lubrication properties. The fabrication was perfumed through stir casting process at different weight composition of reinforcement materials with uniform particle size. Addition of Graphene Oxide was fixed, which was used to improve the wettability between liquid matrix and ceramic reinforcements. The effect of weight composition of the reinforcement materials on density, hardness, tensile strength, sliding wear resistance of AMCs was studied and reported. Microstructure analysis was also carried out on each of casted composites using optical microscopy, SEM and XRD to know fair distribution. The numerical simulation for investigation of residual stresses and damage value for extrusion of fabricated material was carried out through Finite Element Analysis software. The plan and design of numerical simulation experiments was carried out through Box Behnken method at three factors and three levels. The plan and design of numerical simulation experiments was carried out through Box Behnken method at three factors and three levels.The real deformation of fabricated sample at optimum extrusion conditions was carried out on extrusion machine in order to investigate performances such as mechanical property, micro structure, deformability, at the optimum values of input extrusion parameters. The mechanical property such as hardness test, compressive strength test, and as well as for microstructural studies was carried out as per ASTM standards.

### 3.2. Flow chat for the whole process

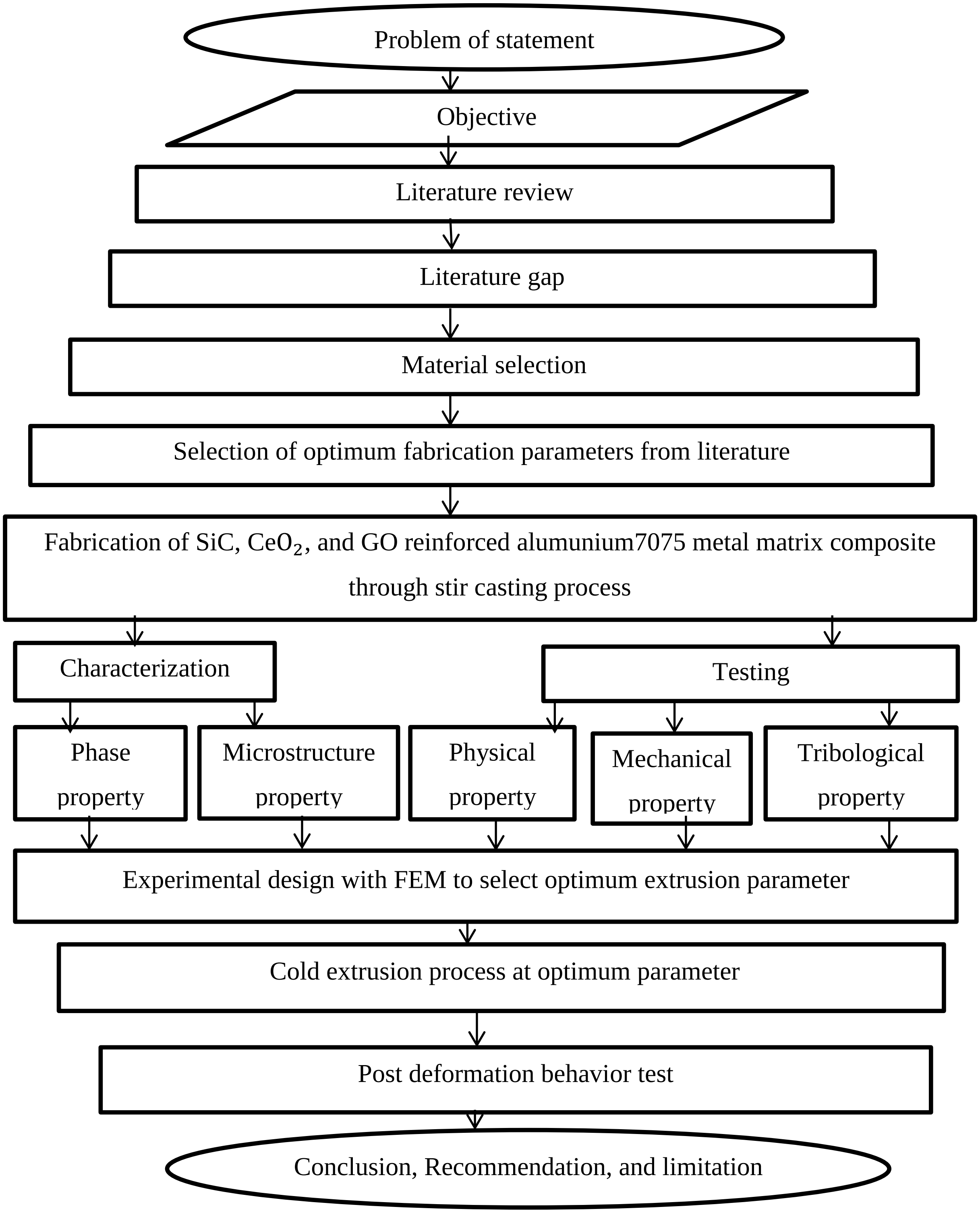


Figure 3.1 Research methodology flow chart

## 3.3. Material

### 3.3.1. Selection of Base Material

The matrix is the main body that provide composites their structure and transfers load between the matrix and reinforcement (S. Senthil et al., 2020). From different type of metal matrix used as base material in composite Aluminum metal matrix has good casting characteristics and used in the aerospace, automobile sector and structural applications due to its low weight and corrosion resistance properties. The Type of aluminum sequence with Main alloy element of the matrix is list in table below according (Singh et al., 2020).

Table 3.1 Different sequence of Aluminum Series

| Type of aluminum sequence | Main alloy element | Application |
|---|---|---|
| Sequence of 1000 | Pure Aluminum | Drawn Tube and chemical Equipment |
| Sequence of 2000 | Copper | Aerospace |
| Sequence of 3000 | Manganese | High strength foil and sheets |
| Sequence of 4000 | Silicon | Sheets |
| Sequence of 5000 | Magnesium | Aerospace and marine |
| Sequence of 6000 | Magnesium and silicon | Aerospace and structural |
| Sequence of 7000 | Zinc | Aero and Auto sector |

Aluminum 7075 from the 7000 series has high fatigue strength, high tensile strength, heat-treatable, high corrosion resistance wrought alloy as compared to all other aluminum series alloys. This alloy is one of the robust aluminum alloys existed, this make it useful in high-stress situations and its low density make the material a fit for applications such as aircraft parts or parts subject to heavy wear. Parashawani Metal Munbia is the source of manufacture with same specific properties and composition material.

Table 3.2 Composition of Al7075-O alloy

| Number | Composition | Amount in Percentage |
|---|---|---|
| 1 | Al | 90% |
| 2 | Zn | 5.6% |
| 3 | Mg | 2.5% |
| 4 | Cr | 0.23% |
| 5 | Cu | 1.6% |

Table 3.3 Mechanical behavior of Al 7075-O aluminum alloy

| Property | Metric |
|---|---|
| Density | 2.81 g/cm3 |
| Ultimate Tensile Strength | 228MPa |
| Tensile Yield Strength | 103 MPa |
| Shear Strength | 331 MPa |
| Fatigue Strength | 159 MPa |
| Modulus of Elasticity | 71.7GPa |

### 3.3.2. Selection of Reinforcement Material

When selecting reinforcing materials, a number of issues have to be considered, including, mechanical properties, thermal and electrical conductivity, Cost, melting point, etc. The characteristics of the reinforcing media determine how structurally effective discontinuously reinforced MMCs is. Common reinforcements in MMCs include ceramic particles (SiC, $Al_2O_3$, $B_4C$), ceramic whiskers ($Al_2O_3$, SiC), and intermetallic compounds (TiAl, NiAl). Ceramic particles enhance strength, stiffness, and hardness, but reduce ductility. Ceramic whiskers significantly improve strength and stiffness, though they also decrease ductility. Intermetallic enhance high-temperature properties and corrosion resistance (Ramnath et al., 2021).

#### 3.3.2.1. Silicon carbide (SiC)

SiC ceramics particles have a crystalline structure contain of carbon (C) and silicon (Si) atoms. The arrangement of particles fluctuates and exhibit different crystal structures such as cubic, hexagonal, or other polytypic based on the synthesis process and conditions. There is different approach used to synthesize SiC particles; the most common approach is thermal decomposition of silicon (Si) and carbon (C) sources in the presence of proper catalysts at elevated temperatures. SiC ceramics stand out as the material with a high strength, high hardness, wear resistance, oxidation resistance, low coefficient of thermal expansion, and high thermal conductivity. It can be applicable in electronics, refractory, wear resistance application like coatings or composites and aerospace industries. Since there is a similarity in thermal expansion rates between silicon carbide and 7075 alloy; reinforcing of silicon carbide to the matrix lead to improve in mechanical strength and, structural integrity, resistance to deformation of the composite material at higher loads and stresses as well downgrades the risk of thermal stress and cracking at the reinforcement-matrix interface (Sonagiri Suresh et al., 2019) . To achieve uniform dispersion and good interfacial bond as well to solve the problem of agglomeration and stress concentrations during reinforcing parameters such as temperature, pressure, and mixing techniques need to be carefully controlled and optimized **(**Ruys, 2023). Parashawani Metal Munbia is the source of manufacture with same specific properties and composition of material.

Table 3.4 Properties of silicon carbide (SiC)

| Properties | SiC |
|---|---|
| Color | Gray |
| Purity | 99% |
| Density (g/cc) | 3.1 |
| Poisson’s ratio | 0.14 |
| Hardness (HB500) | 2800 |
| Compressive strength (C) (MPa) | 3900(C) |

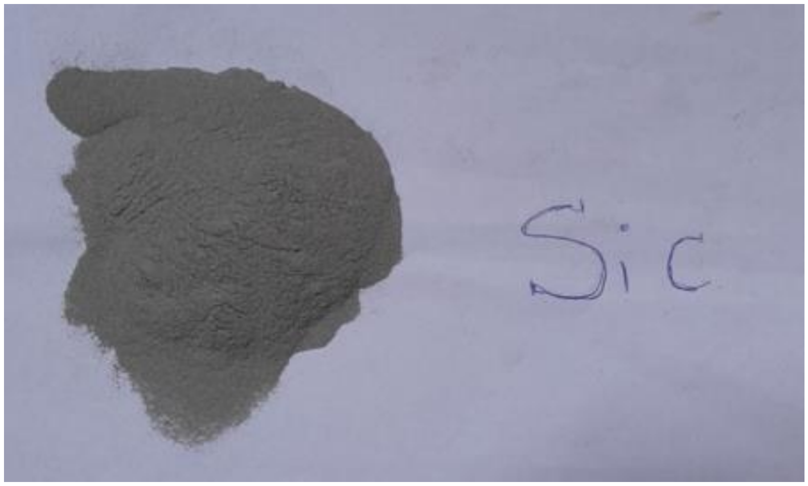


Figure 3.2 Silicon Carbide in Powder form

#### 3.3.2.2. Cerium dioxide $CeO_2$

Cerium dioxide ($CeO_2$) is material composed of cerium and oxygen. High melting point and thermal stability of this material make it excellent choice for high-temperature environments and also its capability to accumulate and discharge oxygen as well reduction-oxidation properties of it to maintaining the chosen oxygen concentration and exchange between different oxidation circumstances respectively makes it number one choice. Additionally, it can improve the tribological properties like friction and wear among contacting surfaces. Parashawani Metal Munbia is the source of manufacture with same specific properties and composition of material.

Table 3.5 Properties of Cerium dioxides ($CeO_2$)

| Type | Cerium dioxide ($CeO_2$) |
|---|---|
| Chemical formula | $CeO_2$ |
| Purity | 99% |
| Color | Black |
| Molar mass g/mol | 172.11 |
| Density g/cm$^3$ | 6.77 |
| Melting point (℃) | 2,727 |


Figure 3.3 Cerium Dioxides ($CeO_2$) in Powder form

### 3.3.2.3.Graphene Oxide (GO)

GO particles has a layered structure result from graphene, consisting of carbon (C) atoms arranged in a hexagonal lattice. The structure of GO particles retains the layered arrangement of graphene but incorporates oxygen-containing functional groups, such as hydroxyl (-OH), epoxy (-O-), and carboxyl (-COOH) groups, which are attached to the carbon lattice. Graphene, a two-dimensional carbon marvel material, has attracted the attention of many academicians internationally due to its exceptional behaviors. The extraordinary behavior of grapheme intrinsic strength and Young's modulus 130 GPa, and 1Tpa,respectively makes it to be an perfect candidate in structural applications as well as high strength and stiffness of graphene make it suitable for energy storage and sensor applications (Dasari et al., 2019). Parashawani Metal Munbia is the source of manufacture with same specific properties and composition of material.

Table 3.6 properties of graphene oxide (GO)

| Property | Amount |
|---|---|
| Carbon purity | ~99 |
| Color | Black |
| Average number of layers | 3-6 |
| Thickness | 0.4 |
| Surface area | $350m^2$/g |


Figure 3.4 The Powder form Graphene Oxide (GO)

### 3.3.3. Identifying matrix and reinforcement

The metal matrix chosen and utilized in this research was 7075 aluminum alloy due to high strength and amazing mechanical properties. Silicon carbide (SiC) was added to increase hardness, cerium di oxide ($CeO_2$) was added to increase wear and corrosion resistance, and small amount of graphine oxide (GO) was also added to improve self-lubrication and wettability between molten metal and solid reinforcement. The selection of reinforcement was perfumed by take into account the cost, properties, and availability of each option.

### 3.3.4. Identification of parameters and its level for casting

The composite was fabricated through a stir casting process with an experimental design constructed based on basic input variables of process parameters like stirring time, stirring speed, particle size , reinforcement weight percentage and pouring temperature .This parameters influence the casting performance so need be controlled very well. In this research, the effect of fabrication process parameter (pouring temperature, stirring speed, stirring time), weight percentage of reinforcement, at different level and optimum process parameter on the surface roughness and hardness is analyzed and identified as follows. The selection of process parameter and their level was performed according to the knowledge obtain from literature, manufacturing and resent information about the composite manufacturing process industry.

Table 3.7 Literature reviews for component weight percentage selection

| Researcher | Matrix | Reinforce-ment | Parameters | | | |
|---|---|---|---|---|---|---|
| | | | Reinforcement ratio | Stirring Speed | Melting Temperature | String time minutes |
| (Samal et al., 2020) | 7075Al | SiC | 2.5%, 5%, 7.5% 10%. | 400 rpm | 750℃ | 8 s |
| (Patel et al., 2019) | 7075Al | -SiC | 2.5%, 5%, 7.5% 10%. | 650rpm | 750℃ | 15–20 |
| (Gukendran et al., 2022) | 7075Al | SiC ,Al2O3 | 0%,2.5%,5%,7.5% | 600 rpm | 700℃ | 10 -15 |
| (Dwivedi et al., 2020) | AA6061 | Sic , rice ash | 0%,2.5%,5%,7.5%,10%,12.5%,15% | 650rpm | 700ºC. | 15 |

Table 3.8 parameters and its level for casting

| S.No | Parameters | | Levels | Unit |
|---|---|---|---|---|
| 1 | Pouring temperature | | 650 | °C |
| 2 | Melting temperature | | 700 | °C |
| 3 | Stirring speed | | 650 | Rpm |
| 4 | Stirring time | | 10 | Minutes |
| 5 | Weight of percentage of matrix | Al 7075 alloy | 81 | Wt.% |
| 6 | Weight percentage of reinforcement | Graphene Oxide | 4 | Wt.% |
| | | Silicon Carbide | 5,7.5,10 | |
| | | Cerium dioxide | 5,7.5,10 | |

### 3.3.5. Experiment design for fabrication of aluminum metal matrix composite

Experimental design for fabrication of aluminum metal matrix composite via stir casting were performed based on the optimum parameters like stirring speed, stirring time and pouring temperature as recommended by most researcher. Weight percentage of silicon carbide and cerium di oxide is made vary to yield needed properties for intended application. Fixed amount of graphene oxide is used to improve wear and wettability between matrix and reinforcement. The combination was performed based on the information according to (Samal et al., 2020) and (Patel et al., 2019).

Table 3.9 Experimental designs for fabrication of the composite

| Samples | Composition | Weight percentage |
|---|---|---|
| S1-sample 1 | 7075 Aluminum alloys | 81 % |
| | Silicon carbide | 5% |
| | Cerium di oxide | 10% |
| | Graphene oxide | 4% |
| S2-sample 2 | 7075 Aluminum alloys | 81% |
| | Silicon carbide | 7.5% |
| | Cerium di oxide | 7.5% |
| | Graphene oxide | 4% |
| S3-sample 3 | 7075 Aluminum alloys | 81% |
| | Silicon carbide | 10% |
| | Cerium di oxide | 5% |
| | Graphene oxide | 4% |
| S4-sample 4(Pure 7075 Aluminum alloys) | Al | 90.0% |
| | Zn | 5.6% |
| | Mg | 2.5% |
| | Cr, and | 0.23% |
| | Cu | 1.6% |

### 3.3.6. Weight estimation for matrix and reinforcement

Total weight mass of matrix and reinforcement needed to fabricated the 7075Al/SiC/$CeO_2$ /GO was selected based on the total specimens require for hardness, compression test, microstructural, wear test and for cold deformation (extrusion) process. All samples were formulated with diameter of 20mm and length of 30cm. The mechanical and tribological behavior of the produced composite materials are largely reliant on the reinforcing weight percentage (wt. %). As a result, the weight percent composition of SiC, GO and $CeO_2$ employed in this research work was determined based on a survey of the literature. The wt.% composition of any reinforcement addition should not exceed 30% to lower the porosity formation in the composite, for better uniform reinforcement distribution, and for suitable densification of the fabricated composite (Ramanathan et al., 2019).Depend on ASTM standard a specimen size needed for the microstructure, hardness, density and corrosion test was Length =7 mm, Diameter =18mm, for the compression test Length = 8mm and Diameter =10mm was required , for the wear test, depending on the ASTMG99-05 standard the sample size used was Length =12mm, Diameter=5.9mm. The length and diameter remain was used for cold extrusion operation. Sample size of 2mm diameter per specimen was considered as allowance to comp set the material loses during hand sawing, filing, machining and grinding. Length =7mm (microstructure, hardness, density and corrosion test) +8mm (compression test) +12mm (wear test) +8 (total allowance size of specimen) +65 (cold extrusion).

Length =100mm,and Diameter=20mm

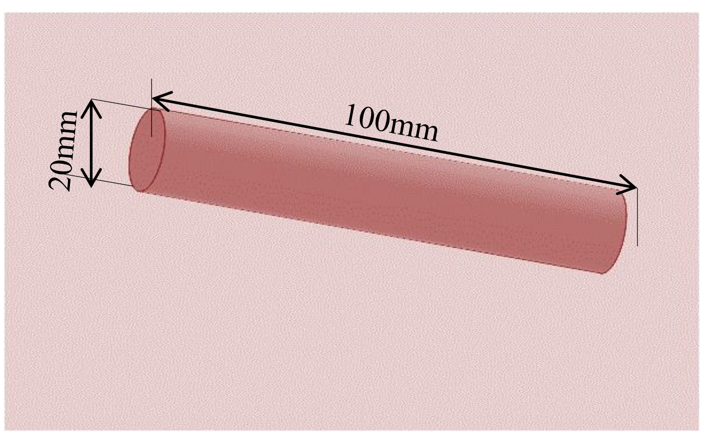


Figure 3.5 Sample Models by solid work

The required volume of material for a cylindrical sample is calculated using eqn. (3.1)

$$V=\frac{\pi}{4} D^2 *L \tag{3. 1}$$

Where, V=Volume of cylindrical shape sample in $mm^3$

L=Length of sample in mm, and

D=Diameter of sample in mm

Depend on the required size total volume of material was calculated as follows

$V=\frac{\pi}{4} D^2 *L=\frac{\pi}{4} 20^2 *100 =31,400 mm^3=31.4 cm^3$

$V_T$ = (31,400$mm^3$*3) = (94,200) for three sample fabricated

The amount of matrix and reinforcement used for each sample was calculated according to weight percentage combination of matrix and reinforcement design in experimental design section. The mass of matrix (7075 aluminum alloy) and reinforcement (SiC, $CeO_2$and GO) present in each sample was calculated by the formula below.

$$m_x=V_T *\rho_x*y \tag{3. 2}$$

Where, $m_x$ = mass or weight of reinforcement or matrix

$\rho_x$=density of matrix or reinforcement

Y=weight percentage of reinforcement or matrix.

Mass or weight of matrix and reinforcement used for each sample was calculated according to weight percentage combination of matrix and reinforcement design in experimental design section.

I. Weight of matrix (7075 aluminum alloy) and reinforcement (silicon carbide, cerium di oxide and graphene oxide ) for sample one :-

Weight (in mass), $m_{7075Al}= V_T *\rho_x*y =31.4cm^3*2.81g/cm^3*0.81=71.469g$

Weight (in mass), $m_{SiC,}= V_T *\rho_x*y =31.4cm^3*3.21\ g/cm^3*0.1=10.079g$

Weight (in mass), $m_{CeO_2,}= V_T *\rho_x*y =31.4cm^3*7.132g/cm^3*0.05 =11.197g$

Weight (in mass), $m_{GO,}$= $V_T$ *$\rho_x$*y =31.4$cm^3$*0.981g/$cm^3$*0.04 =0.985 g

II. Weight of matrix (7075 aluminum alloy) and reinforcement (silicon carbide, cerium di oxide and graphene oxide ) for sample two:-

Weight (in mass), $m_{7075Al}$= $V_T$ *$\rho_x$*y =31.4$cm^3$*2.81g/$cm^3$*0.81=71.469g

Weight (in mass), $m_{SiC,}$= $V_T$ *$\rho_x$*y =31.4$cm^3$*3.21 g/$cm^3$*0.075=7.559g

Weight (in mass), $m_{CeO_2,}$= $V_T$ *$\rho_x$*y =31.4$cm^3$*7.132g/$cm^3$*0.075 =16.795g

Weight (in mass), $m_{GO,}$= $V_T$ *$\rho_x$*y =31.4$cm^3$*0.981g/$cm^3$*0.04 =0.985 g

III. Weight of matrix (7075 aluminum alloy) and reinforcement (silicon carbide, cerium di oxide and graphene oxide ) for sample three:-

Weight (in mass), $m_{7075Al}$,= $V_T$ *$\rho_x$*y =31.4$cm^3$*2.81g/$cm^3$*0.81=71.469g

Weight (in mass), $m_{SiC,}$= $V_T$ *$\rho_x$*y =31.4$cm^3$*3.21 g/$cm^3$*0.05=5.039g

Weight (in mass), $m_{CeO_2,}$= $V_T$ *$\rho_x$*y =31.4$cm^3$*7.132g/$cm^3$*0.1 =22.394g

Weight (in mass), $m_{GO,}$= $V_T$ *$\rho_x$*y =31.4$cm^3$*0.981g/$cm^3$*0.04 =0.985 g

IV. Weight of 7075 for pure aluminum alloys

Weight (in mass), $m_{7075Al}$,= $V_T$ *$\rho_x$*y =31.4$cm^3$*2.81g/$cm^3$*0.81=71.469g

Total mass of matrix used was:-

$M_T$ For (7075 Al) = $m_{7075Al}$(S1+S2+S3+S4) = (71.469g)*4=285.876g

Total mass of reinforcement used was:-

$M_T$ For (SiC) = $m_{SiC,}$ (S1+S2+S3+S4) =5.039g +7.559g +10.079g +0=22.277g

$M_T$ For ($CeO_2$) = $m_{CeO_2,}$ (S1+S2+S3+S4)= 11.197g + 16.795g +22.394g g +0=50.386g

$M_T$ For (GO) = $m_{GO,}$ (S1+S2+S3+S4) = (0.985 g *3) +0=2.955g

Preparation of mold

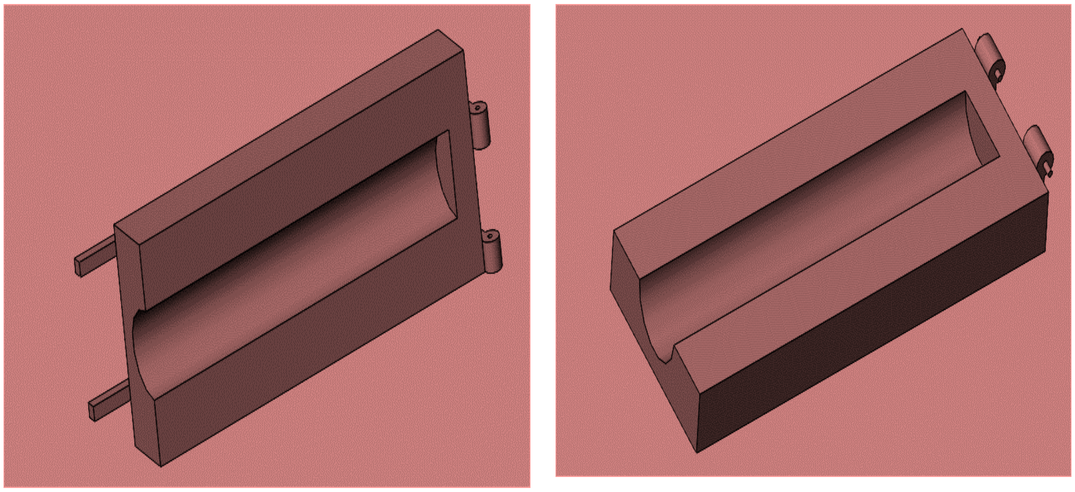

Figure 3.6 Mold model using solid work

### 3.3.7. Fabrication Composite Procedure

The fabrication of SiC, $CeO_2$ and GO -reinforced 7075 Al composite was performed based on the principle used for the stir-casting process. The melting of the matrix happened inside a casting furnace with a Graphite crucible attached to the inside part and a stirrer and motor connected to the above part. First of all, preheating of the furnace was performed with 400°C before introducing metal matrix into the furnace to maintain uniform temperature distribution, energy efficiency, thermal stress reduction, removing residual moisture and contamination. The temperature reading of the process was controlled by thermo couple which was connected to the furnace. Next, weighted matrix (71.469g Al7075 billets) was supplied into the graphite crucible for each casting and melting was kept up until uniform temperature of 700°C was achieved. The argon gas was used to prevent oxidation during melting process because Al7075 alloy contained small amount Mg. Thereafter, the molten metal was made to cool to 650°C to bring into semi-solid-state. Next carefully measured SiC, $CeO_2$ and GO - nano-sized powders were blended by ball milling and preheated at 350 °C for 10 minutes for each sample to, remove moisture content and thermal shock, and for good bonding (Gosavi & Jaybhaye, 2021). After that, a measured and preheated mixture of reinforcement was gradually assimilated into the semi-solid matrix at 650°C pouring temperature while maintaining continuous steering of solution by three bladed stainless steel stirrers (mechanical stirring process) which were set to revolve with average 650 rpms stirring speed for 15 minutes to achieve even dispersion of reinforcement. Reheating of the mixture was continued again until the temperature reading reach 700°C to its liquefied state then the slag is extracted. Later the slag free molten form of SiC, $CeO_2$and GO - nano-sized powders reinforced Al 7075 metal matrix composite was poured into the pre heated(350°C) permanent mold made from iron. Finally cylindrical shaped composite that was solidified at room temperature were extracted from the mold. Generally the above process was employed for all of three samples.

Table 3.10 Fabrication process parameters

| Process | Amount |
|---|---|
| preheating of the furnace | 400°C |
| weighted matrix | 71.469g |
| Melting matrix | 700°C |
| Prevent oxidation | argon gas |
| Semi-solid-state. | 650°C |
| ball milling and preheated | 350 °C for 10 minutes |
| of reinforcement | |
| pouring temperature | 650°C |
| stirring speed | 650 rpms stirring speed for 10 minutes |
| Reheating | 700°C |
| pre heated of mold | 350°C) |

7075 aluminum bar

Chopped bar of 7075 aluminum bar

Measuring the chopped aluminum bar

Measuring the reinforcement weight

Heating of the furnace

Stir cast melting of bar

Figure 3.7 Procedures used for fabrication of hybrid Composite

### 3.3.8. Samples preparation for test

The Fabricated composite samples may have same surface contaminants like dust, particle, lubricants, Oxide Layers, and Contamination from Handling etc. This contamination may cause the in accuracy and in reliability on the test results and need to be removed carefully. Following the flourish fabrication process, the fabricated samples were made clean and in to proper size as ASTM standards for mechanical, physical, Microstructural characterization and tribological test by cutting, grinding, polishing, and etching. This is done to ice the compatibility of samples within the testing machine as well as accuracy and solidness of the result will achieve.

#### 3.3.8.1. Machine and cutting

The surfaces of fabricated sample surfaces were rough and had some slug components on them. To obtain the shape and size required by get rid of undesired parts as well reduce surface roughness; machining on lath accordance to ASTM standards was performed.

| | | |
|---|---|---|
|  |  |  |
| Putting sample on lathe machine | Measure the sample size | Machined sample |

Figure 3.8 Machine and cutting process performed of the developed composite

#### 3.3.8.2. Sectioning

Sectioning is a process of cutting the sample in small and thinner sections to reveal internal part of the sample so that it is easier to examine the region of interest. Sectioning were performed on fabricated reinforced Al7075 composite samples using abrasive cutter as well as hand saw and file to minimize the size of samples as per needed standard. The abrasive cutter work with high speed rotating blade and distilled water cooling system was used to section the fabricated samples as show in figure below.

Figure 3.9 Sectioning of developed composite sample

#### 3.3.8.3. Grinding

Grinding is a process of removing unwanted material or flatting the surface of the samples after sectioning process. The scratch formed on the surface of fabricated Al 7075 composites during grinding process was gradual grinded or removed from the surface using 220, 800, 1200 and 2000 silicon carbide sand papers (from coarse to fine grades). 90 degree from preceding direction of grinding orientation was used to remove the scratch from the surface.

Figure 3.10 The grinding process performed on fabricated composite

#### 3.3.8.4. Polishing

Polishing is the process performed on the surface of the samples by using progressively finer abrasives to eliminate the abrasions, imperfections and roughness that were left behind during grinding process. These processes polish the sample surface and make it more smooth, reflective, and imperfection-free. The fabricated aluminum composite was polished after grinding process using diamond suspension that have two sand wheel rotation at speed using the RB 204 Metpol-II. During the process the speed was made to reduce gradual to keep the material from plastic region deformation.

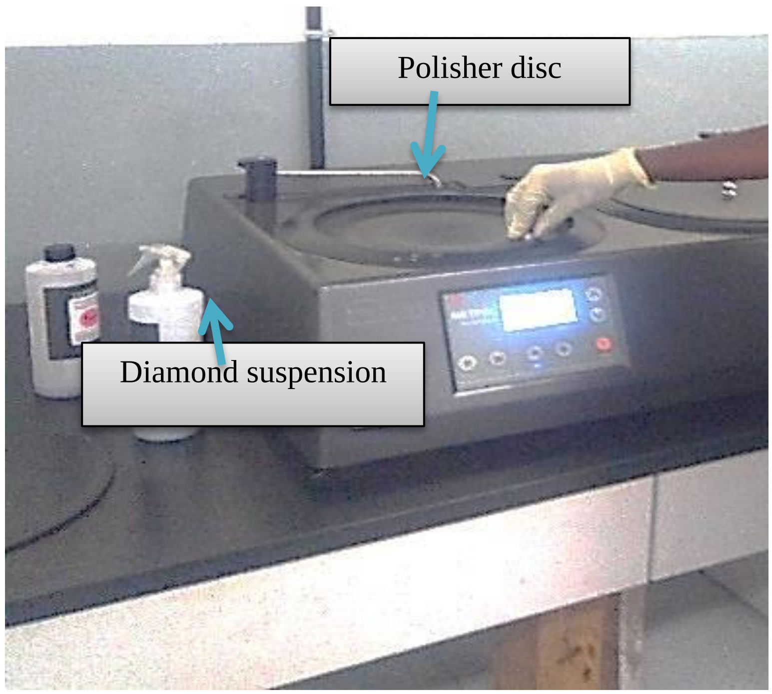


Figure 3.11 Polishing of developed on diamond suspension

#### 3.3.8.5. Etching

Chemical etching is a process performed using particular etchant solution selectively eliminating material from the surface whereas leaving the reinforcement unharmed. Etching was performed on fabricated sample before performing microstructures test. The etchant with 82 ml distilled water chemical 10 ml HCl, 8 ml $HNO_3$ and as well their combination was select based on the behavior of the matrix and reinforcement (Kumar & Shiva, 2022).

Select an appropriate etchant

Dissolving etchant solution

Holding the sample

The chemical selected to the fabricated sample was hydrochloric acid (HCl) and nitric acid ($HNO_3$) ethanol and distilled water.

Putting sample into etchant

Rinse and clean the sample

Figure 3.12 Etching performed on developed composite

Table 3.11 General operation performed on the developed composite to it prepare for test

| Process | Key |
|---|---|
| Machining and cutting | Lath machine |
| Sectioning | abrasive cutter |
| Grinding | 220, 800, 1200 and 2000 silicon carbide sand papers |
| Polishing | diamond suspension |
| Etching | 10ml HCl, 8 ml $HNO_3$ |

## 3.4.Characterization of Microstructures

Microstructural examination is a process used to study the behavior of material at microscopic level and to relate it with macroscopic behavior of material. Microstructural examination using XRD(X- Ray Diffraction),OM(optical) and SEM (Scanning Electron microscope) test was performed on stir casting fabricated SiC, $CeO_2$ ,and GO- 7075 Al composites to know the distribution of reinforcements, Grain size ,types of constituent phase occurrences, porosity as well the interaction between reinforcements and matrix. From the above tests, it is also possible to have better understanding of the mechanical behaviors of specimen: like hardness, strength and wear.

### 3.4.1. X-ray Diffractometer (XRD) characterization

XRD is the method uses X-ray beam from the source into crystal lattice sample in specific target to analyze the phase and crystallographic arrangement of the samples. The detector records the intensity of X-ray beams scatted back in different direction after strike the crystal lattice of the sample as a function of the diffraction angle. The recorded pattern is interpreted through mathematical methods.

#### 3.4.1.1. Phases analysis stir casted composite

The different crystal structures with the stir casting fabricated SiC, $CeO_2$, and GO reinforced 7075 aluminum composite as well the element that form this crystal was studied using the XRD testing instrument called XRD 7000 maxima(XRD, of ASTU). The Phases of the samples was also analyzed by using Cu-Kα (1.5406Å wavelength) radiation that was generated by using voltage of 40 KV and current of 30 mA. In this process at scan rate of 3° per minute 2θ scattering angle is covered with the range of 10° to 80°.

#### 3.4.1.2. XRD peak Analysis

Peaks means in this context, it is a high points with its own intensity ( for phase abundance) and shape ( for crystalline quality) and represent specific crystal structure at that data position( for lattice parameters) (Himabindu et al., 2021). The process used to study the diffraction peak found from X-ray diffraction (XRD) shape is known as XRD peak analysis. This analysis is very important to have better understanding of crystallography, materials characterization, and phase composition**.** To analysis the XRD peaks of fabricated aluminum composite Gauss method was used. The following equation was used for the above investigation.

$$D\ (\mu m) = \frac{K\lambda}{\beta\cos\theta} \qquad (3.3)$$

Where: D is crystal size

$\lambda$ : is the wave length of incident radiation

$\beta$: is order of the diffraction

K: is shape factor

$\theta$ : Braggs angle in degree

The dislocation density is defined as the defects in the sample and is defined as the number of dislocations within a unit volume of the crystalline material (Rai et al., 2023). Dislocations, which are line defects that result from a mismatch or misalignment of the crystal lattice planes, are important for understanding the mechanical characteristics and behavior of materials. Diffraction peaks broaden as a result of local lattice strain caused on by dislocations within a crystal.

$$\delta = \frac{1}{D^2} \qquad (3.4)$$

Where $\delta$ = dislocation density in $nm^{-2}$

$D^2$ = crystallite size of the particles

The existence of defects (such dislocations or vacancies), thermal expansion or contraction, mechanical stress or deformation, or the introduction of impurity atoms into the crystal lattice are some of the causes of lattice strain (Sahoo & Panigrahi, 2021).

$$\varepsilon = \frac{\boldsymbol{\beta}}{4\tan\theta} \qquad (3.5)$$

Where $\boldsymbol{\varepsilon}$ =lattice strain

### 3.4.2. Optical Microscopy (OM) characterization

Microstructure analysis using optical microscopy is a technique uses visible light to examination the microstructure and surface structures of the sample. This technique was employed to examine the metallurgical characteristic of SiC, $CeO_2$ and GO reinforced 7075Al composite using Huvitz HR-300. To perform the test: the samples were prepared to7mm height by 18mm diameter size then grinded with 220, 800, 1200 and 2000 silicon carbide sand papers, further polished by diamond suspension on a two-wheel system RB 204 Metpol-II model polishing instrument and etched via Keller's chemical etchants to acquire smooth surfaces. Well smoothed and etched samples were subjected to low magnification to observe the macroscopic defect such as crack then the magnification was made to increase to examine the distribution of Sic, $CeO_2$ and GO reinforcement with in the matrix as well the phase boundary and grain structure. The image were captured and analyzed.

### 3.4.3. Scanning Electron Microscope (SEM) characterization

SEM analysis is a method that uses a microscope that emits a beam of electron to detect the microstructure future of a sample. This machine (by FT-IR spectrometer in the range of 4000-400 cm-1 Ft/IR-6600 type A )was used to detect and analysis the microstructure and surface characteristics of SiC, $CeO_2$and GO reinforced 7075Al composites ;before and after the wear and compression tests to have better understanding of durability and reliability of the samples. Before perfoming the test ,The samples were made to proper size and polished well.Then the SEM investigation were perform on fabricated samples before and after wear and compression test. The image formed due to the electron beam that was scanned accross the surface of fabricated samples were cuptured using camera on device to study the change in future of surface due to the tests.

## 3.5. Density and porosity measurement and calculation

### 3.5.1. Density of fabricated hybrid composite

Experimental density is knows us the density of an object determined through direct experiments or measurements. The value of experimental density is obtained by measuring the mass and volume of the material and then the ratio of mass to volume of each material is calculated. The mass and volume of the fabricated composite samples were measured on analysis precision balance with a tolerance of 0.0001 to calculate the experimental density. During the calculation process density of the each individual component was taken into account. The theoretical density of composite was calculated according to the following equation (Alaneme & Odoni, 2016).

$$\rho_{theo} = (\rho_{mat} * V_{mat}) + (\rho_{rein} * V_{rein}) \quad (3.\ 6)$$

Where $V_{rein}$ *and* $V_{mat}$ are represent volume fraction (weight percentage) of reinforcement and matrix respectively. $\rho_{theo}$, $\rho_{rein}$ *and* $\rho_{rein}$ is represent density of theoretical, reinforcement and matrix composite respectively. Procedure to test density;-

A. Experimental or actual density for the Al7075 / SiC, $CeO_2$and GO hybrid composite was calculated using Archimedes principles. First off ,the mass of the casted samples in the air was measured using analytical precision balance then the mass of the samples in distilled water was measured by suspected the sample in the water.

The experimental density of the casted samples was measured using the following equation (3.4) (Venugopal & Karikalan, 2021)

$$\rho_{atual} = \frac{M_{air}}{M_{air} - M_{water}} * \rho_w \quad (3.\ 7)$$

Where, $M_{water}$ =mass of casted sample in the measured in distilled water, $M_{air}$ =mass of casted sample in measure in air, $\rho_w$=density of the distilled water 25℃ 1 g/cm$^3$.

Figure 3.13 Measuring the mass of developed composite using Analytical precision balance

### 3.5.2. Calculating Porosity for fabricated hybrid composite

Porosity is physical property of material that measures the amount of small opening or void inside a material. The porosity in material is caused due to air bubbles formation during the manufacturing (stirring) or during pouring into the mold. The material contain porosity has a probability to absorb moisture or liquid then affected by corrosion To have a material with good mechanical properties the amount, size, and distribution of the porosity should be minimize and controlled. The porosity of fabricated samples was measured using Archimedes' method equation (3.5) (Venugopal & Karikalan, 2021).

$$P=\frac{\rho_{th}-\rho_{act}}{\rho_{th}} \tag{3. 8}$$

Where, P= the porosity of the fabricated sample, $\rho_{th}$=the theoretical density fabricated composite sample, $\rho_{act}$=the actual density of the fabricated composite sample.Density of aluminum (Al7075) =2.81 g/cm$^3$, Density of silicon carbide (SiC) =3.21 g/cm$^3$, Density of ($CeO_2$) =7.132 g/cm$^3$, and Density of graphene oxide (GO) =0.981 g/cm$^3$.

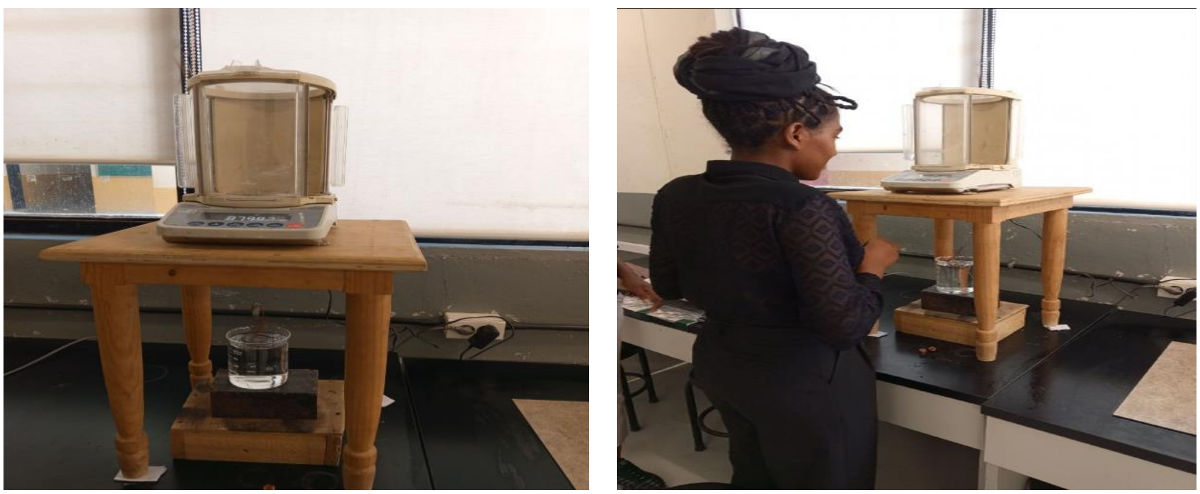

Figure 3.14 Measuring the mass of developed composite in the air and in the water

### 3.6. Hardness test

Hardness is a measure of the ability of a material's resistance or withstands external force such as scratching, indentation, penetration or deformation applied to its surface without undergoing permanent damage. The hardness of the fabricated reinforced aluminum 7075 composite was tested on Vickers hardness test machine to evaluate the fitness of fabricated composites to the specified engineering applications. The Vickers hardness test (HVS-50) employed has square base pyramid diamond indenter with an angle of 136 among opposite faces at the vertex. Cylindrical sample Length =7 mm, Diameter =18mm was employed to perform the test according to ASTM E3-95 using Vickers Hardness test (HVS-50). The 10 kgf load was applied to the face of composite sample for average time of 10 second to test the hardness of the material according to ASTM E384-17. A load of 10 kgf for 10 seconds was applied at different positions three times to calculate an average value the hardness.

$$HV=0.102\times 2F\,[\sin\frac{\mathbf{136^{\circ}}}{\mathbf{2}}]/d^2 \qquad (3.\ 9)$$

Where, HV=the Vickers hardness value (kgf /$mm^2$ ), F=the subject force (kgf), d= surface area indentation ($d_1$ &$d_2$) in mm. In addition, the percentage of improvement in hardness of the materials which in turn means properties was calculated using the equation below.

$$\text{Improvement (\%)} = \frac{\text{New}(X_o)\text{-original}(X_i)}{\text{Original}(X_i)} \times 100 \qquad (3.\ 10)$$

Where, $X_o$ is the original hardness of pure alloy whereas ($X_i$) is the average hardness of the fabricated samples.


Figure 3.15 Measuring the hardness developed composite

### 3.7. Wear test

The wear test is the test performed on material to assess the durability and performance of product under normal use. The dry wear test was performed on SiC, $CeO_2$ ,and GO reinforced 7075 Al composite on computerized micro pin –on-disc tribometer TR-20MICRO wear tester machine found in Addis Abeba science and Technology University. To perform test the following steps was used. First, the fabricated samples were made to size of 5.9 mm diameter and 12 mm length as per ASTM G99 standard and the samples surfaces that came in contact during the test was also made clean as needed. Then, the wear test parameters such as load

(30), wear track diameter (50 mm), time duration (10 min), and sliding distance (500mm) were selected according literature and material properties. After that, the mass of the samples before performing the test were measured and recorded to calculate the mass loss that was occur during the test. Subsequently, the test was performed and data related to wear rate, friction coefficient, sliding rate of the samples were carefully recorded. Finally, the mass after the test was taken as well the surfaces of the samples after the test were analyzed using SEM to assess wear profile and the surface damage. Coefficient of friction can be calculate using Archard's law (Samal et al., 2020).

$$\text{Volume loss (mm}^3\text{)} = \frac{\text{Initial mass in gram-Final mass in gram}}{\text{Density (g/mm}^3\text{)}} \text{x}100 \quad (3.\ 11)$$

$$\text{Wear rate (mm}^3\text{/mm)} = \left(\frac{\text{Volume loss}}{\text{Sliding distance}}\right) \times 100 \quad (3.\ 12)$$

$$\text{Coefficient of friction (COF)} = \frac{\text{Volume loss} \times \text{Hardenessof the material}}{\text{Applied load} \times \text{Sliding distance}} \quad (3.\ 13)$$

Figure 3.16 Testing of the wear resistance of developed composite material

**3.8. Compression strength test**

A compression test is a common mechanical test used to determine the compressive strength and behavior of a material. It involves applying a compressive load or force to a test specimen and measuring its response to the applied load .Compression test was performed on reinforced 7075 aluminum metal matrix composite. The apparatus used to perform the test was universal testing machine (UTM), and vernier caliper also used to measure length and diameter before and after the test. Three cylindrical shaped spacemen of 8 mm diameter to 10 mm length was prepared using lathe machine According to ASTM E-9 standard. The length of the spacemen was measured using the vernier caliper and grinded by 220 sand papers to make sure that the proper size is used. The proper diameter to length sized spacemen was kept at the center of the cross cell so that uniform loading can be assured to the spacemen. Then movable cross cell is used for Appling load and lower slowly until it touch the spacemen. Load is applied gradually by opening the valve and pressing start button until space start to fail. The Extensometers reading give the change in length of the spacemen due to compression load. Once the elastic region is reached spacemen start to burgle out, pointer stop for a moment and then start to move backward direction. The compression was performed on the prepared sample using progressive loads until 50KN.the load was applied until specimen fracture or deform completely.

Before compression test

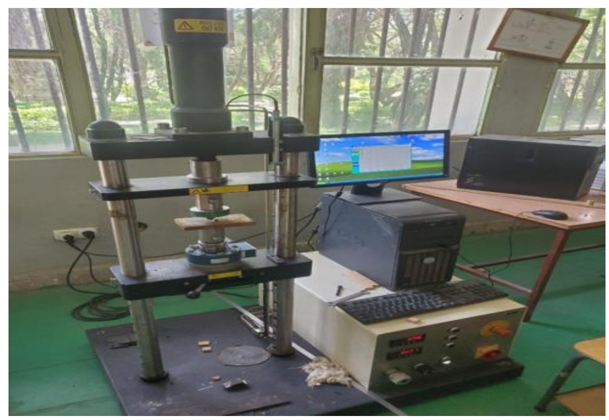

Mounting the sample

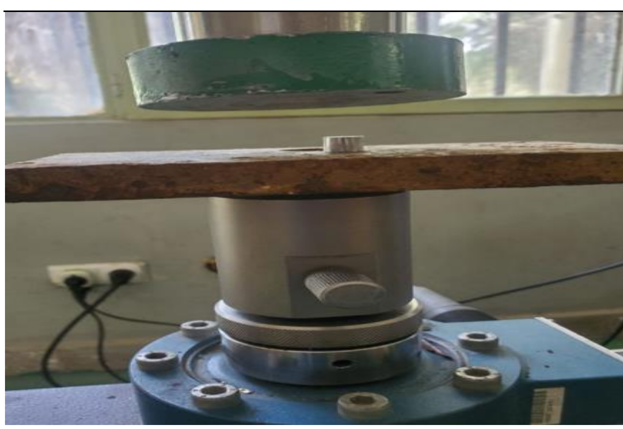

Prepare for Compression

After compression

Figure 3.17 Procedure used to test the compression strength of developed composite

### 3.9. Testing of corrosion resistance behavior of developed composite

Corrosion test is the test performed on fabricated samples to evaluate the performance and duration of specimen in harsh environments without degradation for intended application. Corrosion tests were performed on the fabricated sample to investigate the effect of weight percentage of reinforcement on corrosion resistance material. To perform the above test , the sample with 15mm diameter and 4mm length was prepared and polished with 220,800,1200, and 200 SiC  sand paper to remove un wanted scratch  from the surface of specimen. Then diamond post with double disk polishing machine was used to remove left over material on the surface that is impossible to remove by different grade of sand paper. Finally, the well prepared samples were immersed in 3% NaCl solution for 30 minutes. (Sambathkumar et al., 2017) Electrochemical analyzer (SP300EC) was utilized to do the corrosion test. TAFEL plots is the effective and easy method used to analysis the electrochemical properties of material (Olani et al., 2023).Tafel curves were produced by adjusting potential volt range of -250mV catholically and +250Mv anodically verses corrosion potential (Ecorr) at scan rate of 1mV/s.

$$\text{Corrosion rate (CR)} = 0.13 Icorr. \left(\frac{\mathrm{Ew}}{\mathrm{d}}\right) \tag{3. 14}$$

Where, $Icorr$= the corrosion rate, $Ew$=Equivalent weight of specimen in (g), and d= Density of materials (g/$cm^3$). Corrosion rate in measurement was calculated by using formula.

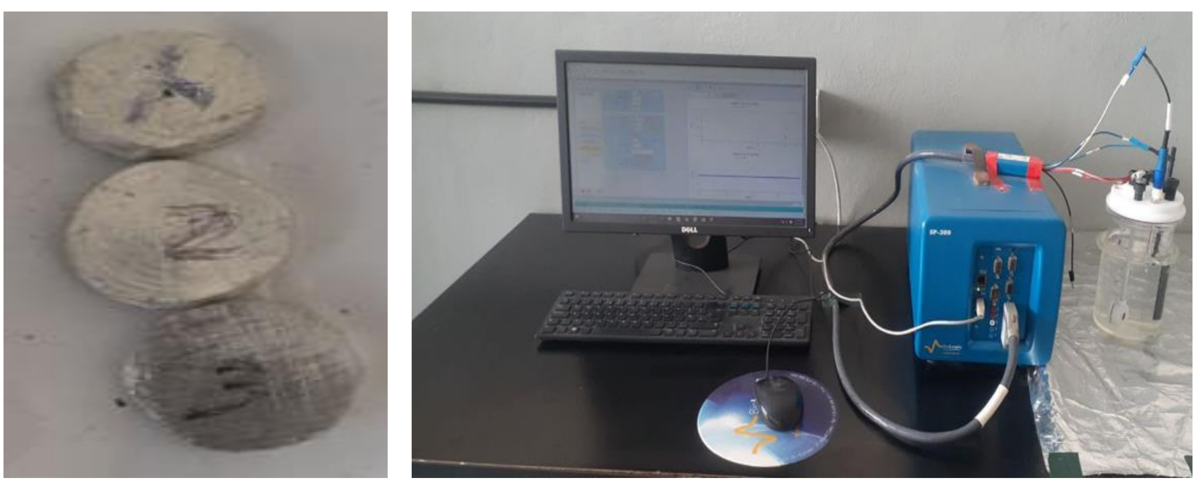

Figure 3.18 Corrosion on developed composite in 3%NaCl Electrochemical Analyzer

### 3.10. Sample selection by Signal- to noise ratio(S/N)

Signal-to-noise ratio (SNR or S/N) is used measure the quality of a signal relative to the background noise. It is defined as the ratio of the mean to the standard deviation of the output. S/N ratio has performance characteristics expressed as lower-the-better, nominal- the –better and higher -the –better. The mean response of the experimental data was evaluated by transforming the output data into S/N ratio. The S/N ratio represents a measure of quality features and is calculated as follows for three condition of performance characteristic (N S & AS, 2019).

Condition 1: Larger - the- better

$$\frac{S}{N} = -10\log_{10}\left(\frac{1}{n}\right)\sum_{1}^{n}\frac{1}{Yij^2} \qquad (3.\ 15)$$

Where: n is the number of replications, $Yij^2$ observation response value for i =1, 2, 3…n and j=1, 2, 3…m, this equation is applied where maximization of the quality is point of interest. It is referred to the larger -the –better type of the problem.

Condition 2.Nominal –the- better

$$\frac{S}{N} = 10\log_{10}\frac{\mu^2}{\sigma^2} \qquad (3.\ 16)$$

Where $\mu = \frac{y_1+y_2+y_3+\cdots+y_n}{n}$ and $\sigma^2 = \sum_{i}^{n-1}\frac{(yi-y)^2}{n-1}$ is suitable for normalizing problem.

Condition 3: Smaller –the-better

$$\frac{\mathbf{S}}{\mathbf{N}} = -10\log_{10}\left(\frac{1}{n}\sum_{1}^{n}Yij^2\right) \qquad (3.\ 17)$$

Where: n is the number of replications, ${Y_{ij}}^2$is the observation response value

The extruded effect would be minimized for quality product. In this paper, since damage, effective stress and load have to be minimized the smaller-the-better characteristic was selected to yield the optimum results. Thus, the S/N ratio condition was expressed in the logarithmic transformation of the loss function.

### 3.11. Analysis of variance (ANOVA)

ANOVA is a standard statistical technique that is used to analyze experimental data. It was used to determine which parameters have a significant influence on the quality attribute. It also used to determine the influence of all control parameters using idea of percentage contribution. The Percent contribution measure associated influence of each control parameter on the performance characteristic of results in the analysis of variance. This analysis used a significance level of 5%, corresponding to a 95% level of confidence. Based on its statistical findings, it is determined that the existence or absence of significant variation in the output. The significance value in the ANOVA is the P value. The P value is the probability of obtaining F value, accepting the null hypothesis. Subsequently compering P value with significance level which is $\alpha(0.05)$ then decided ANOVA as significant when p is less than 0.5 and as insignificant for above 0.5 values.

### 3.11.1. Sample selection using Grey Relation Analysis

Multi objective optimization is a mathematical optimization approach that involves simultaneously optimizing multiple objective functions. The complex relationships between various parameters and objectives, and make informed decisions that optimize the overall performance of the extrusion process while balancing the trade-offs between competing goals was also explore by this approach. This optimization approach was used in this work to analysis; the interaction of responses, the combine effect of input extrusion parameters on the responses and to find the global value. Procedure used in the process for selection of fabricated reinforced aluminum metal matrix composites sample for defining the new material in the 3D deform software was listed down:

**Step 1:** Based on the type of quality characteristic, transform original response data to S/N ratio using related formula stated.

**Step 2:** Normalize the data to minimize variability and the effect of using numerous units to make comparability easy. Normalize using $Y_{ij}$ as $Z_{ij}(0\_Z_{ij}\_1)$ where, $Z_{ij}$ represents the normalized for ith experimental/trial and the jth dependent variable/response. For normalizing S/N ratio with larger-the-better performance characteristic and small-the-better the following equation is used respectively.

$$Z_{ij} = \frac{\text{Yij-Ymin}}{\text{Ymax-Ymin}} \tag{3. 18}$$

$$Z_{ij} = \frac{\text{Ymax-Yij}}{\text{Ymax-Ymin}} \tag{3. 19 }$$

**Step 3:** Determine grey relational coefficient (GRC) for normalized S/N ratio values.

$$\mathrm{GRC_{ij}} = \frac{\Delta_{\min} + \delta\Delta\max}{\Delta ij_{ij} + \delta\Delta\max} \tag{3. 20}$$

Where i=1,2,3…,n is number of experiments and j=1,2,3,…,m is the responses.

$GRC_{ij}$ =GRC for ith trial,$\Delta$=absolute difference between $Y_{oj}$ and $Y_{ij}$ ,$\Delta_{max}$=maximum value of $\Delta$,$\Delta_{min}$=minimum value of $\Delta$,$\delta$=is the distinguishing coefficient ($0 \leq \delta \leq 1$)

$Y_{0j}$=optimum performance value or the ideal normalized value of jth response

$Y_{ij}$=the ith normalized value of jth response/dependent variable $\Delta$

**Step 4:** calculate the grey analysis grade ($GRGi$)

$$\mathrm{GRGi} = \frac{1}{\mathrm{m}} \sum \mathrm{GRCi} \tag{3. 21}$$

Where m is the number of responses

### 3.12. Secondary operation

Secondary operation contain the following main parts

- ✓ Identifying the input extrusion parameter and response
- ✓ input extrusion parameter and response was combine by box behnken inside design expert
- ✓ Input the combined extrusion parameter into the 3D-deform software to find the response value
- ✓ Use design-expert then box-behnken again to check the significant of the result
- ✓ If the result is significant use mat lab to find optimum point for the extrusion.

#### 3.12.1. Identify parameters and its level for extrusion

In this research, the effect of deforming process parameter (extrusion speed, extrusion ration and extrusion temperature) three different levels and optimum process parameter on the deforming rate will be analyzed and identified. The parameter that can describe the response behavior during deformation very well was choosing.

Table 3.12 Selected extrusion parameter of developed composite (Kumar et al., 2019)

| Parameters | Units | Levels | | | Response |
|---|---|---|---|---|---|
| | | 1 | 2 | 3 | Damage, load, and effective stress |
| Extrusion ratio | mm/s | 6 | 8 | 10 | |
| Ram speed | - | 2.5 | 3 | 3.5 | |
| Billet temperature | ℃ | 185 | 225 | 265 | |

### 3.12.2. Experimental design

The design of experiments (DOE) is a system used to carry modeling and analysis of the effect of input parameter on the response. The experimental design for cold extrusion was performed based on the properties and size of fabricates samples. From extrusion parameters: based on their effect on the process, extrusion speed, extrusion ratio and extrusion temperature were selected as extrusion process parameters. Die length of 20 mm and mesh size of 80,000 for work piece, 70,000 for each die was used. The effect of these parameters on the on damage, stress and required load for extrusion was investigated utilizing multi objective optimization using mat lab 21 software to perform the GRA.

### 3.12.3. Simulation Procedure – DEFORMTM- 3D

DEFORMTM-3D V-11 software was used to run FEM simulations process. Finite element modeling of cold extrusion process to determine, punch load, strain stress distribution, material flow and other parameter is very important procedure that helps to acquire essential information needed to perform the fabrication process. The above model was used to generate the cold extrusion process of Al7075/SiC, $CeO_2$, and GO using DEFORM-3DV11 software. CATIA software was used to model the work piece, top die, bottom die and holder. STL format of the models was then transferred to the DEFORM-3D. DEFORM-3D has three levels below to perform the simulation fully (Sifakis & Barbič, 2022).

- Preprocessor level
- Simulation engine level

- Post –processor level

**Preprocessors level: -** it is the stage used to create and input the necessary data base file into the system before initiating the simulation process. Under preprocessing stage, geometry modeling, geometry discretize, define the border condition, preloading, and mess modification operations was performed.

Stress equilibrium balance equation:-

$\sigma_{ij,j}=0$

Where, $\sigma_{ij,j}$= the stress at the boundary surface

**Boundary equation:-**

$\sigma_{ij}=F_j$ , $u_i = U_i$

Where, $F_j$ =the force on border surface, $\sigma_{ij}$=stress on the border surface, $U_i$ =deformation velocity at on the border surface

Compatibility with incompressibility condition:-

$$\dot{\varepsilon}=\frac{1}{2}(u_{i,j}+u_{ji}) \qquad \varepsilon_v=u_{i,j}=0 \tag{3. 22}$$

Where, $\dot{\varepsilon}$= the strain rate at the border

**Constitutive equations:-**

$$\sigma'_{i,j}=\frac{2\bar{\sigma}}{3\dot{\bar{\varepsilon}}}\dot{\varepsilon}_{i,j} \qquad \bar{\sigma}=\sqrt{\frac{3}{2}(\sigma_{i,j}\ \sigma_{j,i})} \qquad \bar{\varepsilon}=\sqrt{\frac{3}{2}(\dot{\varepsilon}_{i,j}\varepsilon_{ji})} \tag{3. 23}$$

Where, $\bar{\sigma}$=the effective stress, $\bar{\varepsilon}$ =the effective strain, $\dot{\bar{\varepsilon}}$ =the effective strain rate $\dot{\varepsilon}_{i,j}$= strain rate, the weak form of rigid plastic equation can be obtain.

$$\int_{v}^{-}\varepsilon\delta\bar{\varepsilon}dV+K\int_{V}^{-}\varepsilon_v\delta\varepsilon_v dV-\int_{SF}^{-}F_i\delta u_i dS=0 \tag{3. 24 }$$

Where, s=the surface area of sample=the surface volume of the sample being examine, is the penalty constant.Defining the fabricated material was performed based on compression test result for simulation. Only the work piece's flow stress should be specified when using DEFORM 3D software to solve an isothermal forming problem involving rigid dies and rigid-plastic work piece. Flow stress expressed by Hollomon's equation (Hao et al., 2017).

$$\overline{\sigma}=k\dot{\varepsilon}^{n} \tag{3. 25 }$$

Where, $\bar{\sigma}$ is flow stress, $\dot{\varepsilon}$ is true strain; K is material constant and n is strain hardening constant. At temperatures below the recrystallization temperature, the strain rate mostly determines the flow stress.

$$\overline{\sigma} =C\dot{\varepsilon}^{n} \tag{3. 26}$$

Power law used as constitutive equation to determine flow stress for simulation of aluminum composite developed during cold deformation.(Jain et al., 2017) The values of parameter used to define the fabricated material properties were inputted into 3Ddeform software through power law equation found in 3Ddeform software**.**

$$\overline{\sigma}=C\overline{\varepsilon}^{n}\dot{\overline{\varepsilon}}^{m}+y \tag{3. 27}$$

Depend on the above equation the fabricated material was defined. Where, n is strain exponent, m is strain rate exponent, C is material constant and y represented initial yield value. During a compression test, the initial yield stress is determined using the stress-strain curve. The boundary between elastic and plastic behavior is known as the yield stress.

$$\varepsilon = \log(1+e) \tag{3. 28}$$

Where, ε is true strain

$$\overline{\sigma} = S(1+e) \tag{3. 29}$$

Where, σ is true stress, e is engineering strain and S is engineering stress. The metal's behavior throughout the forming process is determined by the strain hardening exponent (n). Stain hardening exponent and strain rate exponent is calculated by below equation.

$$n=\frac{d\log(\sigma)}{d\log(\varepsilon)} \tag{3. 30}$$

$$m=\frac{d\log(\sigma)}{d\log(\dot{\overline{\varepsilon}})} \tag{3. 31}$$

$\log(\sigma) = \log(k) + n\log(\varepsilon)$

K is Strength coefficient

Material defining using the 3D-deform

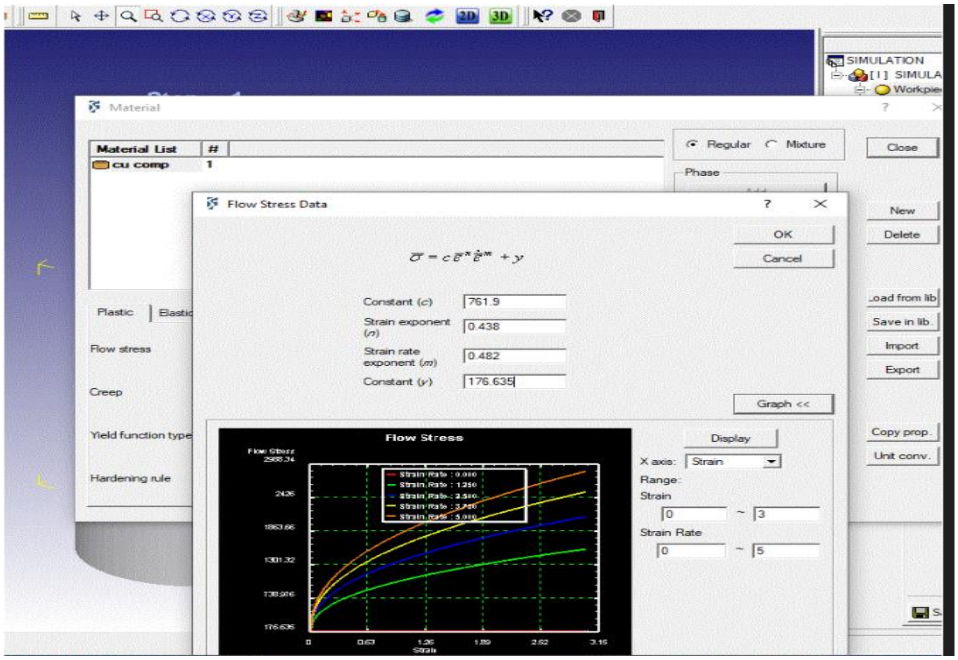


Figure 3.19 Material defining and meshed parts in preprocessors level

Meshed workpies Holder Top die Bottom die

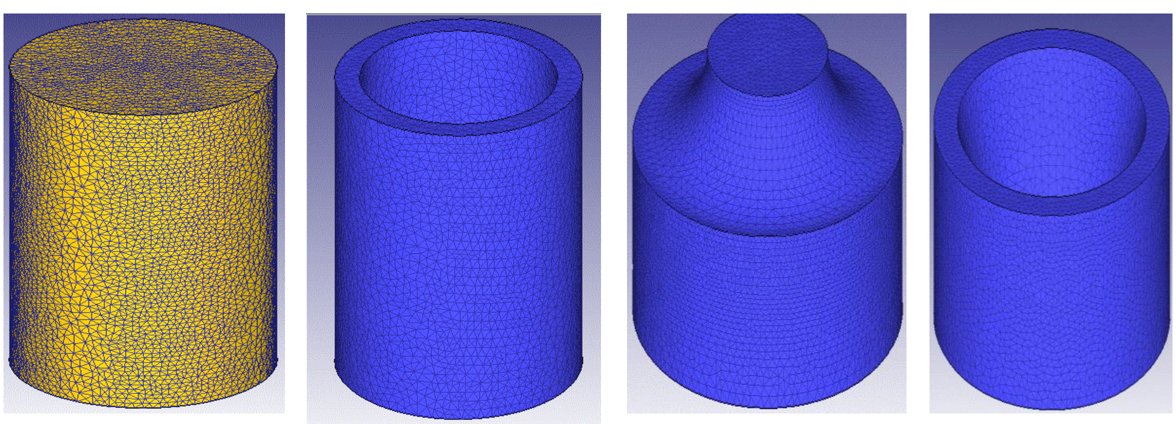

Figure 3.20 The meshed part of work pies, holder, top die and bottom

**Simulation engine level**:-it is the frame work that performs actual numerical analysis and simulation based on the input parameters. It communicates with different parts of the software like automatic mesh generation, message, and log file system to build a new mesh and writes status information of the work piece, while it is running. Algorithm and numerical methods were used to define the leading equation that was used to evaluating the deformation conduct of the material being simulated.

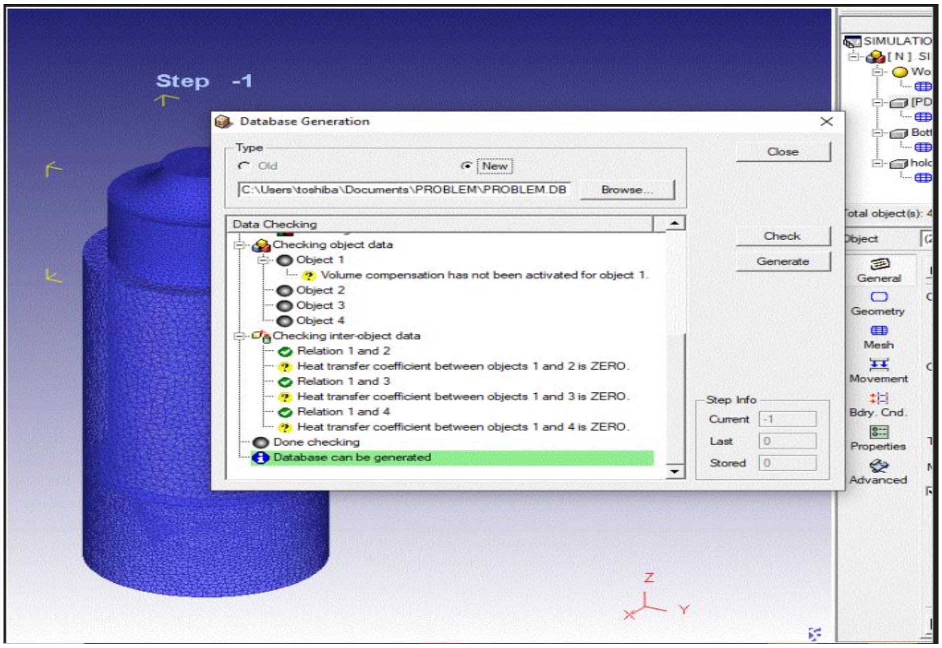


Figure 3.21 Data base generation stage in Simulation engine level

**Post processor level**: - it the level used after simulation engine stage is completed to analysis the result of simulation. This stage used to provide the meaningfully information about the result obtain from simulation stage and interpret it. The result extracted from simulation engine stage is used as input for post processing process. Under this stage data import, manipulation, visualization, analysis, and comparisons were performed.  The following equations were used to analysis the rigid-plastic behavior.

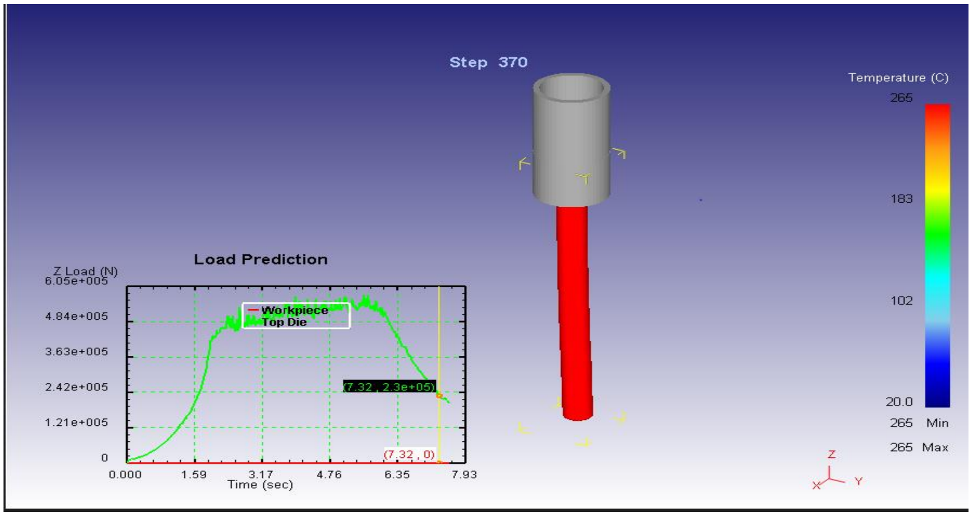


Figure 3.22 Response in post processor

#### 3.12.4. Multi-objective Optimization of Process Parameters Using GA

Genetic algorithm is techniques that generate solutions to multi-objective optimization problems by using equation extracted from design of expert into MATLAB. Genetic algorithms contain natural evolution such as Inheritance, mutation, selection, and crossover. The main objective of introducing a Genetic Algorithm (GA) in this work was to optimize the extrusion process parameters to obtain the low value of damage, load and effective stress for better surface finish.

### 3.13. Real deformation process

#### 3.13.1. Design and Fabrication of die for deforming

Die profile an important to guiding the flow of material by applied force/load through ram in hot extrusion process. Flow of material in extrusion process is directly influenced by die profile and friction condition between ram and work piece or billet, profile angle like: stream line die, cosine die. Cosine die selected because of enables greater flexible of design and improved material flow with reduced defects, reduced distortion of the final extruded shape(Huang et al., 2019). Cosines die to help minimize the residual stress within the extruded material which improves quality and performance the final product. The load requirement for the deformation process was determined by using a cosine die with the punch, billet, and container, and the geometry was designed by solid work software. After designed cosine die selected material AH13 die steel stock material was found in Addis Ababa from MIDI and made through machining process. The hydraulic press was pressed by the applied load, resulting in an optimal value and die fabrication based on the extrusion ratio.

Figure 3.23 Die design and fabrication

### 3.13.2. Cold extrusion of developed composite

The Cold deformation (cold extrusion) was performed on fabricated composite to improve the properties of the casted sample further. The operation was performed based on the optimum extrusion parameter (extrusion ratio, ram speed, and extrusion temperature). To reduce friction force SiC, $CeO_2$ and GO reinforced 7075Al composite was pre heated to 263.6537℃ as well solid lubricant graphite powders together with semi-solid lubricant grease used. Then the pre heated casted billet (with temperature below recrystallization) was extruded using 10.074(KN) and ram speed 2.5m/s and extrusion ration 6:1. SiC, CeO2 GO reinforced7075Al composite was extruded to from 20mm to 8.15 mm through cold extrusion.

.Figure 3.24 Cold deforming using hydraulic pressure

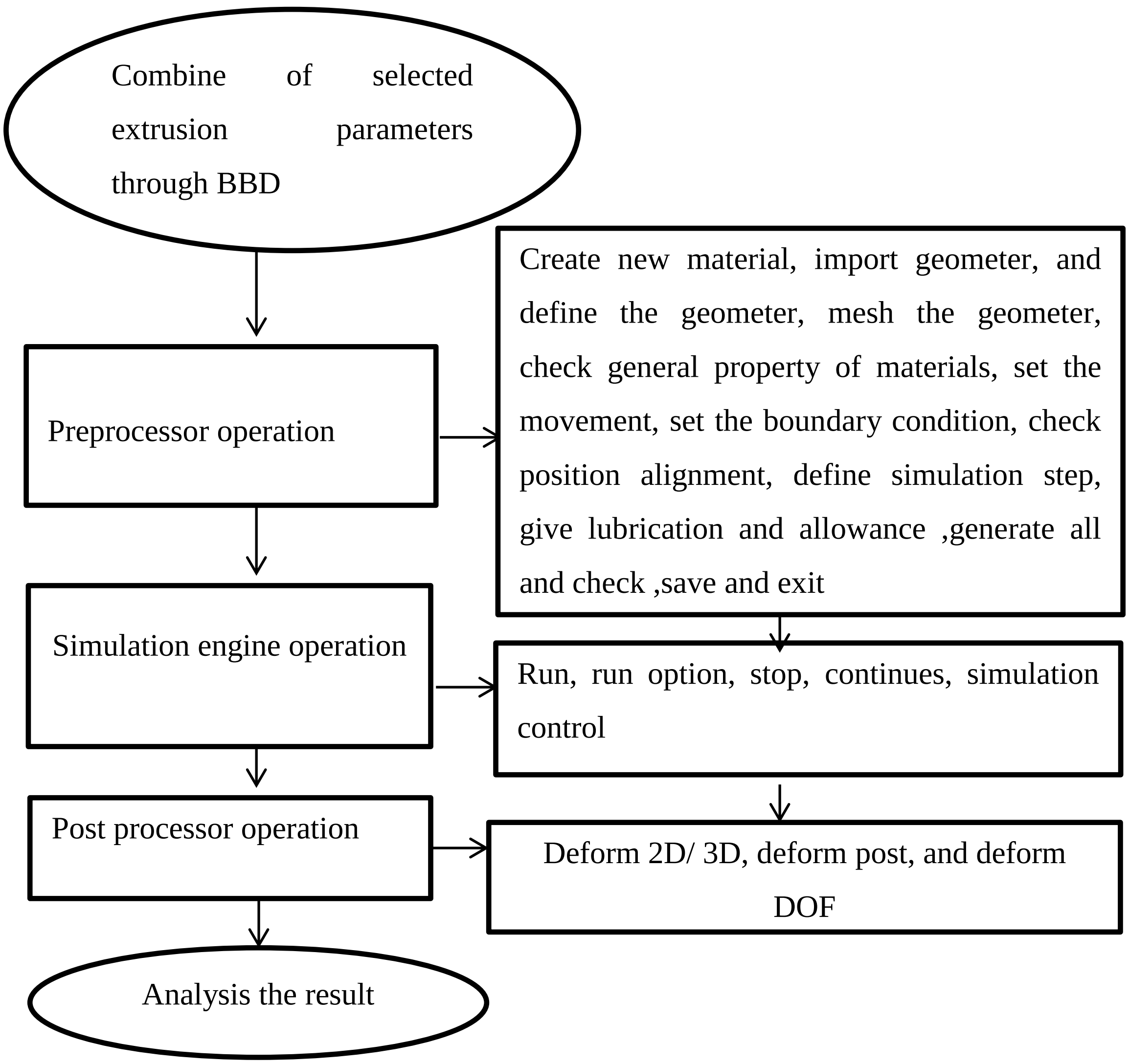


Figure 3.25 General procedure in simulation

Table 3. 1 Tool and equipment used there function

| S.No | Equipment with tool | Function |
|---|---|---|
| 1 | Analytical precision balance | Measure the mass |
| 2 | Ball milling machine | Blended the powder reinforcement together |
| 3 | Abrasive cutter | To section the alloy bar into piece for the fabrication process |
| 4 | Stir casting | Fabricate the composite material |
| 5 | Lathe machine | To prepare the fabricated sample for the test as per ASTM standard |
| 6 | Grinder and polisher | For removal, smooth, and finishing, surface material |
| 7 | Extrusion machine | To deform fabricated composite |
| 8 | Optical microscope | To study the microstructure behavior material |
| 9 | SEM | Characterize the hybrid composite surface and analysis the behavior of the fabricated composite surface after wear test. |
| 10 | XRD(X-Ray Diffraction) | Analyze Crystal Structure, Phase Identification, Crystallographic Orientation |
| 11 | Universal testing machine (UTM) | To Measure the compression strength of materials |
| 12 | Vickers hardness tester | Measure the hardness of the samples |
| 13 | Pin on disc | Wear resistance of fabricated sample |
| 14 | Image J Software | To analysis the image to measuring grain size and porosity |

## CHAPTER

## RESULTS AND DISCUSSION

### 4.1. Introduction

The manufacturing of reinforced aluminum 7075metal matrix composite through stir casting techniques followed by forming process had shown significant result in improving physical, mechanical, and tribological properties.in this section and sub section the discussion was performed on the result obtain from the fabrication of SiC, $CeO_2$ ,and GO- reinforced Al 7075 composite at selected optimum values followed by cold deform at optimum extrusion parameters obtained using FEM simulation conducted via 3 DEFORM V11 software.

#### 4.1.1. Analysis of synthesized samples behaviors

The samples contain different weight percentage of SiC, $CeO_2$ ,and GO-reinforcement was fabricated. The value of the reinforcement ration was selected based on the optimum ratio provide optimum result in most article. Those ratios were the amount of reinforcement combine with the matrix (Al7075) and provide the best properties. The combination of different weight percentage SiC, $CeO_2$ ,and GO with matrix (Al7075) was listed below.

Table 4.1Composition of SiC, Ceand GO reinforced Al7075 composite

| Fabricated Sample code | Composition |
|---|---|
| $S_1$ | 81%Al7075 +10% $CeO_2$+5% SiC+4%GO |
| $S_2$ | 81%Al7075+7.5%$CeO_2$+7.5%SiC+4%GO |
| $S_3$ | 81%Al7075+5%$CeO_2$+10%SiC+4%GO |
| $S_4$ | 90%Al+5.6%Zn+2.5%Mg+0.23%Cr+1.6%Cu |

### 4.2. Characterization of fabricated sample

The microstructure examination was perfumed on fabricated sample to observe structure of samples at the micro level. Characterizing and calculating the arrangement distribution of component materials was mainly examined through this method. The shape, size and distribution of Sic, $Ceo_2$, and GO reinforcement within Al 7075 matrix of fabricated sample was studied using optical and scanning electron microscope.

### 4.2.1. X-RD Analysis of developed composite

#### 4.2.1.1.Phase Analysis of stir cast fabricated

The X- ray diffraction pattern of (90%Al+5.6%Zn+2.5%Mg+0.23%Cr+1.6%Cu)($S_{pure}$) (81%Al7075+10%$CeO_2$+5%SiC+4%GO)$S_1$,(81%Al7075+7.5%$CeO_2$+7.5%SiC+4%GO)$S_2$, and ( 81%Al7075+5%$CeO_2$+10%SiC+4%GO)($S_3$) were observed in angle between (10°-2θ-80°) at scan speed 3°/min. The diffraction peaks of fabricated sample were compared to XRD-JCPDS files of various materials for strong peak as drawn on figure below. The Sic and $CeO_2$ can be seen as small peak when compare to the matrix material 7075 Al in XRD plotted graphs. This deference in peak size was observed to the weight percentage variation (Bhowmik et al., 2020). The peak for GO was not observed clearly because small amount of Nano particle weight percentage was used. The tallest peak was seen at angle of (44.69855°), and (2 0 0) JCPDS card number for Al. This was observed due to high concentration of the material in sample. For Sic, the peak was formed at angle of (38.43666°) and (1 1 1) JCPDS card number (S Suresh et al., 2019).For $CeO_2$, the peak was formed at angle of (65.13481°) and (2 2 0) JCPDS card number. The next visible peak was formed for Mg at angle (78.18107°) and (3 1 1) JCPDS card number was formed. This angle indicated the visibility of the combination (Sambathkumar et al., 2017).

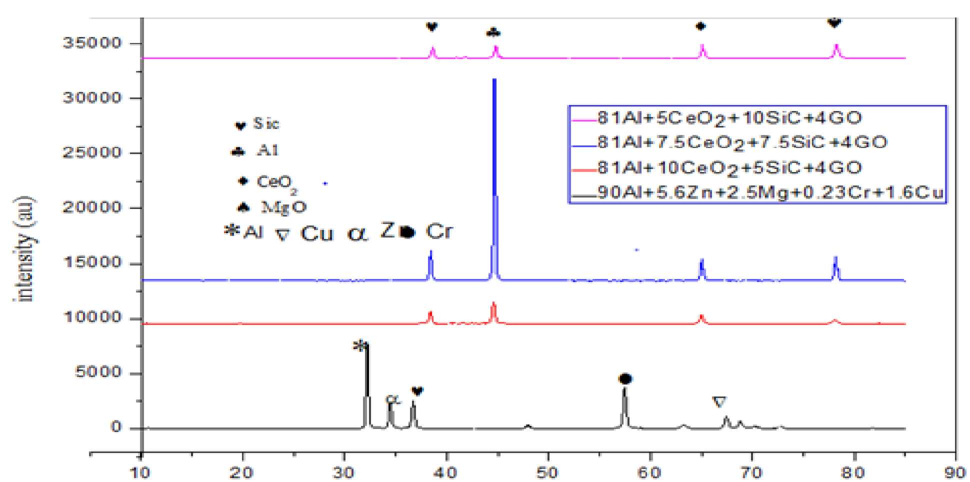


Figure 4.1The peak point height of fabricated sample

The increases in intensity of the peaks after reinforcement indicated the improvement in the crystallinity or ordered arrangement of atoms in the material. The reinforcement added result in the reduction of dislocations and grain boundaries as well increase crystallographic orientations. These intern result the increment in intensity of sharper peaks and formation additional diffraction peak. Sometime it is also result in formation of new compounds.

#### 4.2.1.2.Dislocation Density, Lattice Strain and Crystalline Sizes of Samples

Crystalline or grain size was calculated for all of four samples using origin soft ware depend on data taken from XRD test. Scherrer equation was used to calculate the average crystalline size based on peak widening seen in the XRD pattern. Based on this equation 0.9 and 0.15406(Å) values of shape factor (K) and X-ray wavelength (λ) respectively was used to connect peak widening (β), X-ray wavelength (λ), full width at half maximum (FWHM), and the crystalline size (D) (Sun et al., 2020).The sample with best properties was selected based on calculated average crystalline size values and intended application. The smaller average crystalline size enhances hardness and strength while, finer enhance resistance to deformation, fatigue resistance, and creep resistance, in other hand, larger increases ductility and toughness. Depend on the result indicated in table below k (0.96) and λ (Ȧ) (0.15406) was taken and the Dislocation Density and Lattice Strain, and Crystalline Sizes of Samples was calculate according to Scherrer rule and equation. From table below it was conclude that, the decrement in dislocation density and Lattice Strain shows the improvement in properties. Especially Sample two shows more decrement in dislocation density and Lattice Strain than other fabricated sample. This indicates the better properties enhancement.

Table 4.2 Dislocation Densities and Lattice Strain Crystalline Sizes of Samples

| Sample | Data from XRD peak analysis | | Experimental Calculation using Scherrer equation | | |
|---|---|---|---|---|---|
| | Peak position 2θ (°) | FWHM$\beta$(°) | D(μm)= $\frac{K\lambda}{\beta cos\theta}$ | $\delta = \frac{1}{D^2}$ $*10^{-3}(\mu m)^{-2}$ | $\varepsilon = \frac{\beta}{4\tan\theta}$ $*10^{-3}$ |
| | 32.23061 | 0.25816 | 33.45502 | 0.893464 | 3.898718 |

| | | | | | |
|---|---|---|---|---|---|
| Sample pure | 34.49343 | 0.29922 | 29.03552 | 1.186153 | 4.20555 |
| | 36.73399 | 0.35441 | 24.66845 | 1.643298 | 4.657622 |
| | 47.98272 | 0.42441 | 21.3991 | 2.183781 | 4.160985 |
| | 57.4954 | 0.37764 | 25.06043 | 1.592293 | 3.003766 |
| | 63.28494 | 0.52463 | 18.57741 | 2.897543 | 3.714755 |
| | 67.46788 | 0.4307 | 23.16529 | 1.863478 | 2.814254 |
| | 68.83987 | 0.53624 | 18.75733 | 2.842222 | 3.414626 |
| | 70.21646 | 0.56308 | 18.0128 | 3.082033 | 3.494748 |
| | 72.72767 | 0.45063 | 22.86545 | 1.912672 | 2.670476 |
| Average | | | 23.49968 | 2.009694 | 3.6035 |
| Sample one | 38.41425 | 0.33557 | 26.1837 | 1.45860 | 4.202928 |
| | 40.70338 | 0.48398 | 18.28549 | 2.9909 | 5.693042 |
| | 41.5234 | 0.37521 | 23.64967 | 1.7879 | 4.318555 |
| | 44.61802 | 0.33912 | 26.4469 | 1.42971 | 3.606242 |
| | 65.01048 | 0.40166 | 24.49503 | 1.66664 | 2.750432 |
| | 78.09511 | 0.57571 | 18.55779 | 2.90367 | 3.096813 |
| Average | - | - | 22.93643 | 2.03957 | 3.944669 |
| Sample two | 38.43666 | 0.26752 | 18.84637 | 0.926884 | 3.348511 |
| | 44.69855 | 0.23239 | 22. 60434 | 0.671008 | 2.466326 |
| | 65.06579 | 0.32657 | 18.13657 | 1.101063 | 2.233862 |
| | 78.18107 | 0.40544 | 22.36743 | 1.438349 | 2.17757 |
| Average | - | - | 19.78346 | 1.034326 | 2.556567 |
| Sample three | 44.81628 | 0.31142 | 28.81979 | 1.203978 | 3.29543 |
| | 38.62366 | 0.33596 | 26.17001 | 1.460133 | 4.18319 |
| | -12.17329 | 18.02897 | 0.462833 | 4668.214 | -737.726 |
| | 41.87214 | 0.22491 | 39.49973 | 0.640932 | 2.565068 |
| | 41.87214 | 8.14141 | 1.091197 | 839.8338 | 92.85168 |
| | 65.13481 | 0.33941 | 29.00764 | 1.188434 | 2.318611 |
| | 78.27386 | 0.44969 | 23.7885 | 1.767119 | 2.411239 |
| | 78.39682 | 1.89195 | 5.659138 | 31.22478 | 10.12244 |
| Average | - | - | 19.312355 | 693.1916 | -77.4973 |

### 4.2.2. Optical microscopy analysis

The distribution of reinforcement particle in the Al 7075 matrix was studied using optical microscope. The distribution Sic, $Ceo_2$, and GO with the matrix at different fraction where examined carefully with 100x, 200x and 500x magnification scale. To clearly observe the distribution of reinforcement etchant was used. Using Image software the grain boundary was analyzed based on the image extracted from optical microscope examination.

#### 4.2.2.1.Distribution of reinforcement particles in the matrix

The optical test was perfumed to check the distribution of SiC, $CeO_2$ ,and GO with in the 7075 Al metal matrix. The analysis performed on image recorded from optical test showed that the matrix material 7075Al shows uniform distribution though out the sample. Visual examination shows that relatively homogeneous distribution of SiC, $CeO_2$ ,and GO particle within each other and the matrix in terms of both spatial arrangement and density. This result showed that the stir casting fabrication method used was effective in accomplishing uniform distribution the above reinforcement within the employed matrix. The recorded image was shown in figure below. Sample two shows sound fabrication output.

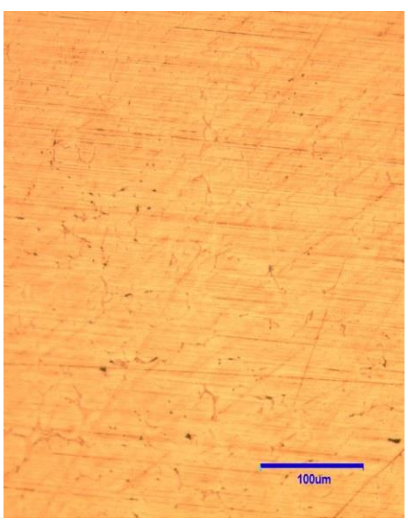


$S_1$ at100x before etching

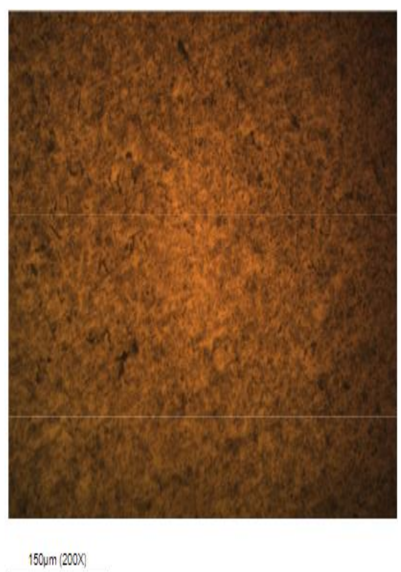


$S_1$ at 200x after etching

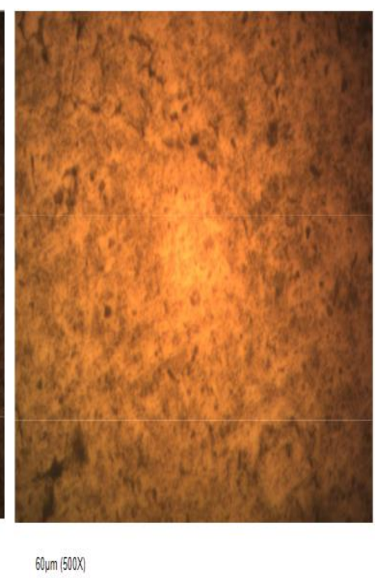


$S_1$ at 500x after etching

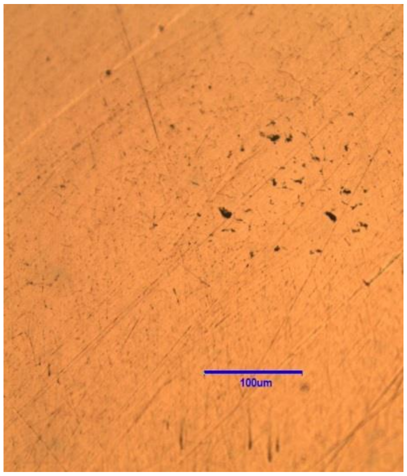


$S_2$ at 100x before etching

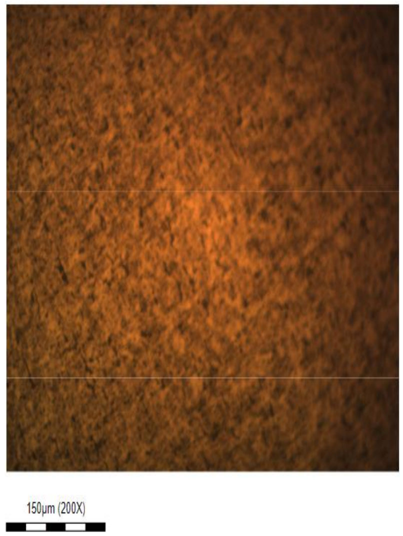


$S_2$ at 200x after etching

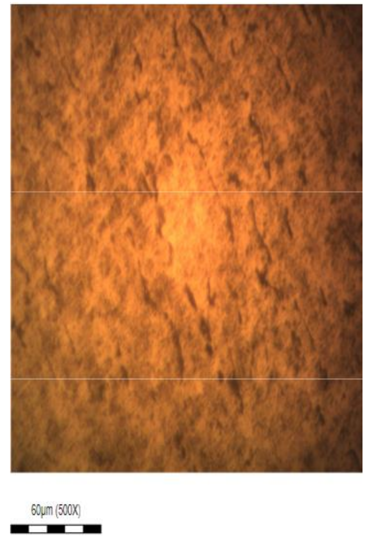


$S_2$ at 500x after etching

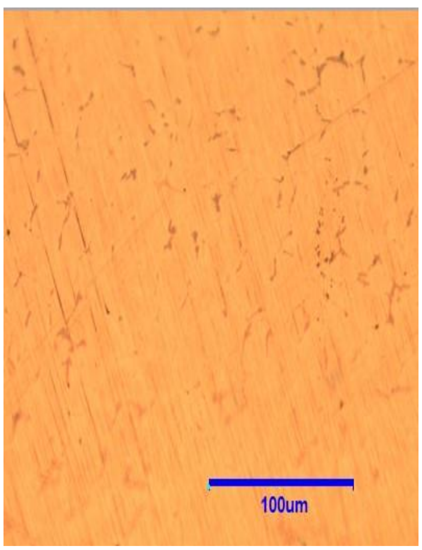


$S_3$ at 100x before etching

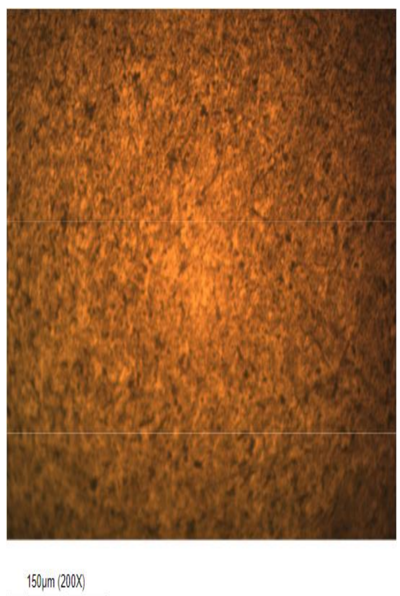


$S_3$ at 200x after etching

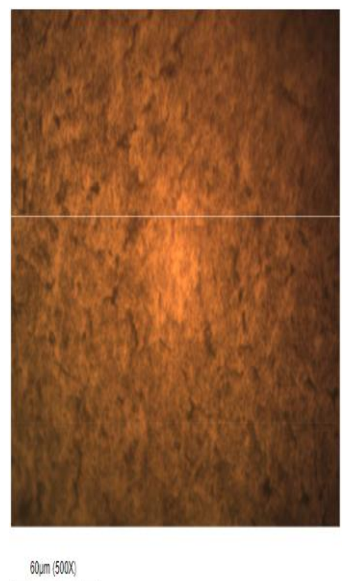


$S_3$ at 500x after etching

Figure 4.2 optical test image of hybrid developed composite

As the amount of weight percentage of reinforcement increases the microstructure image become dense and darker but the distribution of reinforcement still good and uniformly bonded to the matrix aluminum. The presence SiC and $CeO_2$ particle could inhibit the movement dislocation and increases the strength of the material (Mohal, 2017).

#### 4.2.2.2. Grain size calculation

The grain size and porosity content of stir cast fabricated samples were calculated using the Image J software. From analysis of image recorded from optical test using Image J software through ASTM E112-Line intercept methods, the average of five trial taken for each sample was found as :Sample one, with 81% Al7075 +10% $CeO_2$+5% SiC+4% GO combination showed that the average grain size of 19.025μm aswell porosity percentage of 0.219%, Sample two ,with 81% Al7075+7.5% $CeO_2$+7.5% SiC+4% GO combination showed that the average grain size of 18.7514μm as well porosity percentage of 0.0162%, and sample three with 81% Al7075+5% $CeO_2$+10% SiC+4% GO combination showed that the average grain size of 18.7532 μm as well porosity percentage of 0.982%,.This analysis showed that the incorporation of different reinforcement like ceramic and oxide with different ratio have effect on the grain growth within the 7075 Al matrix. Concerning porosity, the combination of hard ceramics (SiC) and oxides ($CeO_2$, GO) reduce the porosity and contributed slight increase in density. Depending on the results, sample two with low grain size and porosity (18.7514μm) and 0.0162%, was preferred. This is because smaller grains and porosity offer more grain boundaries and finer microstructure, which act as barriers to dislocation movement and improve the material's strength, hardness, toughness and fatigue resistance.

Table 4.3 Grain size calculated for developed composite using Image j

| Sample | Grain size | Porosity |
|---|---|---|
| $S_1$(81%Al7075+10%$CeO_2$+5%SiC+4%GO) | 19.025μm | 0.219% |
| $S_2$ ( 81%Al7075+7.5%$CeO_2$+7.5%SiC+4%GO) | **(18.7514μm)** | 0.0162% |
| $S_3$( 81%Al7075+5%$CeO_2$+10%SiC+4%GO) | 18.7532 μm | 0.982. |

### 4.2.3. Surface morphology analysis

The surface morphology analysis was perfumed on the fabricated samples using Scanning Electron Microscope (SEM). The behavior of samples surface were analyzed based the images recorded during SEM test. From the image it was found that, the uniform distribution of SiC, $CeO_2$ ,and GO, reinforcement with the 7075Al matrix, and due to poor wettability of molten 7075 aluminum matrix with hard reinforcement during fabrication process same micro holes and grooves was seen.

| | | |
|---|---|---|
| 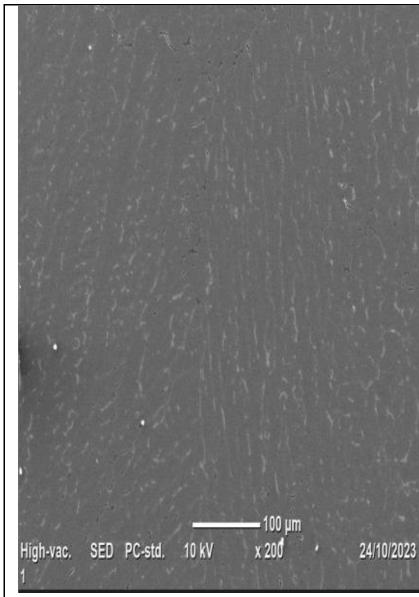 | 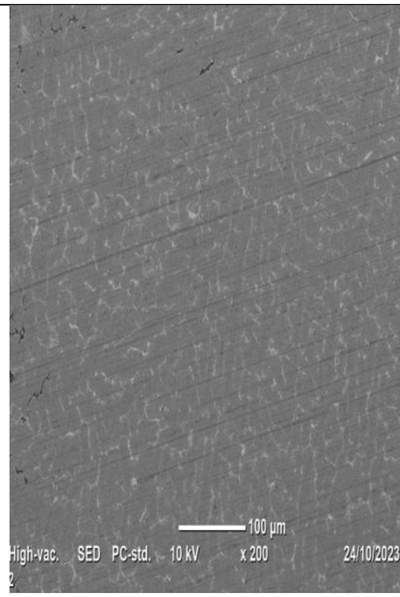 | 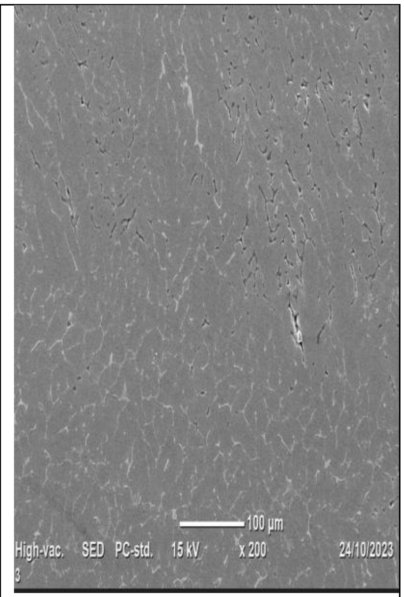 |
| Sample One | Sample Two | Sample Three |

Figure 4.3 SEM test image of developed composite at 100x for sample 1, 2,3

### 4.3. Analysis of Density and Porosity of fabricated Sample

The theoretical and actual density of SiC, $CeO_2$ ,and GO reinforced Al7075 metal matrix composite was calculated by the rule of mixture using Archimedes principle. These values were calculated based on the value of mass measured in the air and the water using Analytical precision balance. The reinforcement particles that have lower density result in lower porosity which in turn result in higher density of fabricated composite.in other hand, reinforcement particles with higher density sink to the bottom and result in porosity during fabrication of the composite and makes density higher (Hammar Ilham Akbar & Wibowo, 2020). For each fabricated sample the value of density recorded was list down in table below. The second sample with 7.5 % Silicon carbide and 7.5% Cerium di oxide 4% Graphene oxide have 3.09099 theoretical densities and 3.011 actual densities with 0.02584 porosity values. These porosity is low when compare to the other reinforced and pure samples. Having high actual density and low porosity when compare to other means sample has high hardness. This intern means has good particle distribution.

Table 4.4 Measure mass in air and in the water SiC, $CeO_2$, and GO reinforced Al7075

| Samples | Mass in the air | Mass in the water |
|---|---|---|
| $S_1$(81%Al7075+10%$CeO_2$+5%SiC+4%GO) | 4.571 | 2.7059 |
| $S_2$ (81%Al7075+7.5%$CeO_2$+7.5%SiC+4%GO) | 4.252 | 2.9067 |
| $S_3$ ( 81%Al7075+5%$CeO_2$+10%SiC+4%GO) | 5.055 | 3.1776 |
| $S_4$(90%Al+5.6%Zn+2.5%Mg+0.23%Cr+1.6%Cu) | 3.8056 | 1.5565 |

The relationship between Theoretical and actual density of SiC, Ce$\mathbf{O_2}$ ,and GO reinforced Al7075 fabricated sample was analyzed based on the connection between actual density and the porosity (Rajasekaran & Pugazhenthi, 2020).

Table 4.5Theoretical and actual density of SiC, $CeO_2$, and GO reinforced Al7075 sample

| Samples | Theoretical density ($g/cm^3$ ) | Actual density ($g/cm^3$) | Porosity percentage |
|---|---|---|---|
| Sample one | 3.18904 | 2.451 | 0.2314 |
| Sample two | **3.09099** | **3.011** | **0.02584** |
| Sample three | 2.99294 | 2.692 | 0.10054 |
| 7075 Al alloy | 2.903488 | 1.692 | 0.41725 |

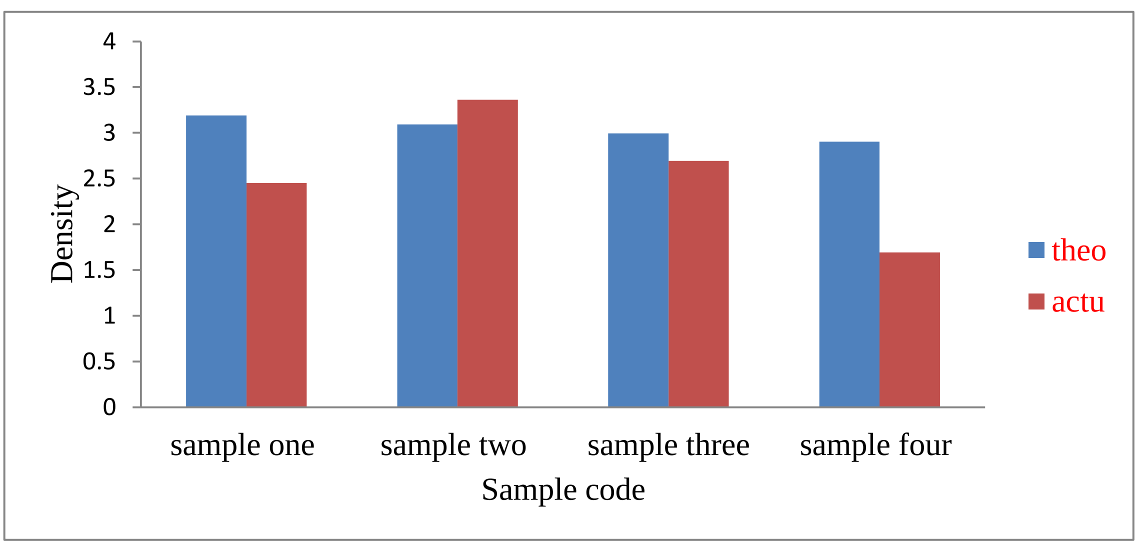


Figure 4.4 Actual verses theoretical density of SiC, $CeO_2$ and GO reinforced Al7075

## 4.4. Analysis the Hardness of Developed Composite

The hardness test was performed on three reinforced and one pure 7075 aluminum metal matrix using Vickers hardness tester. The three trials were taken for each of four samples and average values of the trial was calculated for each. The average hardness of 228.37, 240.5 and 232.13(HV) was recorded for sample 1, 2 and 3 respectively. The hardness of the $S_1$(81%Al7075+10%$CeO_2$+5%SiC+4%GO),$S_2$(81%Al7075+7.5%$CeO_2$+7.5%SiC+4%GO)and $S_3$ (81%Al7075+5%$CeO_2$+10%SiC+4%GO) was improved when compare to sample that was fabricate 5%,7.5% and 10% of sic 7075 Al composite (Rajasekaran & Pugazhenthi, 2020) The sample two has high values of hardness value. Sample two (81%Al7075+7.5% $CeO_2$+7.5% SiC+4%GO) shows hardness increment of 95.84 HV or 66.25% when compare to pure sample which has a hardness of 144.66.

Table 4.6 Hardness values of SiC, $CeO_2$, and GO reinforced Al7075 metal matrix

| Sample code | Hardness(HV) | | | | |
|---|---|---|---|---|---|
| | Trial one | Trial two | Trial three | Average value | %of Improvement |
| $S_1$ | 237.6 | 216.6 | 230.9 | 228.37 | 57.87% |
| $S_2$ | 236.6 | 231.9 | 253.0 | **240.5** | **66.25**% |
| $S_3$ | 215.7 | 230.9 | 249.8 | 232.13 | 60.47% |
| $S_4$ | 140.3 | 143.7 | 150 | 144.66 | - |

Hardness values verse reinforcement type and ration was analyzed and the best hardness was found when the ratio of both reinforcement reach 7.5%.

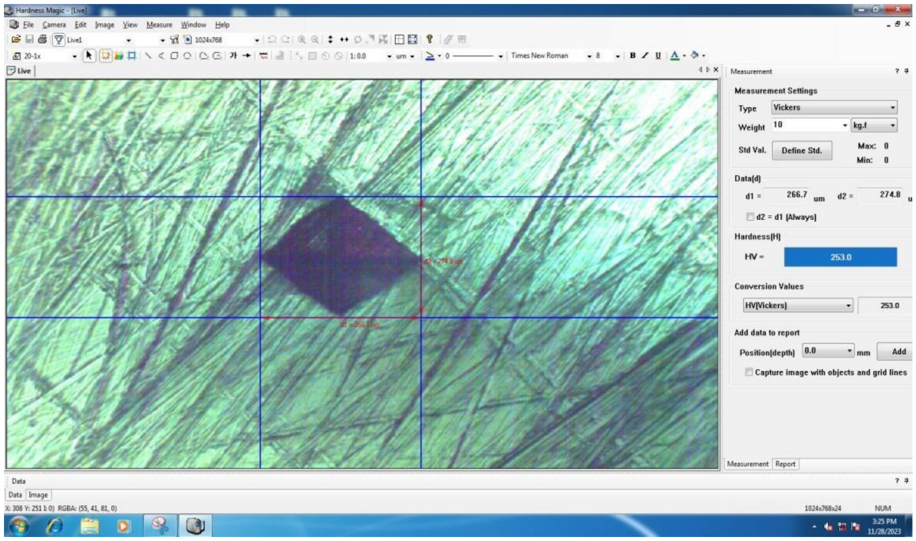

Figure 4.5 Hardness test trial three of (81%Al7075+7.5%CeO_2+7.5%SiC+4%GO)

## 4.5.Wear test

The wear rate tests were perfumed on SiC, $CeO_2$ ,and GO reinforced 7075 Al metal matrix composite using pin on disc.Sample two shows decrease in wear, friction force as well coefficient of friction as time the material exposed to the wear environment increases when compared with the other two as shown in figure below. It was known that less wear, friction force as well coefficient rate it implies better tribological and mechanical properties.

### 4.5.1. Sliding distance rate

Sliding distance is linear distance covered by a point on the pin as it slides through crossways to the surface of the disc. The wear behaviors of the material largely depend on the sliding distance as well sliding time. Melting and formation of hardened layer on the contact surfaces of AMMC's and wear testing tool during wear testing process cause the wear rate to increases simultaneously with both sliding distance time(Kumar et al., 2022). High amount of sliding velocity cause high pressure between the counter disc plate and pin contact surface. The high pressure formed between the surface intern causes high friction heat which enhance the formation surface temperature and accelerate oxide layer generation (Bhowmik et al., 2020). High sliding distance means more contact surface.

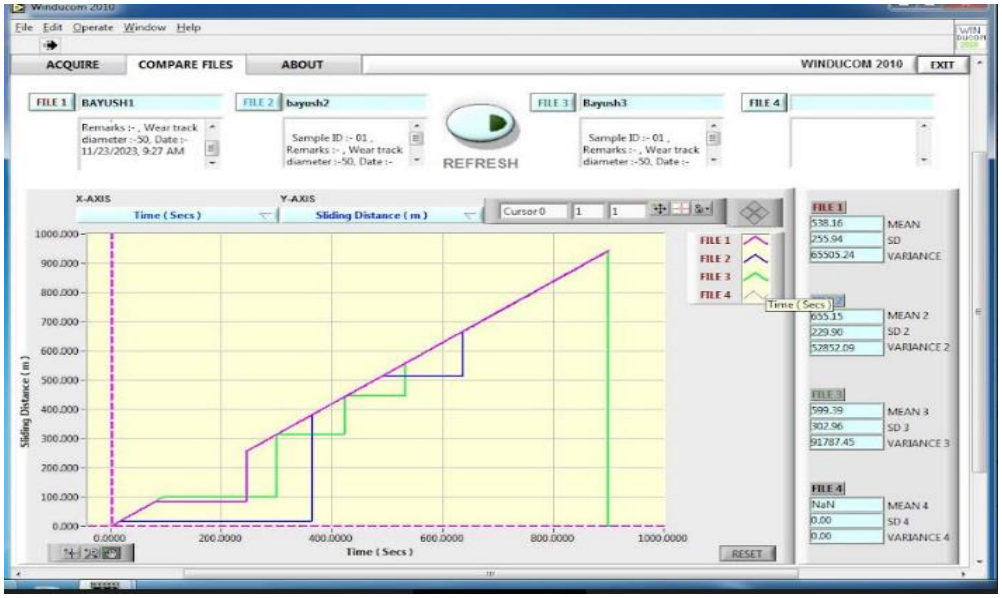


Figure 4: 1 Sliding distance verses time for fabricated sample 1, 2, 3,

### 4.5.2. Coefficient of friction (COF) with time

Coefficient of friction (COF) is  dimensionless quantity that used to measure the resistances of material to slide when become connect .The Coefficient of friction (COF) verses time for fabricated sample was recorded during wear test perfumed using 30N load  ,500 m sliding distance, 400rpm  parameter was showed in figure below.


Figure 4: 2 Coefficient of friction verse time for fabricated sample1, 2, and 3

Coefficient of friction verse time relation of (81%Al7075+10%$CeO_2$+5%SiC+4%GO), (81%Al7075+7.5%$CeO_2$+7.5%SiC+4%GO) and (81%Al7075+5%$CeO_2$+10%SiC+4%GO) samples were interpreted to analyze the wear behaviors. The coeffent of friction was calculated for the sample based on Archard's law.

Table 4.7 Coefficient friction calculate value

| Sample | Coefficient of friction |
|---|---|
| $S_1$(81%Al7075+10%$CeO_2$+5%SiC+4%GO) | 0.01465 |
| $S_2$( 81%Al7075+7.5%$CeO_2$+7.5%SiC+4%GO) | **0.00306** |
| $S_3$(81%Al7075+5%$CeO_2$+10%SiC+4%GO) | 0.019 |

From figure below it was analyzed that, at the beginning of the test the initial transient phase were observed where COF fluctuation with time due to surface initial wear influence, alteration in surface roughness and topography. After initial phase steady states were observed were COF relatively constant due to stable friction. Starting from around 350.000 wear transition phase (COF fluctuation) was observed due to removal of material, formation debris, and contacting surface change. Sample two or (81%Al7075+7.5%$CeO_2$+7.5%SiC+4%GO) stay longer steady stage. Sample one or (81%Al7075+10%$CeO_2$+5%SiC+4%GO) start wear transition phase sooner than other. Sample three or (81%Al7075+5%$CeO_2$+10%SiC+4%GO) show more COF value.

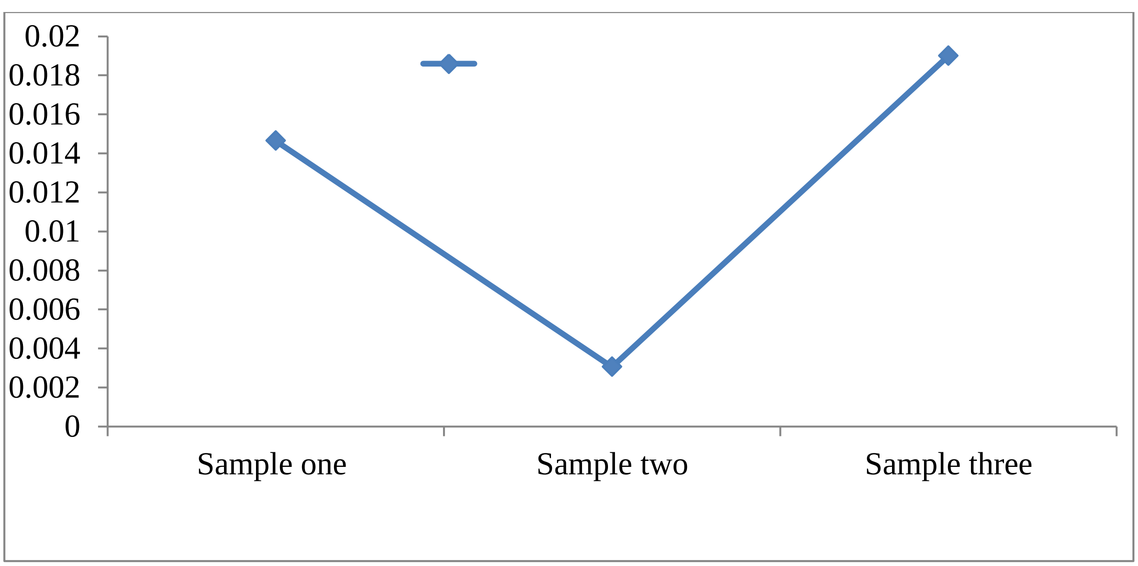


Figure 4.6 Coefficient of friction of developed sample taken at average selected parameters

#### 4.5.3. Friction force with time

The resistive force that resists the relative motion between two surfaces in contact is knows as friction force. From the graph it was seen that as the time of the wear processed the friction force rate decreases. The sample with (81%Al7075+7.5%$CeO_2$+7.5%SiC+4%GO) combination shows that gradual decrement in friction forces as the process proceed as shown in figure.

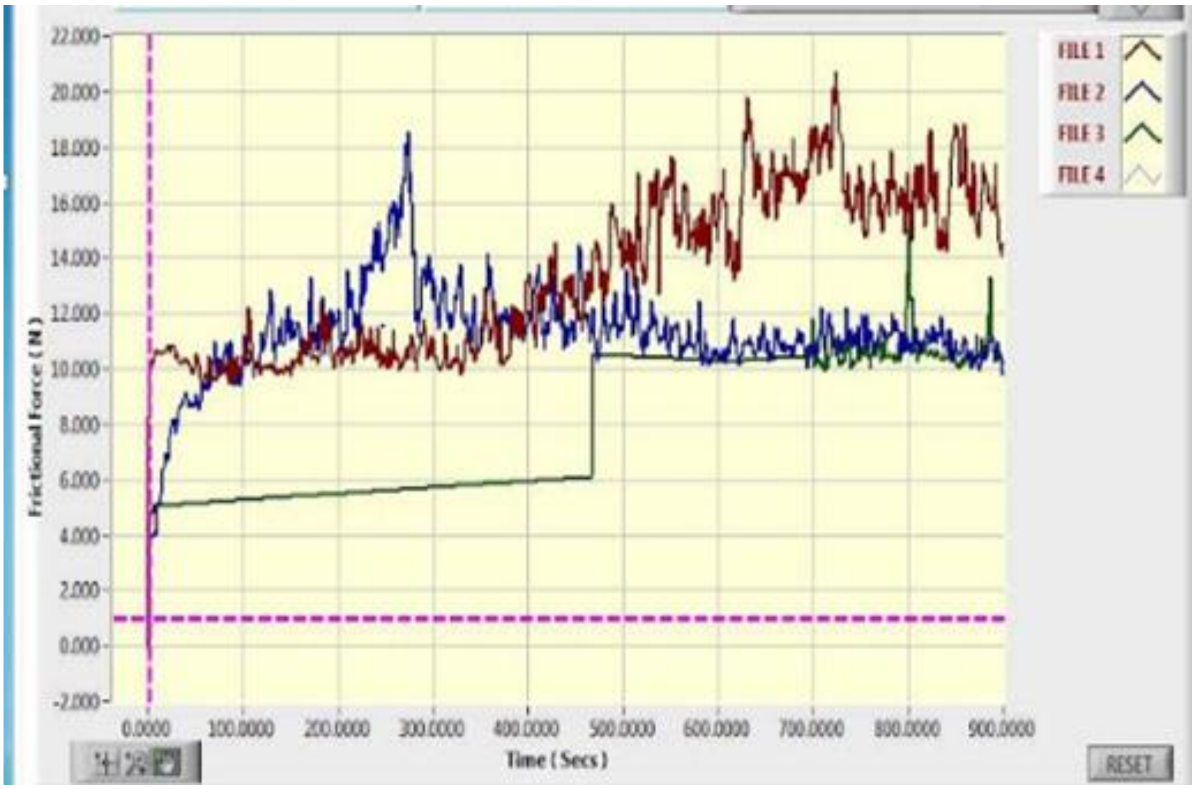


Figure 4: 3 Friction force verses time for sample 1,2,3

#### 4.5.4. Wear rate

The wear rate is refers as the measure of how quickly a material is lost over a time from the surface of a sample when subjected to friction, abrasion or other mechanical load. The mass of the sample before and after wear test were measured and recorded to calculate the wear rate and volume loss happen on fabricated sample during wear test .the results were list down on table below. The volume loss and wear rate for samples were calculated and tabulated below. The sample with minimum wear rate value has better wear resistance properties.

Table 4.8 The volume loss and wear rate of fabricated sample

| Sample | Mass before wear test | Mass after wear test | Volume Loss (%) | Wear rate (%) |
|---|---|---|---|---|
| $S_1$(81%Al7075+10%$CeO_2$ +5%SiC+4%GO) | 0.7812 | 0.7976 | 0.6628 | 0.19256 |
| $S_2$(81%Al7075+7.5%Ce $O_2$+7.5%SiC+4%GO) | 0.7978 | 0.7690 | 1.022 | **0.19129** |
| $S_3$(81%Al7075+5%$CeO_2$+ 10%SiC+4%GO) | 0.7794 | 0.7460 | 1.2401 | 0.24802 |


Figure 4: 4 wear rate verses time for sample 1, 2,3

From the wear verse time plot it was observed that 81%Al7075+7.5%$CeO_2$+7.5%SiC+4%GO sample combination show small wear rate when compare to the wear rate other two samples.

### 4.5.5. Wear morphology analysis of developed composite

The Wear morphology analysis were perfumed on the fabricated samples post wear test to analysis materials surface and wear behaviors of material using scanning electron microscope SEM. From the image taken from SEM test it was found that same micro cracks and delamination were see. The SEM image for three fabricated sample at different magnification were list in figure below.

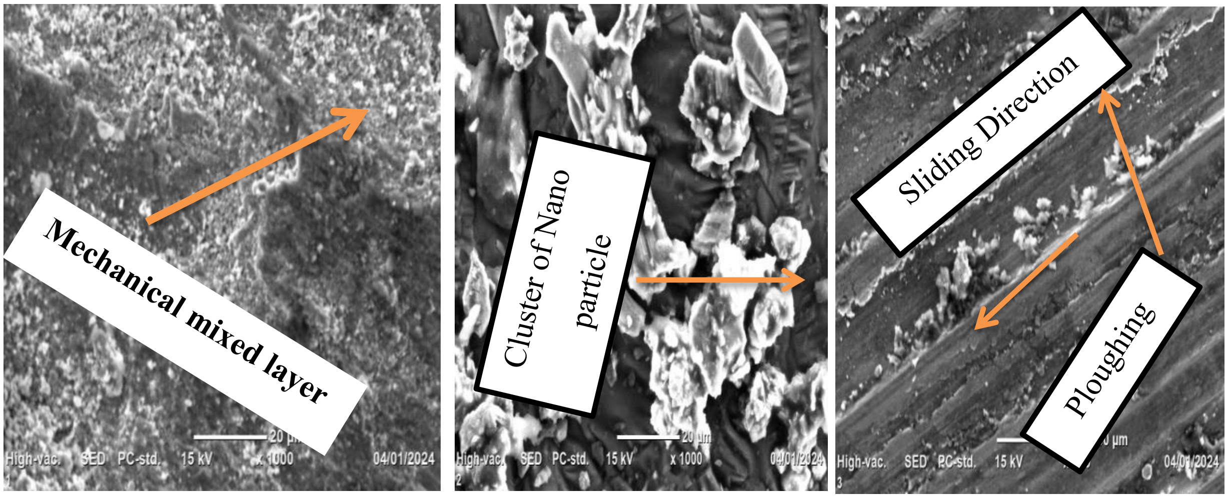


$S_1$ at 1000x magnification S at 1000x magnification $S_3$ at 1000x magnification

Figure 4.7 Wear morphology images of developed composite from SEM

### 4.6. Compression test

The compression test was performed on SiC, $CeO_2$ ,and GO, reinforced 7075Al composite by universal testing machine to examine the performance of the material under the compressive loading condition. The stress-strain graph for each sample was drawn for each sample depend data taken after compression test. The fabricated composites with 81% Al7075 +10% $CeO_2$+5% SiC+4% GO, 81% Al7075+7.5% $CeO_2$+7.5% SiC+4% GO and 81% Al7075+5% $CeO_2$+10% SiC+4% GO showed significant yield and ultimate compressive strength The result taken from compression test showed that the enhancement of strength and stiffness compared to the pure 7075 Al alloy . These improvements in properties result from addition of reinforcement. Generally from SEM and compression test sample two can effectively withstand compression load and better mechanical properties. This because the addition of SiC as well $CeO_2$ enhance the compression load resistance of fabricated material.

Table 4.9 Yield and ultimate strength of fabricated material

| Sample | Yield strength | Ultimate strength |
|---|---|---|
| $S_1$(81%Al7075+10%$CeO_2$+5%SiC+4%GO) | 110Mpa | 413Mpa |
| $S_{2(}$81%Al7075+7.5%$CeO_2$+7.5%SiC+4%GO) | 150Mpa | 490 Mpa |
| $S_{3(}$81%Al7075+5%$CeO_2$+10%SiC+4%GO) | 40Mpa | 432Mpa |

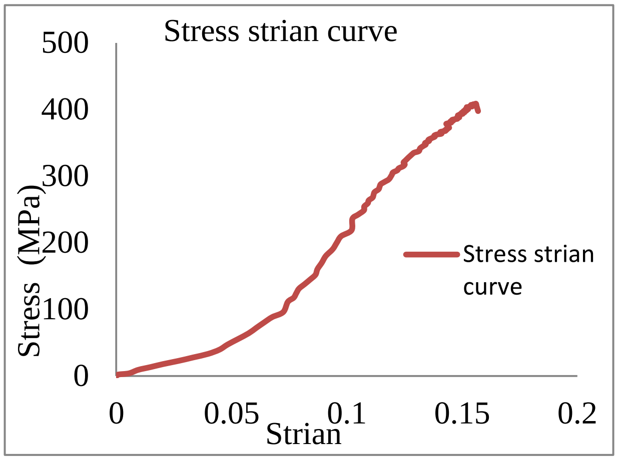


S1

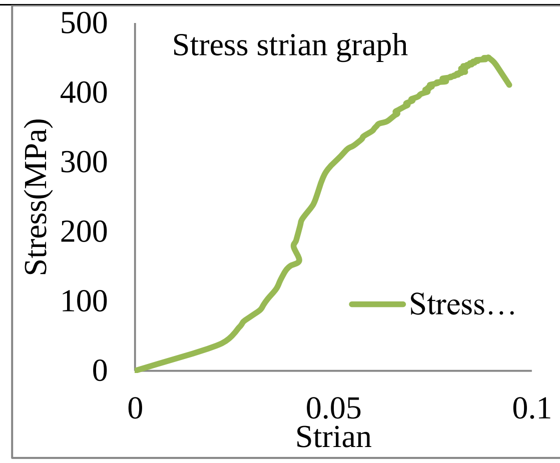


S2

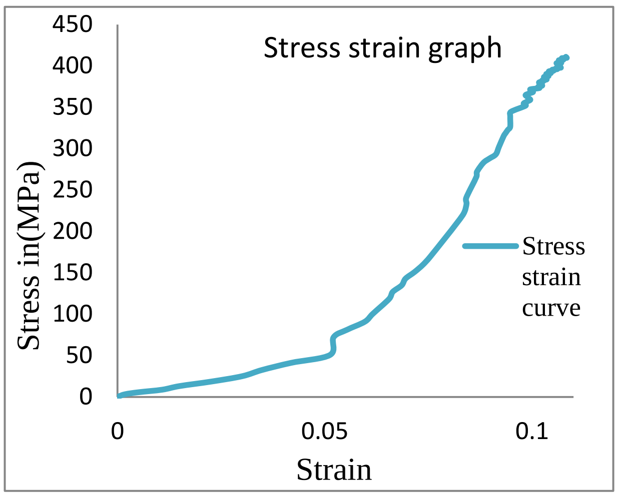


S3

Stress-strain graph of three samples drawn based on result obtain from compression test

Figure 4.8 The stress verses strain graph for sample 1, 2,3

### 4.6.1. Compression Fractography analysis of developed composite

The Compression fractography study were perfumed on SiC, $CeO_2$ ,and GO, reinforced 7075 Al composite to analysis the surface features, microstructure, and failure mechanisms of the material using SEM. This test reveals same micro cracks, and porosity on sample surface which were not possible to visualize with naked eyes after compression. The SEM image taken at different magnification for three fabricated samples that contain different ration of reinforcement percentage was listed down in figure below.

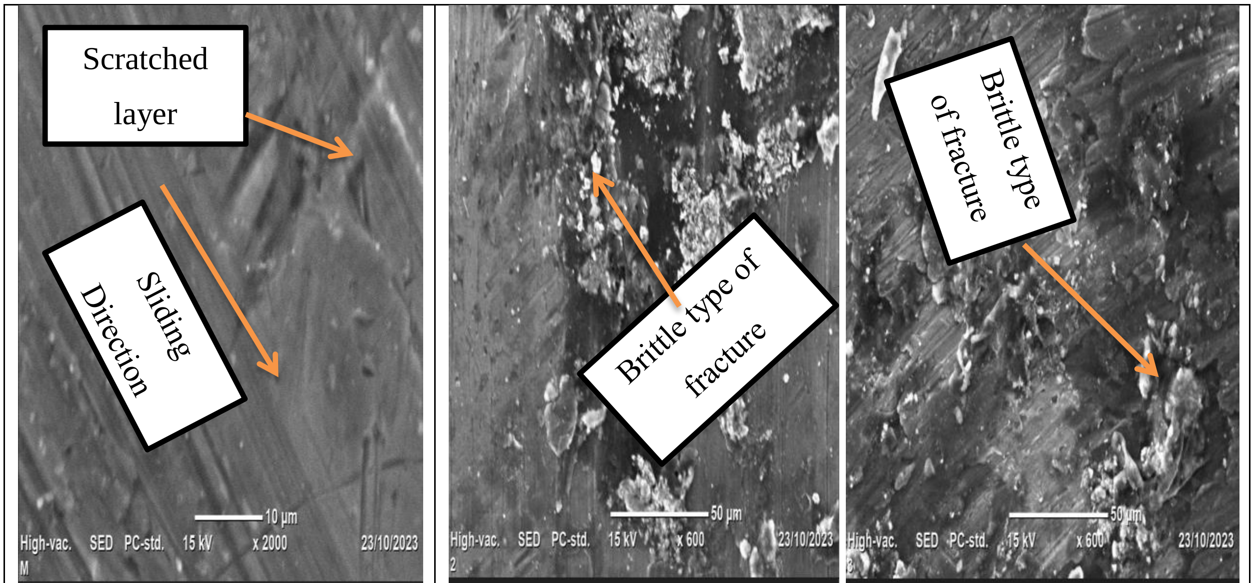


| | | |
|---|---|---|
| Sample One | Sample Two | Sample Three |

Figure 4.9 Compression test graph for sample 1, sample 2 and sample 3 respectively

**4.7. Corrosion test result**

The electrochemical analysis were perfumed on stir cast fabricated reinforced 7075Al composite samples using 3.5 % NaCl solution at room temperature to understand the corrosion resistance behavior of material according to (Sambathkumar et al., 2017).To detected the Potentio dynamic polarization of the samples the TAFEL estimation method was used. The TAFEL curve were plotted for three fabricated composite as showed in figure below using test data extracted during potentio dynamic polarization test. From these curve corrosion: current densities (Icorr), potentials (Ecorr), anodic (βa), cathode (βc), slopes and corrosion rate was obtain for each samples. Equivalent weight of composite in3% NaCl solution was calculated and listed in table below.

Table 4.10 Cathode and anode current and voltage value

| Sample | Corrosion current ($I_{corr}$)(mA/$cm^2$) | Corrosion potential ($E_{corr}$ )(V) | Bc | Ba | corrosion rate(mm/year) |
|---|---|---|---|---|---|
| Sample one | -1.46948161 | -0.77451516 | -0.364339 | 0.021 | 0.00079 |
| Sample Two | -1.03854699 | -0.835308989 | 0.064 | -0.09352 | 0.00044 |
| Sample hree | -1.679134615 | -0.768567416 | 0.026 | -0.26 | 0.00086 |

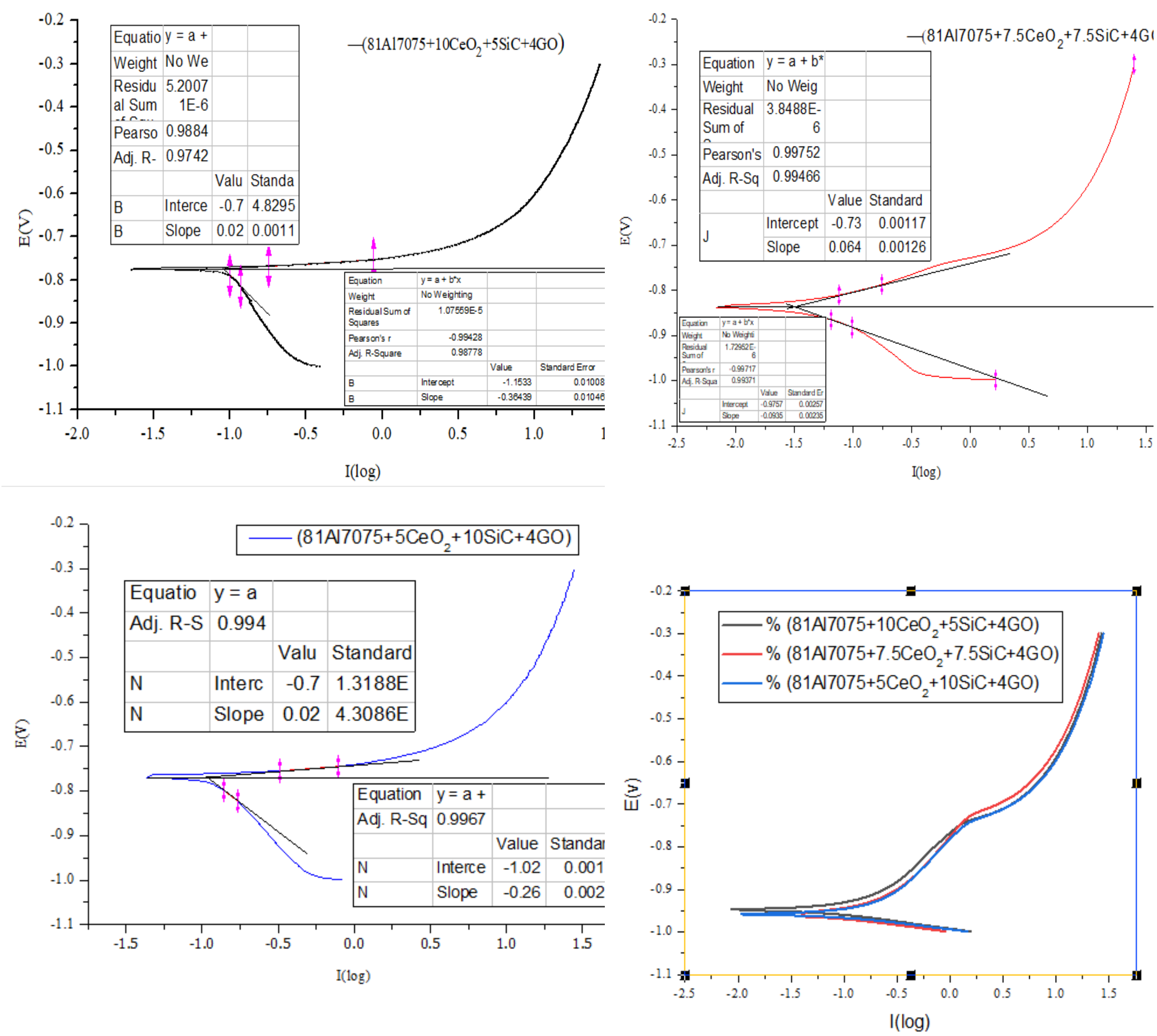


Figure 4.10 Tafel plots of copper matrix hybrid composite specimens in 3.5%NaCl solution

In corrosion analysis the slope indicated the rate corrosion over a time period. Steeper slope suggests a higher corrosion while a flatter slope indicates a slower corrosion rate. The intercept and slope used to analysis corrosion behavior of a material. Negative intercept and a positive slope may show an initial period of accelerated corrosion while a positive intercept and a negative slope may propose a decrease in corrosion rate over time. The improve in corrosion resistance was due the formation protective layer on the surface composite, in addition to, uniform distribution of nanoparticles in the matrix and effective dispersion (Kumar et al., 2023).

## 4.8. Sample selection for simulation

Careful selection of sample was performed in order to optimize the input cold extrusion parameter based on simulation using 3D deform to ensure accurately connection of the stir casting process and the next deforming process. Depend on the test result of the samples; the sample with best properties was selected. Sample with 81%7075Al-7.5%SiC-7.5%$CeO_2$ – 4%GO of weight percentage combination was selected.

### 4.8.1. Sample selection using S/N ratio

The Sample code(S). Hardness(HD), Compressive strength(CS), Corrosion rate(CR),and Wear rate(WR).

**Step1**: Transformation of experimental data obtain from the test result into S/N ratios

Table 4.11 Transformation of experimental data obtain from the test result into S/N ratios

| Experimental results | | | | | S/N ratio(dB) | | | |
|---|---|---|---|---|---|---|---|---|
| S | HD (HV) | CS (MPa) | CR | WR | HD | CS | CR | WR |
| S1 | 228.370 | 413.0 | 0.05880 | 0.612560 | 47.150 | 52.320 | 24.610 | 4.240 |
| S2 | 240.50 | 490.0 | 0.05040 | 0.191290 | 47.620 | 53.800 | 25.940 | 14.350 |
| S3 | 232.130 | 432.0 | 0.05320 | 0.248020 | 47.310 | 52.700 | 25.480 | 12.100 |

**Step2:** Normalization of S/N ratio was perform

Table 4.12 Normalization of S/N ratio was perform

| Sample | Hardness (HV) | Compressive Strength (MPa | Corrosion Rate | Wear Rate |
|---|---|---|---|---|
| S1 | 0.98 | 0.97 | 0.95 | 0.23 |
| S2 | 1.00 | 1.00 | 1.00 | 0.77 |
| S3 | 0.99 | 0.98 | 0.98 | 0.65 |

**Step3**: Determination of deviation sequence

Table 4.13 Determination of deviation sequence

| Sample | Hardness (HV) | Compressive Strength (MPa | Wear Rate | Corrosion Rate |
|---|---|---|---|---|
| $S_1$ | 0.020 | 0.030 | 0.770 | 0.050 |
| $S_2$ | 0.000 | 0.000 | 0.230 | 0.000 |
| $S_3$ | 0.010 | 0.020 | 0.350 | 0.020 |

**Step 4** Determine grey relational coefficient.

Table 4.14 Determine grey relational coefficient developed composite

| Sample | Hardness (HV) | Compressive Strength (MPa) | Wear Rate | Corrosion Rate | Grey Relational Coefficient | Grey Relational Grade |
|---|---|---|---|---|---|---|
| $S_1$ | 0.63640 | 0.63640 | 0.39340 | 0.63640 | 0.63640 | 0.55070 |
| $S_2$ | 1.00000 | 1.00000 | 0.63640 | 1.00000 | 1.00000 | 0.90910 |
| $S_3$ | 0.81820 | 0.63640 | 0.48780 | 0.63640 | 1.00000 | 0.65450 |

**Step 5** Rank of the fabricated sample by gray analysis

Table 4.15 Rank of the fabricated sample by gray analysis

| Sample | Grey Relational Grade | Rank |
|---|---|---|
| **Sample two** | 0.90910 | One |
| Sample three | 0.65450 | Two |
| Sample one | 0.55070 | Three |

The selected material help in defining the material properties during numerical simulation process in preprocessing stage. Because the fabricated material was new and the software does not know the material so to make the software to identify and process the operation for new material, the properties of new material need to be identified and introduced to the software. For this purpose ranking and selecting the best sample is needed.

Table 4.16 Properties of selected sample used as input parameter to define the material in preprocessing of simulating process

| S.No | Define parameters | Data /formula | Source of data |
|---|---|---|---|
| 1 | Compression strength | 490 Mpa | From compression test |
| 2 | Density | 3.011g/$cm^3$ | From Archimedes principles and experimental data |
| 3 | Flow stress constitutive equation | $\bar{\sigma}$=C$\bar{\varepsilon}^n \dot{\bar{\varepsilon}}^m$+y | From DEFORM 3D software |
| 4 | Constants define in power low<br>C=material constant<br>n=strain exponent<br>m=strain rate exponent<br>y=initial yield value | <br>C=1348.155Mpa<br>n=0.491<br>m=0.01<br>y=170Mpa | Calculated Based on compression strength of fabricated sample |
| 5 | The meshing | 80,000 mesh for work ship | |
| 6 | Coefficient of friction | 0.3 | As lubricated condition was taken |

### 4.9. Numerical simulation of developed composite for deformation behavior analysis through cold extrusion

The simulation operation was performed for cold extrusion 81%7075Al-7.5%SiC-7.5%$CeO_2$ –4%GO composite to evaluate the effect of extrusion parameters (extrusion ratio, ram speed and billet temperature) on the response (damage, load and effective stress) during the deformation of the fabricated material through cold extrusion process. The operation was performed on 3D deform software. Cosine die as well Extrusion ration, ram speed and billet temperature was selected as input extrusion parameter since they have significant effect on extrusion responses based on previous studies as well cosine die was selected . The selected extrusion parameter was combined through Box Behken (BBD) method found in Design – Expert software. The experiments were performed to identify optimum process parameter. The response damage, load, and effective stress value recorded due to selected input parameter was taken to design –expert again to check the significant of the process and value.

Table 4.17 Input parameter and response combination through BBD

| Run | Factor 1<br>A:Extrusion ratio | Factor 2<br>B:Ram speed | Factor 3<br>C:Temperature (℃) | Response 1<br>Damage | Response 2<br>load 2(KN) | Response 3<br>stress (Mpa) |
|---|---|---|---|---|---|---|
| 1 | 6 | 3.5 | 225 | 0.658 | 254 | 2010 |
| 2 | 6 | 2.5 | 255 | 0.68 | 243 | 1290.55 |
| 3 | 8 | 3 | 225 | 0.9 | 332 | 2325 |
| 4 | 6 | 3 | 265 | 0.742 | 269 | 1979.24 |
| 5 | 8 | 3.5 | 265 | 0.7713 | 282 | 2272 |
| 6 | 8 | 2.5 | 185 | 0.7863 | 305 | 2301 |
| 7 | 8 | 3 | 255 | 0.9 | 332 | 2325 |
| 8 | 8 | 3 | 255 | 0.9 | 332 | 2325 |
| 9 | 6 | 3 | 185 | 0.5893 | 222 | 2585.18 |
| 10 | 10 | 3 | 265 | 0.7713 | 285 | 2509.04 |
| 11 | 10 | 3.5 | 255 | 0.752 | 279 | 2010.05 |
| 12 | 8 | 3.5 | 185 | 0.75 | 273 | 2244 |
| 13 | 10 | 3 | 185 | 0.875 | 311 | 2554.76 |
| 14 | 10 | 2.5 | 225 | 0.94 | 364 | 2223.69 |
| 15 | 8 | 2.5 | 265 | 0.899 | 326 | 1629.88 |

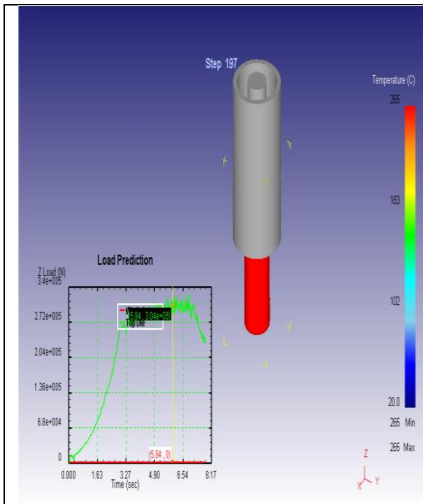

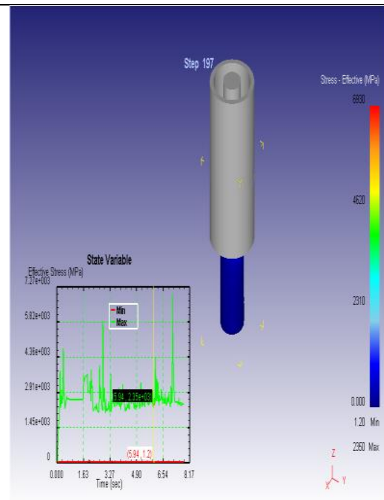

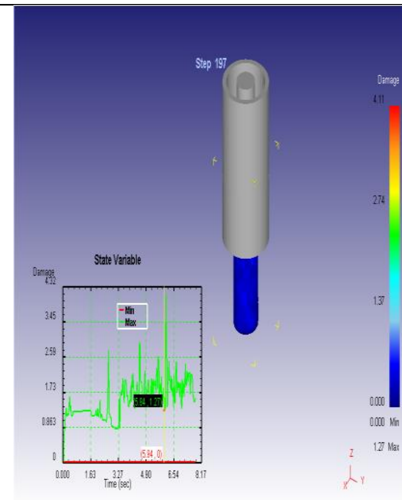


Response of load, effective stress and damage respectively for input 6,3.5m/s, and 255°C

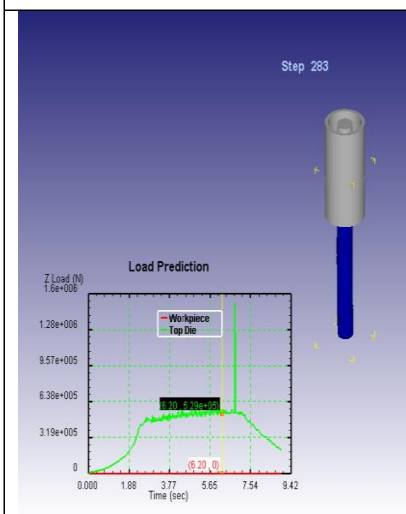

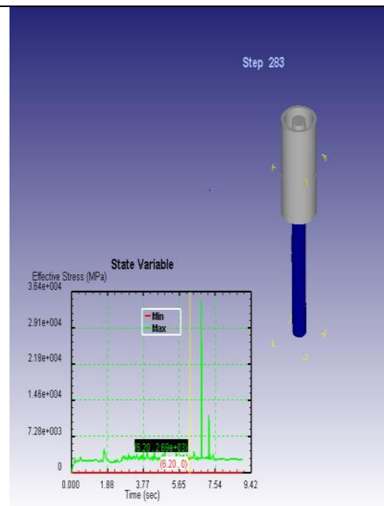

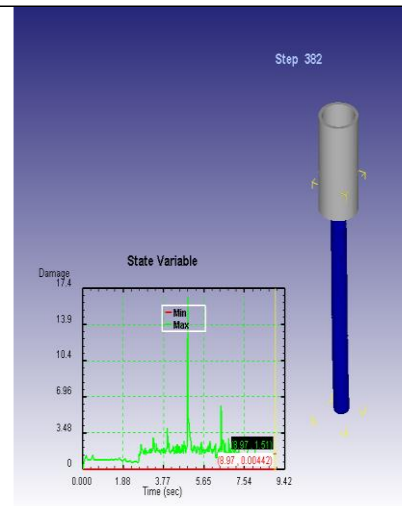


Response of load, effective stress and damage respectively for input 6,2.5m/s, and 255°C

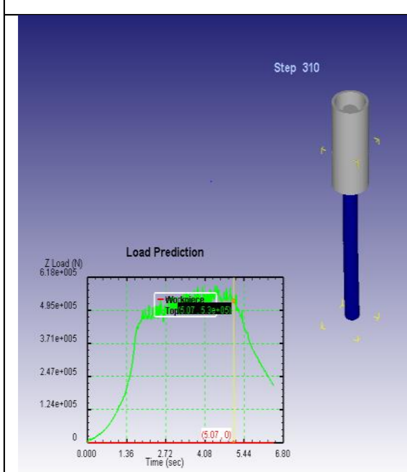

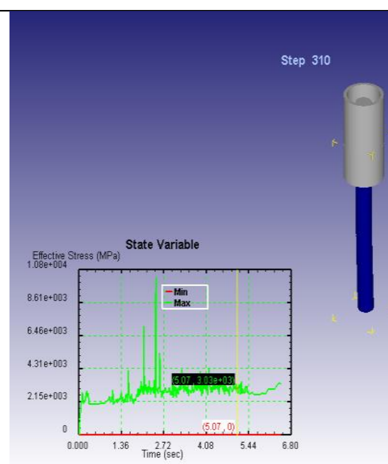

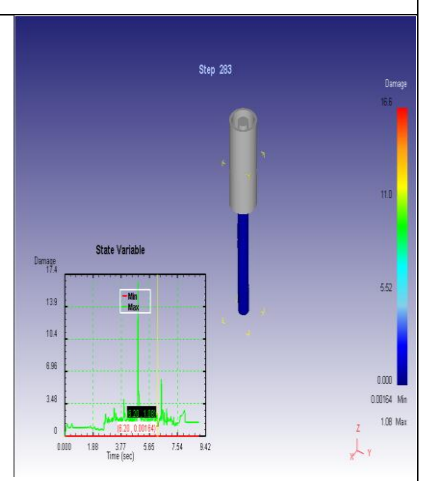

Response of load, effective stress and damage respectively for input 8,3m/s, and 255℃

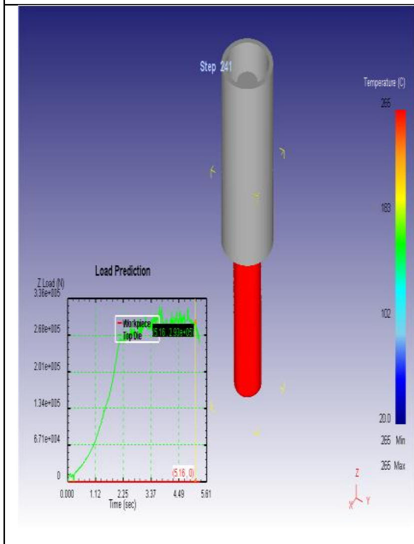


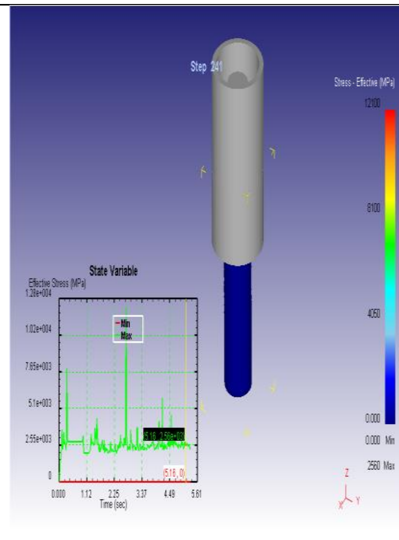


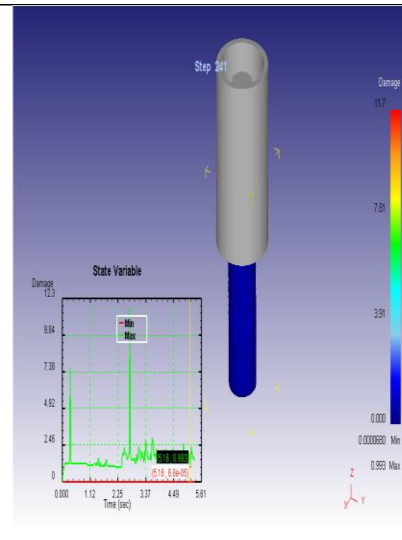


Response of load, effective stress and damage respectively for input 6,3m/s, and 265℃

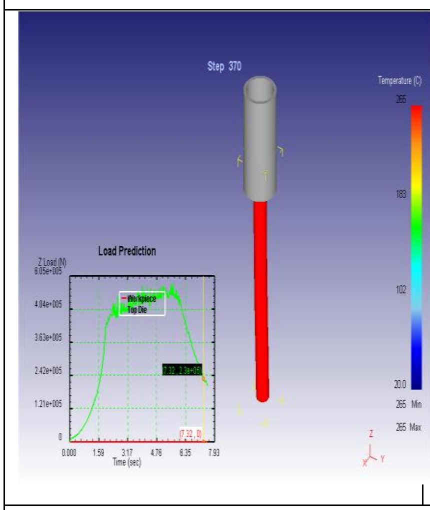


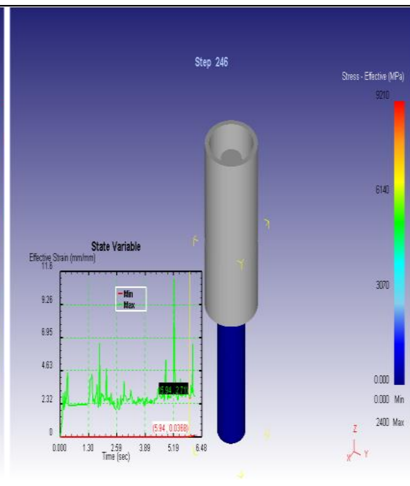


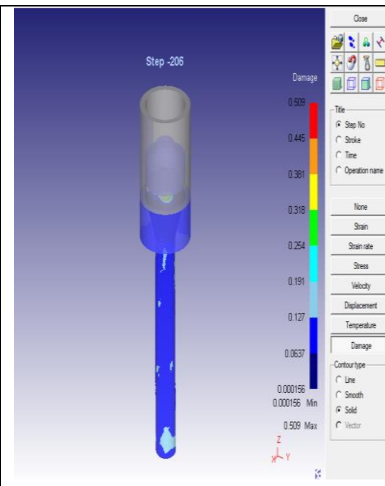


Response of load, effective stress and damage respectively for input 6,3.5m/s,and 265℃

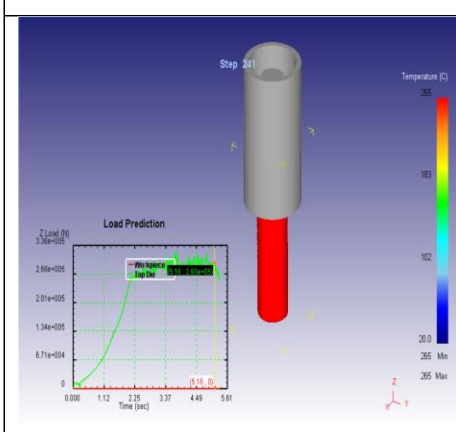


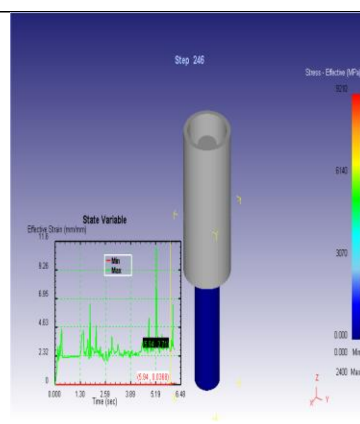


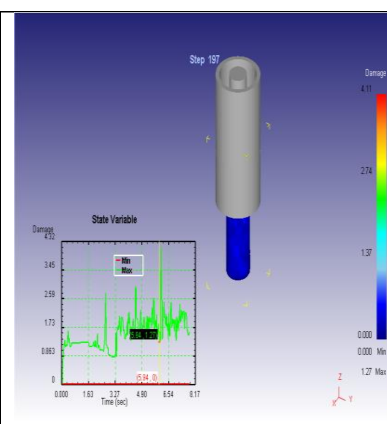


Response of load, effective stress and damage respectively for input 8,3.5m/s,and 265℃

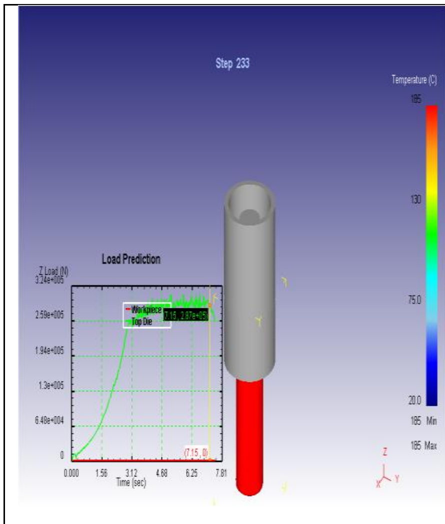

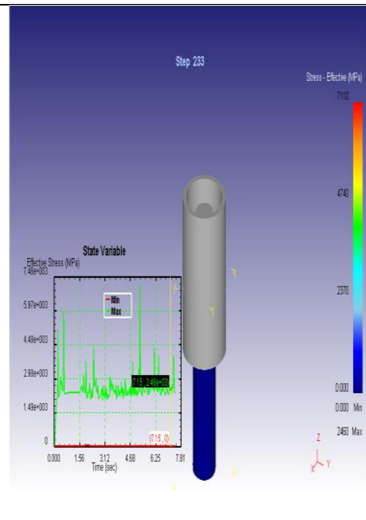

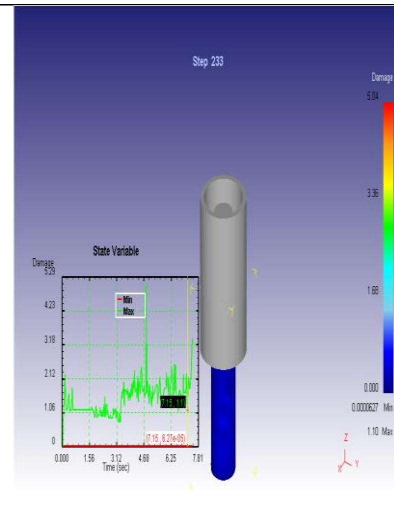


Response of load, effective stress and damage respectively for input 8,2.5m/s,and 185℃

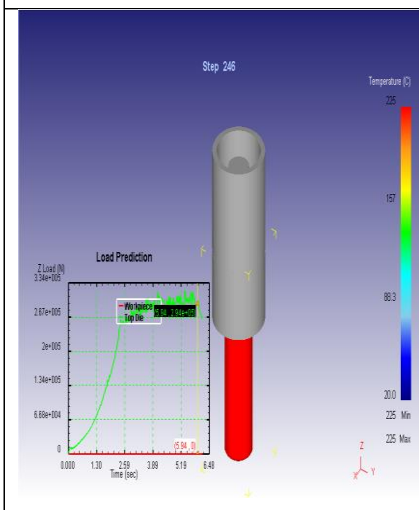

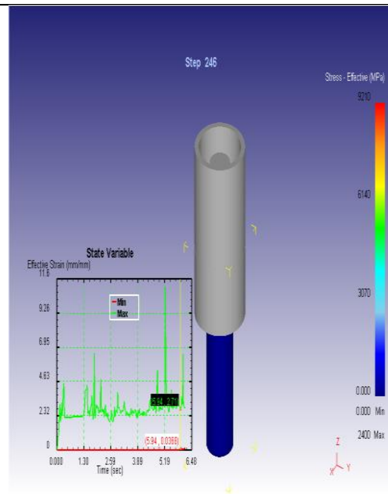

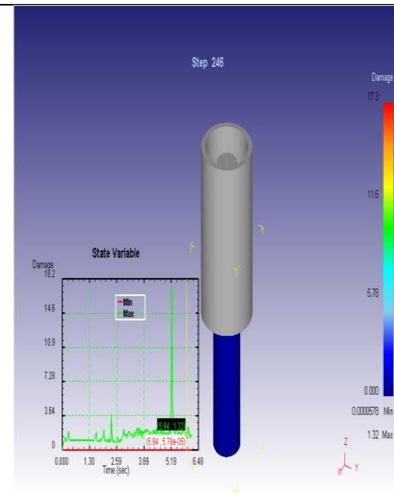


Response of load, effective stress and damage respectively for input 8,3m/s,and 255℃

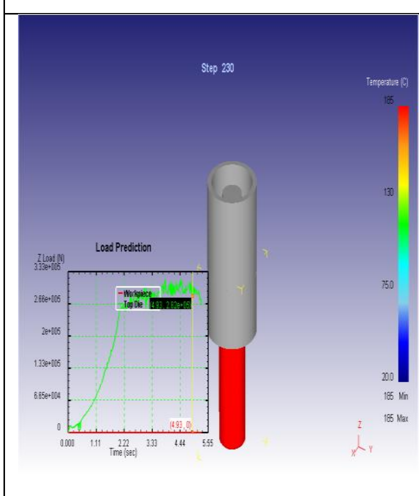

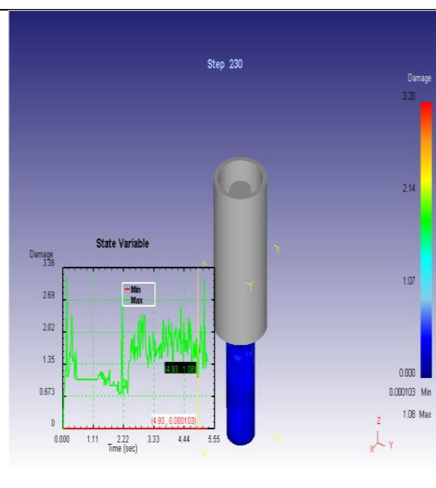

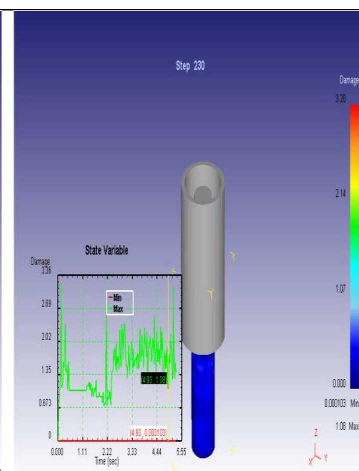


Response of load, effective stress and damage respectively for input 6,3m/s,and 185℃

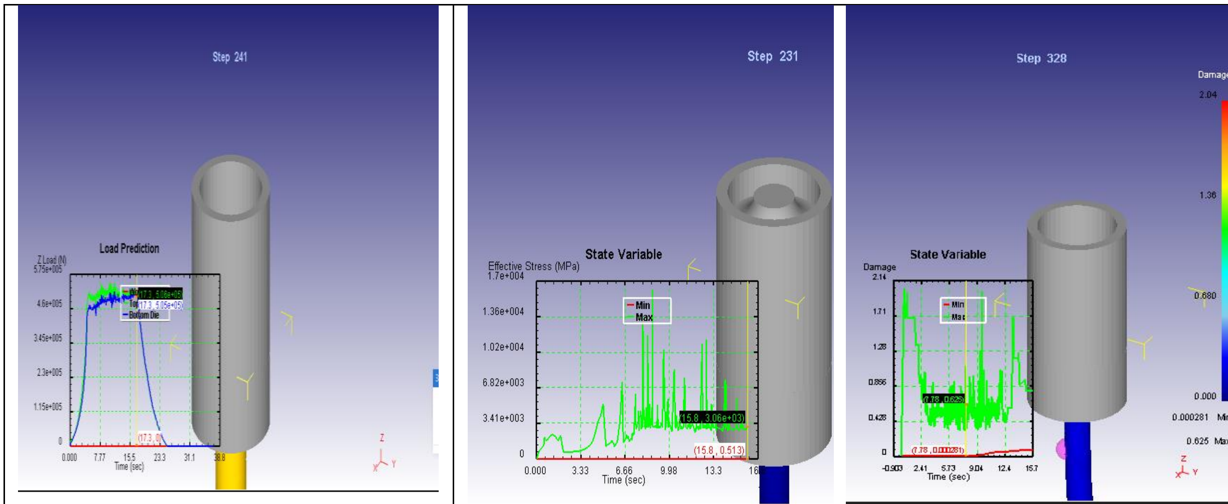


Response of load, effective stress and damage respectively for input 10,3m/s,and 265℃

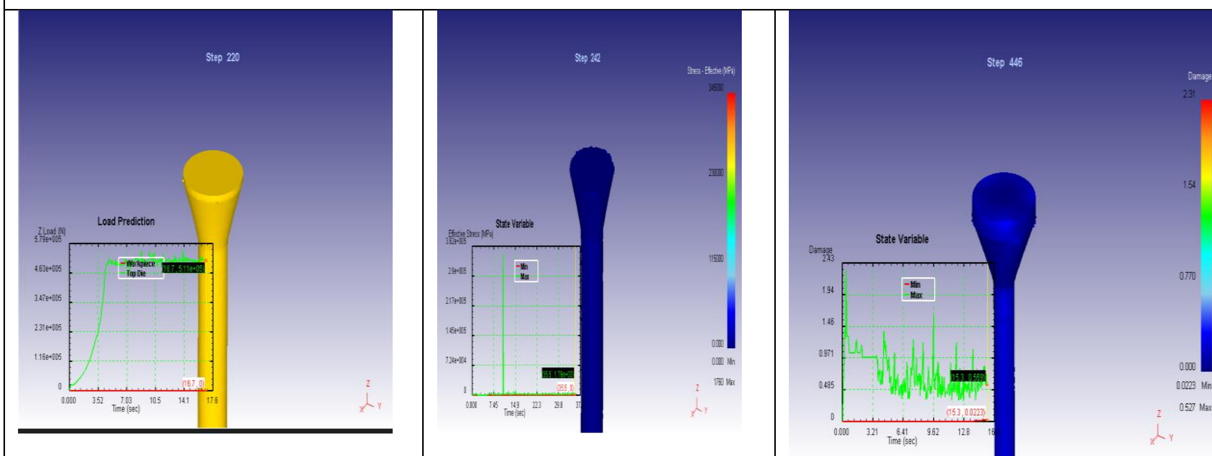


Response of load, effective stress and damage respectively for input 10,3.5m/s,and 255℃

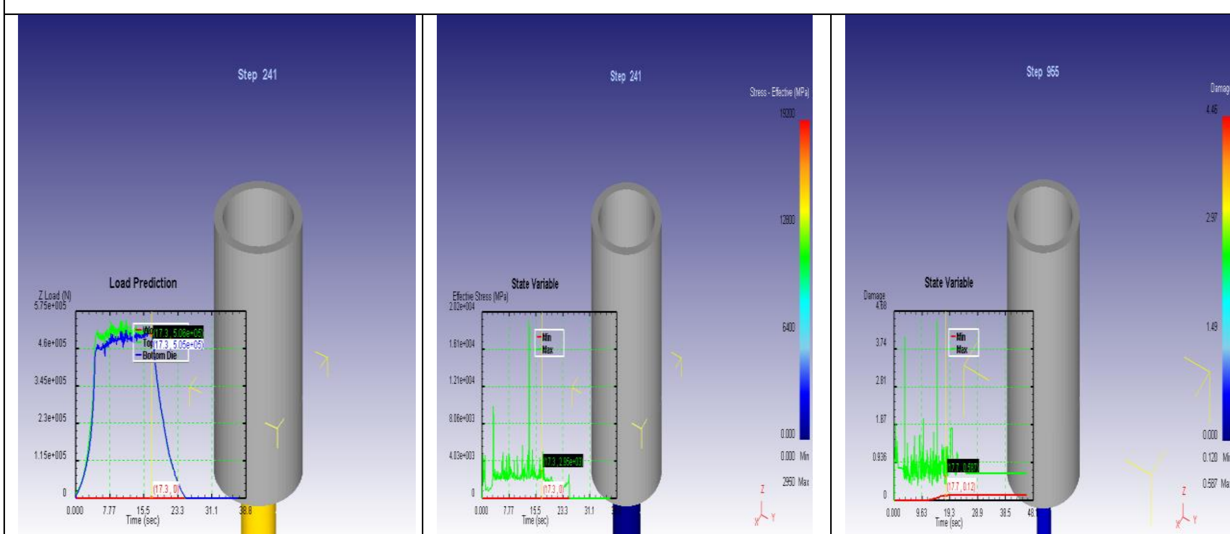


Response of load, effective stress and damage respectively for input 8,3.5m/s, and 255℃

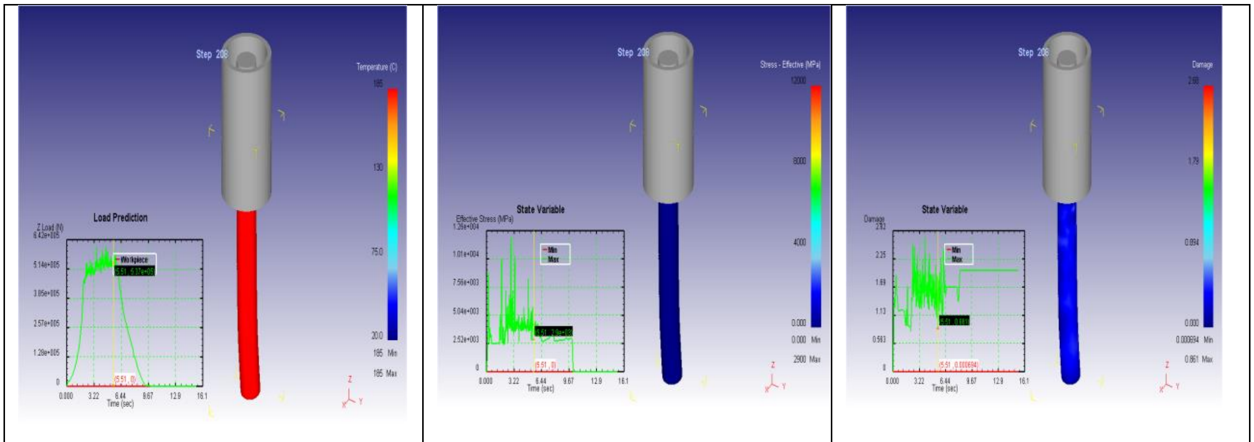

Response of load, effective stress and damage respectively for input 10,3m/s ,and 185℃

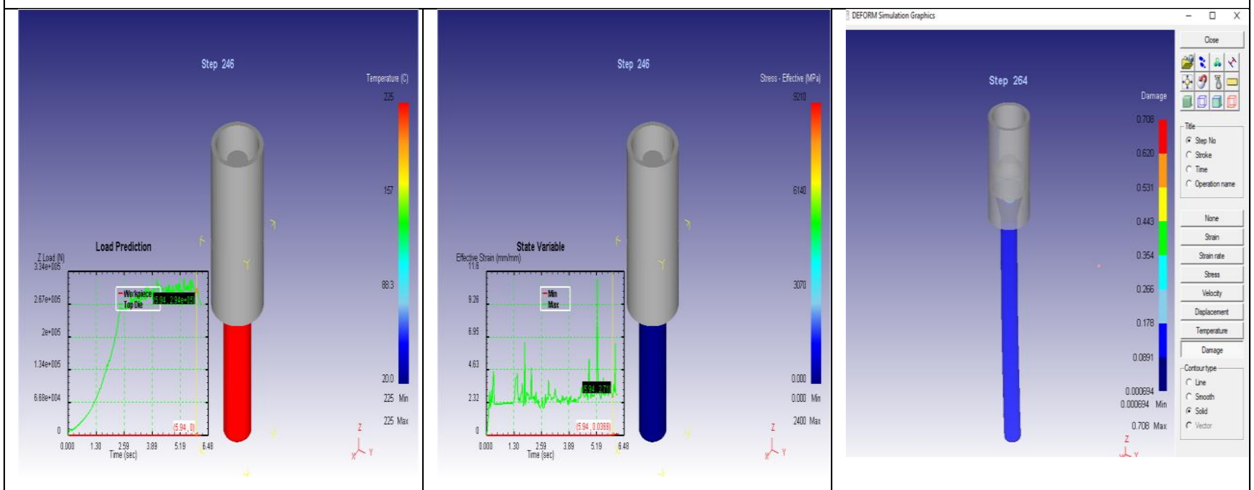

Response of load, effective stress and damage respectively for input 10,2.5m/s ,and 255℃

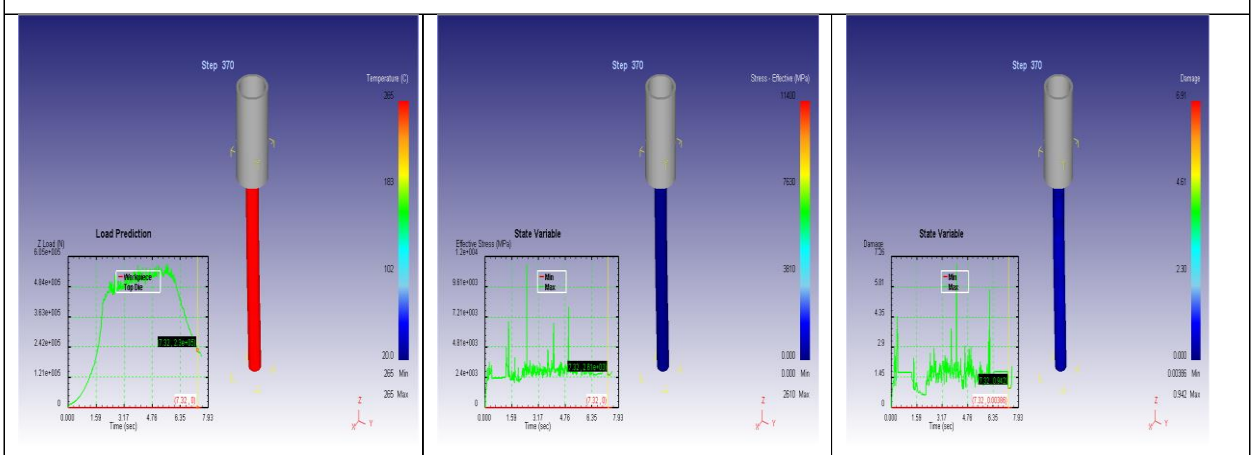

Response of load, effective stress and damage respectively for input 10,2.5m/s ,and 265℃

Figure 4.11 Load, effective stress, damage response taken for each combination of input parameter

### 4.9.1. Damage analysis of simulated composite

#### 4.9.1.1.Statistical Analysis damage

The statistical Analysis was performed on damage response to analysis the effect of input parameters on damage during cold extrusion fabricated sample. The input extrusion parameter with damage response that was predicted through simulation using 3D deform software was checked (significance of the relation) with response surface methodology of design of expert software. The fit summary program in design expert computed the influence of all model term on damage and generated the statistics p-values, lack of fit and R-squared. Table of Quadratic model, Sequential Model Sum of Squares showed that quadratic model was suggested whereas cubic was aliased i.e., it is the ultimate order model that justifies significantly because the variation in the response (p-value small), and reasonable agreement between Adjusted R-squared and Predicted R-squared (within 0.2 of each other).

Table 4.18 Quadratic model for damage in fit summary

| Source | Sequential p-value | Lack of Fit p-value | Adjusted $R^2$ | Predicted $R^2$ | |
|---|---|---|---|---|---|
| Linear | 0.0446 | - | 0.3708 | 0.1584 | |
| 2FI | 0.3274 | - | 0.4246 | 0.1616 | |
| Quadratic | 0.0002 | - | 0.9752 | 0.8585 | Suggested |
| Cubic | | | 1.0000 | | Aliased |

Table 4.19 Sequential Model Sum of Squares for damage

| Source | Sum of Squares | Df | Mean Square | F-value | p-value | |
|---|---|---|---|---|---|---|
| Mean vs. Total | 9.46 | 1 | 9.46 | | | |
| Linear vs. Mean | 0.0776 | 3 | 0.0259 | 3.75 | 0.0446 | |
| 2FI vs. Linear | 0.0254 | 3 | 0.0085 | 1.34 | 0.3274 | |
| Quadratic vs. 2FI | 0.0491 | 3 | 0.0164 | 60.28 | 0.0002 | Suggested |
| Cubic vs. Quadratic | 0.0014 | 3 | 0.0005 | | | Aliased |
| Residual | 0.0000 | 2 | 0.0000 | | | |
| Total | 9.62 | 15 | 0.6411 | | | |

#### 4.9.1.2. Analysis of Variance for damage

In Design of Experiments (DOE), the significance and contribution of independent variables on the response variable was analyzed by ANOVA. The important terms in the model were identified based on low value of P. From the table of Analysis of Variance for damage it was observed that The Model F-value of 62.25 suggests the model is significant and only a 0.01% probability that an F-value this greater could happen due to noise. P-values less than 5% imply model terms are statistically significant. Significant model terms were observed for A, B, C, AB, AC, BC, $A^2$, $B^2$, and $C^2$ also. The insignificant model term was indicated by the Values greater than 10%.From the table of Fit of statistics of damage of material it was observed that the model fit the data because the change between Predicted R-Squared and Adjusted R squared is less than 0.2.the model can be used navigate the design space because Adequate Precision ratio of 26.427 is greater than 4.the Percentage of contribution was calculated by dividing sum of squares of individual source by sum of square of Cor Total.

Table 4.20 Analysis of Variance result for damage

| Source | Sum of Squares | Df | Mean Square | F-value | p-value | | Percentage of contribution |
|---|---|---|---|---|---|---|---|
| Model | 0.1521 | 9 | 0.0169 | 62.25 | 0.0001 | Significant | 99.087% |
| A-extrusion ratio | 0.0559 | 1 | 0.0559 | 206.02 | $< 0.0001$ | | 36.41% |
| B-ram speed | 0.0175 | 1 | 0.0175 | 64.39 | 0.0005 | | 11.4% |
| C-temperature | 0.0042 | 1 | 0.0042 | 15.42 | 0.0111 | | 2.736% |
| AB | 0.0069 | 1 | 0.0069 | 25.37 | 0.0040 | | 4.495% |
| AC | 0.0164 | 1 | 0.0164 | 60.52 | 0.0006 | | 10.68% |
| BC | 0.0021 | 1 | 0.0021 | 7.69 | 0.0392 | | 1.368% |
| $A^2$ | 0.0368 | 1 | 0.0368 | 135.63 | $< 0.0001$ | | 23.97% |
| $B^2$ | 0.0067 | 1 | 0.0067 | 24.70 | 0.0042 | | 4.36% |
| $C^2$ | 0.0115 | 1 | 0.0115 | 42.22 | 0.0013 | | 7.49% |
| Residual | 0.0014 | 5 | 0.0003 | | | | |
| Lack of Fit | 0.0014 | 3 | 0.0005 | | | | |
| Pure Error | 0.0000 | 2 | 0.0000 | | | | |
| Cor Total | 0.1535 | 14 | | | | | |

Table 4.21 Fit of statistic perfumed for damage

| | | | |
|---|---|---|---|
| Std. Dev. | 0.0165 | $R^2$ | 0.9912 |
| Mean | 0.7943 | Adjusted $R^2$ | 0.9752 |
| C.V. % | 2.07 | Predicted $R^2$ | 0.8585 |
| | | Adeq Precision | 26.4272 |

Regression Model for damage $= -7.38778 + 0.746094X_1 + 1.51856\ X_2 + 0.026082\ X_3 - 0.0415\ X_1\ X_2 - 0.00080125\ X_1\ X_3 - 0.0011425\ X_2\ X_3 - 0.0249688\ X_1^2 - 0.1705\ X_2^2 - 3.48281e\text{-}05X_3^2$

Where, $X_1$ is stand for A or extrusion ratio or, $X_2$ is stand for or ram speed, $X_3$is stand for C or temperature.

#### 4.9.1.3. Parametric influence on damage

The graph of predict plot verses actual on figure (a) showed that the actual value follow a normal distribution, thus follow straight line and the graph of Normal % probability of vs. internally studentized residual figure (b) which is a plot of the internally studentized residual versus the ascending predicted response values used to tests assumption of constant variance and the plot showed a random scatter or constant range of internally studentized residual cross the graph that indicates there is no need for a transformation. So, the model is suitable to conduct analysis on effect of individual parameters on surface roughness

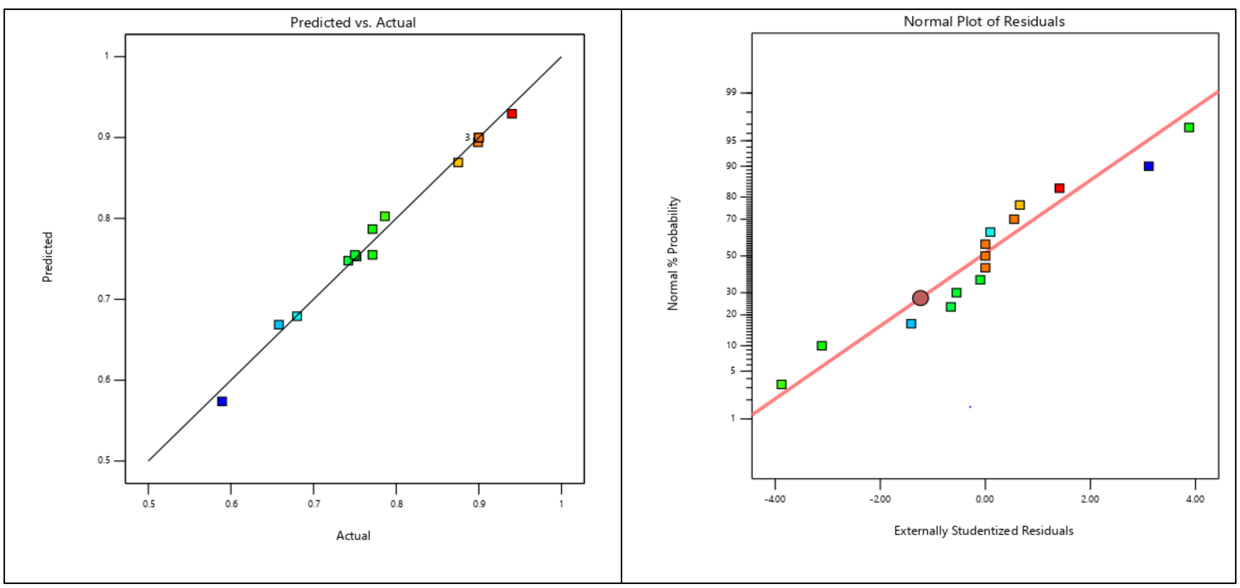


Figure 4.12 (a) predict plot verses actual and (b) Normal % probability of vs. internally studentized residual for damage

#### 4.9.1.4. Effect of extrusion parameter on damage

The contribution percentage of each extrusion parameter was calculated from ANOVA table. This percentage was recorded for extrusion ratio 36.41% Ram speed 11.4%and billet temperature 2.736%. Based the value of the contribution parameters extrusion ratio with largest percentage have more effect. Closely relate the value of ram speed and temperature percentage contribution and small value and did not effect on damage. But extrusions ration have effect on damage response. The ANOVA with p values of extrusion ratio (P< 0.001) and R-square value result 99.087 of table with extrusion ratio is significant factors effect on damage

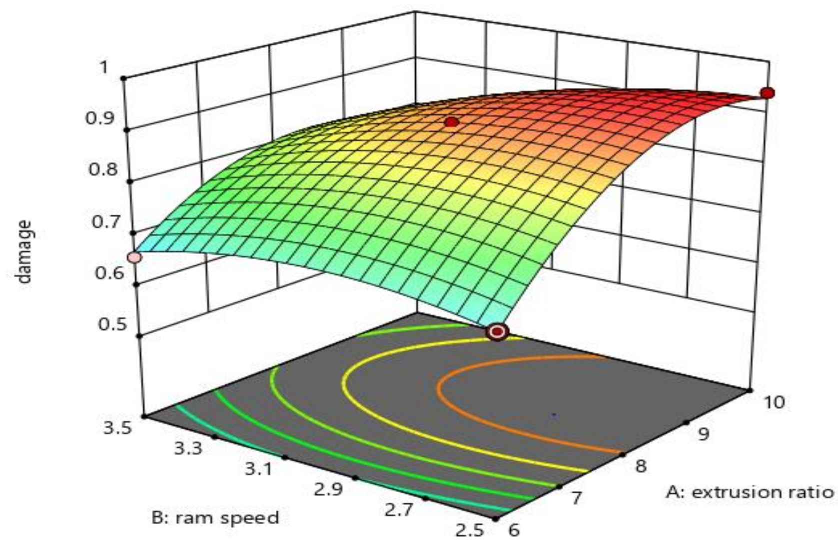


Figure 4.13 Effect of extrusion parameter on damage

### 4.9.2. Analysis load of simulated composite

#### 4.9.2.1. Statistical Analysis of load

The statistical Analysis was performed on load response to analysis the effect of input parameters on load during cold extrusion of fabricated sample. The input extrusion parameter with load response that was predicted through simulation using 3D deform software was checked (significance of the relation) with response surface methodology of design of expert software. The fit summary program in design expert computed the influence of all model term on load and generated the statistics p-values, lack of fit and R-squared. Table of Quadratic model, Sequential Model Sum of Squares showed that quadratic model was suggested whereas cubic was aliased i.e., it is the ultimate order model that justifies significantly because the variation in the response (p-value small), and reasonable agreement between Adjusted R-squared and Predicted R-squared (within 0.2 of each other).

Table 4.22 Fit summary result for load

| Source | Sequential p-value | Lack of Fit p-value | Adjusted $R^2$ | Predicted $R^2$ | |
|---|---|---|---|---|---|
| Linear | 0.0424 | | 0.3772 | 0.1523 | |
| 2FI | 0.3059 | | 0.4416 | 0.1427 | |
| Quadratic | 0.0004 | | 0.9713 | 0.8362 | Suggested |
| Cubic | | | 1.0000 | | Aliased |

Table 4.23 Sequential Model Sum of Squares for load

| Source | Sum of Squares | Df | Mean Square | F-value | p-value | |
|---|---|---|---|---|---|---|
| Mean vs. Total | 1.296E+06 | 1 | 1.296E+06 | | | |
| Linear vs. Mean | 11012.75 | 3 | 3670.92 | 3.83 | 0.0424 | |
| 2FI vs. Linear | 3672.25 | 3 | 1224.08 | 1.42 | 0.3059 | |
| Quadratic vs. 2FI | 6661.18 | 3 | 2220.39 | 50.29 | 0.0004 | Suggested |
| Cubic vs. Quadratic | 220.75 | 3 | 73.58 | | | Aliased |
| Residual | 0.0000 | 2 | 0.0000 | | | |
| Total | 1.318E+06 | 15 | 87834.60 | | | |

#### 4.9.2.2. Analysis of Variance for load

From the table of Analysis of Variance for load it was observed that The Model F-value of 53.72 suggests the model is significant and only a 0.01% probability that an F-value this greater could happen due to noise. P-values less than 5% imply model terms are statistically significant. Significant model terms were observed for A, B, C, AB, AC, BC, $A^2$, $B^2$, and C2 also. The insignificant model term was indicated by the Values greater than 10%.From the table of Fit of statistics of damage of material it was observed that the model fit the data because the change between Predicted R-Squared and Adjusted R squared is less than 0.2.the model can be used navigate the design space because Adequate Precision ratio of 26.4274 is greater than 4.The Percentage of contribution was computed by dividing sum of squares of individual source by sum of square of Cor Total.

Table 4.24 Analysis of Variance result for load

| Source | Sum of Squares | df | Mean Square | F-value | p-value | | Percentage of contribution |
|---|---|---|---|---|---|---|---|
| Model | 21346.18 | 9 | 2371.80 | 53.72 | 0.0002 | (significant) | 98.976% |
| A-extrusion ratio | 7875.12 | 1 | 7875.12 | 178.37 | < 0.0001 | | 36.51% |
| B-ram speed | 2812.50 | 1 | 2812.50 | 63.70 | 0.0005 | | 13.040% |
| C-temperature | 325.13 | 1 | 325.13 | 7.36 | 0.0421 | | 1.5075% |
| AB | 2304.00 | 1 | 2304.00 | 52.19 | 0.0008 | | 10.683% |
| AC | 1332.25 | 1 | 1332.25 | 30.18 | 0.0027 | | 6.17728% |
| BC | 36.00 | 1 | 36.00 | 0.8154 | 0.4079 | | 0.1669% |
| $A^2$ | 4752.06 | 1 | 4752.06 | 107.63 | 0.0001 | | 22.03% |
| $B^2$ | 456.98 | 1 | 456.98 | 10.35 | 0.0235 | | 2.1188% |
| $C^2$ | 2193.75 | 1 | 2193.75 | 49.69 | 0.0009 | | 10.17% |
| Residual | 220.75 | 5 | 44.15 | | | | |
| Lack of Fit | 220.75 | 3 | 73.58 | | | | |
| Pure Error | 0.0000 | 2 | 0.0000 | | | | |
| Cor Total | 21566.93 | 14 | | | | | |

Table 4.25 Fit Statistics result for load

| | | | |
|---|---|---|---|
| Std. Dev. | 6.64 | $R^2$ | 0.9898 |
| Mean | 293.93 | Adjusted $R^2$ | 0.9713 |
| C.V. % | 2.26 | Predicted $R^2$ | 0.8362 |
| | | Adeq Precision | 26.4274 |

Regression Model for Z load = -2550.47 + 282.516 $X_1$ + 455.25 $X_2$ + 9.28984 $X_3$ -24 $X_1$ $X_2$ - 0.228125 X1 $X_3$-0.15 X2 $X_3$ -8.96875 $X_1^2$ -44.5 $X_2^2$ -0.0152344 $X_3^2$

#### 4.9.2.3. Parametric influence on load

The graph of predict plot verses actual load on figure (a) showed that the actual value follow a normal distribution, thus follow straight line and the graph of Normal % probability of vs. internally studentized residual figure (b) which is a plot of the internally studentized residual versus the ascending predicted response values used to tests assumption of constant variance and the plot showed a random scatter or constant range of internally studentized residual cross the graph that indicates there is no need for a transformation. So, the model is suitable to conduct analysis on effect of individual parameters on surface roughness

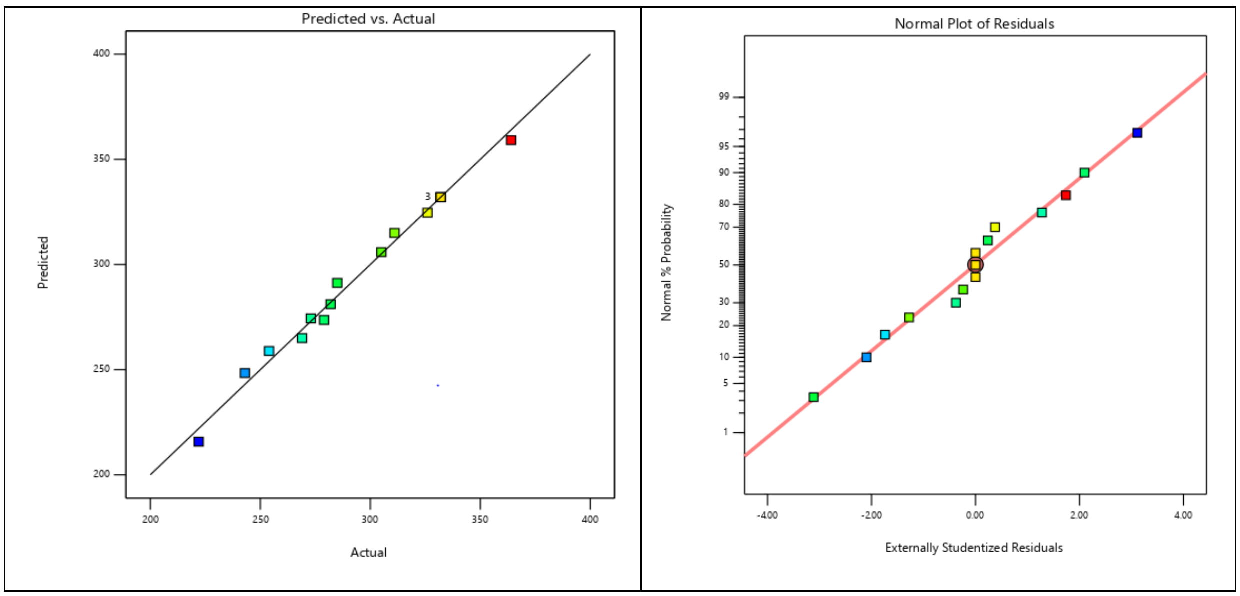


Figure 4.14 (a) predict plot verses actual and (b) Normal % probability of vs. internally studentized residual for load

#### 4.9.2.4. Effect of extrusion parameter on load

The contribution percentage of each extrusion parameter was calculated from ANOVA table. This percentage was recorded for extrusion ratio 36.51%. Ram speed 13.040% c and billet temperature 1.5075%. Based the value of the contribution parameters extrusion ratio with largest percentage have more effect. Closely relate the value of ram speed and temperature percentage contribution and small value and did not effect on damage. But extrusions ration have effect on load response. The ANOVA with p values of extrusion ratio (P< 0.001) and R-square value 98.976as result of table with extrusion ratio is significant factors effect on load.

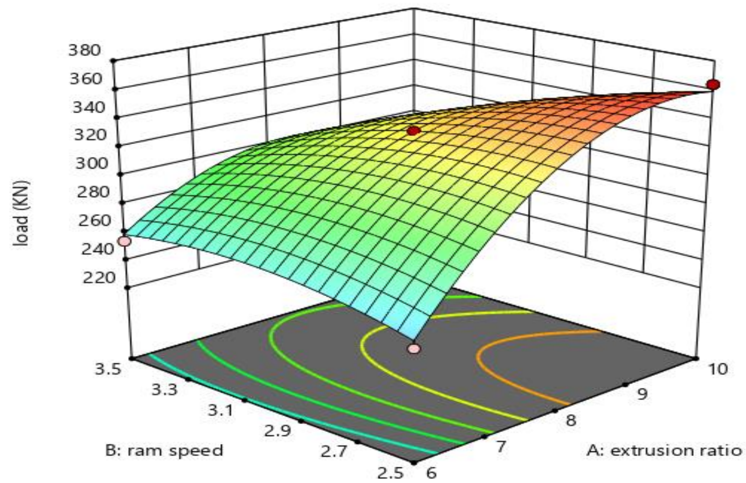


Figure 4.15 Effect of extrusion parameter analyze on load

#### 4.9.3. Effective stress analysis of simulated composite

##### 4.9.3.1.Statistical of effective stress

The statistical Analysis was performed on effective stress response to analysis the effect of input parameters on effective stress during cold extrusion of fabricated sample. The input extrusion parameter with effective stress response that was predicted through simulation using 3D deform software was checked (significance of the relation) with response surface methodology of design of expert software. The fit summary program in design expert computed the influence of all model term on effective stress and generated the statistics p-values, lack of fit and R-squared. Table of Quadratic model, Sequential Model Sum of Squares showed that quadratic model was suggested whereas cubic was aliased i.e., it is the ultimate order model that justifies significantly because the variation in the response (p-value small), and reasonable agreement between Adjusted R-squared and Predicted R-squared (within 0.2 of each other).

Table 4.26 Fit summery result for effective stress

| Source | Sequential p-value | Lack of Fit p-value | Adjusted $R^2$ | Predicted $R^2$ | |
|---|---|---|---|---|---|
| Linear | 0.1650 | | 0.1840 | -0.3325 | |
| 2FI | 0.2535 | | 0.3070 | -0.9379 | |
| Quadratic | 0.0005 | | 0.9596 | 0.7691 | Suggested |
| Cubic | | | 1.0000 | | Aliased |

Table 4.27 Sequential Model Sum of Squares result for effective stress

| Source | Sum of Squares | Df | Mean Square | F-value | p-value | |
|---|---|---|---|---|---|---|
| Mean vs. Total | 7.091E+07 | 1 | 7.091E+07 | | | |
| Linear vs. Mean | 5.972E+05 | 3 | 1.991E+05 | 2.05 | 0.1650 | |
| 2FI vs. Linear | 4.081E+05 | 3 | 1.360E+05 | 1.65 | 0.2535 | |
| Quadratic vs. 2FI | 6.351E+05 | 3 | 2.117E+05 | 44.08 | 0.0005 | Suggested |
| Cubic vs. Quadratic | 24013.49 | 3 | 8004.50 | | | Aliased |
| Residual | 0.0000 | 2 | 0.0000 | | | |
| Total | 7.258E+07 | 15 | 4.839E+06 | | | |

#### 4.9.3.2.Analysis of Variance for effective stress

From the table of Analysis of Variance for effective stress it was observed that The Model F-value of 37.95 suggests the model is significant and only a 0.04%probability that an F-value this greater could happen due to noise. P-values less than 5% imply model terms are statistically significant. Significant model terms were observed for A, B, C, AB, AC, BC, $A^2$, $B^2$, and C2 also. The insignificant model term was indicated by the Values greater than 10%.From the table of Fit of statistics of damage of material it was observed that the model fit the data because the change between Predicted R-Squared and Adjusted R squared is less than 0.2.the model can be used navigate the design space because Adequate Precision ratio of 26.4274 is greater than 4.The Percentage of contribution was calculated by dividing sum of squares of individual source by sum of square of Cor Total.

Table 4.28Analysis of Variance result for effective stress

| Source | Sum of Squares | Df | Mean Square | F-value | p-value | | Percentage contribution |
|---|---|---|---|---|---|---|---|
| Model | 1.640E+06 | 9 | 1.823E+05 | 37.95 | 0.0004 | (Significant) | 98.557% |
| A-extrusion ratio | 2.565E+05 | 1 | 2.565E+05 | 53.41 | 0.0008 | | 15.414% |
| B-ram speed | 1.407E+05 | 1 | 1.407E+05 | 29.30 | 0.0029 | | 8.455% |
| C-temperature | 2.000E+05 | 1 | 2.000E+05 | 41.63 | 0.0013 | | 12.01% |
| AB | 2.177E+05 | 1 | 2.177E+05 | 45.32 | 0.0011 | | 13.08% |
| AC | 78461.61 | 1 | 78461.61 | 16.34 | 0.0099 | | 4.715% |
| BC | 1.119E+05 | 1 | 1.119E+05 | 23.31 | 0.0048 | | 6.72% |
| $A^2$ | 21775.99 | 1 | 21775.99 | 4.53 | 0.0865 | | 1.308% |
| $B^2$ | 4.909E+05 | 1 | 4.909E+05 | 102.22 | 0.0002 | | 29.50% |
| $C^2$ | 93170.66 | 1 | 93170.66 | 19.40 | 0.0070 | | 5.5991% |
| Residual | 24013.49 | 5 | 4802.70 | | | | |
| Lack of Fit | 24013.49 | 3 | 8004.50 | | | | |
| Pure Error | 0.0000 | 2 | 0.0000 | | | | |
| Cor Total | 1.664E+06 | 14 | | | | | |

Table 4.29 Fit statistics result effective stress

| | | | |
|---|---|---|---|
| Std. Dev. | 69.30 | $R^2$ | 0.9856 |
| Mean | 2174.29 | Adjusted $R^2$ | 0.9596 |
| C.V. % | 3.19 | Predicted $R^2$ | 0.7691 |
| | | Adeq Precision | 22.3658 |

$$\text{Regression Model Stress} = -4428.6 + 702.633\,X1 + 9000.66\,X2 - 87.7269\,X_3 - 233.272\,X_1 X_2 + 1.75069 X_1 X_3 + 8.364\,X2\,X_3 - 19.1991\,X12 - 1458.52\,X_2^2 + 0.099282\,X_3^2$$

### 4.9.3.3.Parametric influence on effective stress

The graph of predict plot verses actual effective stress on figure (a) showed that the actual value follow a normal distribution, thus follow straight line and the graph of Normal % probability of vs. internally studentized residual figure (b) which is a plot of the internally studentized residual versus the ascending predicted response values used to tests assumption of constant variance and the plot showed a random scatter or constant range of internally studentized residual cross the graph that indicates there is no need for a transformation. So, the model is suitable to conduct analysis on effect of individual parameters on surface roughness

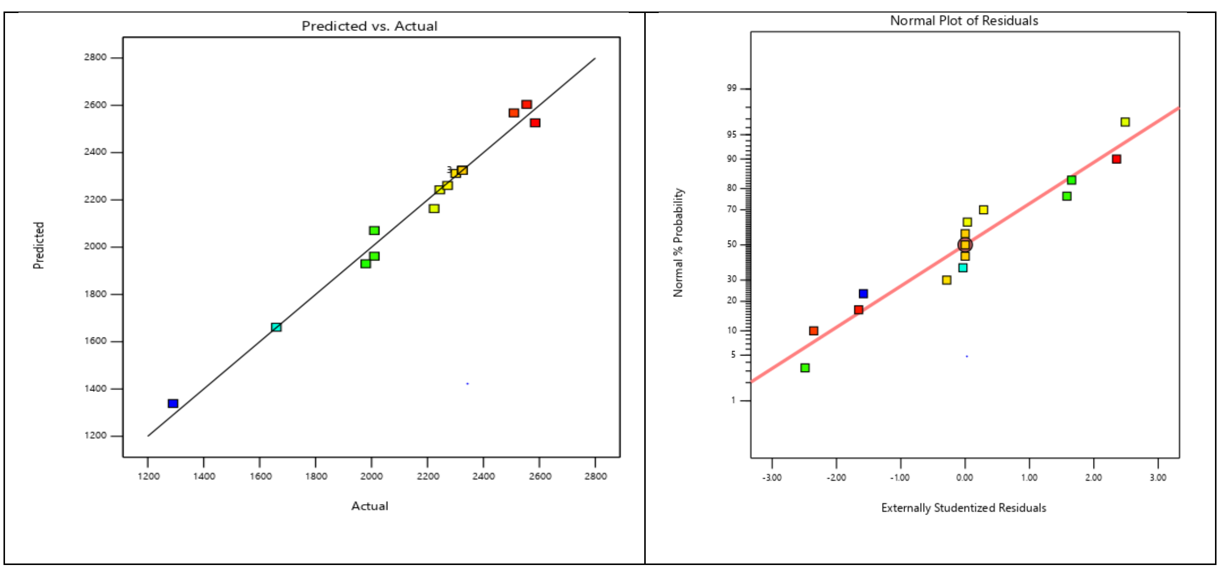


Figure 4.16 (a) Predict plot verses actual and (b) Normal % probability of vs. internally studentized residual for effective stress

#### 4.9.3.4. Effect of extrusion on effective stress

The contribution percentage of each extrusion parameter was calculated from ANOVA table. This percentage was recorded for extrusion ratio 15.414%Ram speed 8.455%and billet temperature 12.01%.Based the value of the contribution parameters extrusion ratio with largest percentage have more effect. Closely relate the value of ram speed and temperature percentage contribution and small value and did not effect on damage. But extrusions ration have effect on effect stress response. The ANOVA with p values of extrusion ratio (P< 0.001) and R-square value result 98.557 as of table with extrusion ratio is significant factors effect on effective stress.

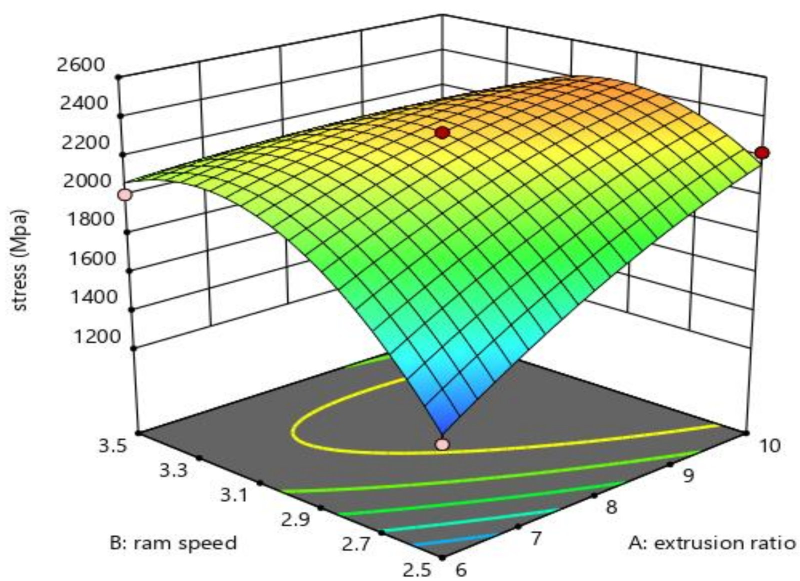


Figure 4.17 Effect of extrusion parameter on effective stress

## 4.10. Optimization response through gray analysis

The three combination of parameter obtain from optimization through gray analysis that can provide best result after deformation through. Depend on the value in table below the one that have best effect deformation processes selected and the operation was preceded.

Table 4.30 Optimization response through gray analysis with mat lab

| | Damage | Load(N) | Effective stress | Extrusion ratio | Ram speed | Extrusion temperature |
|---|---|---|---|---|---|---|
| 1 | 0.513567 | -4867.99 | 2366.097 | 6 | 2.5 | 185 |
| 2 | 0.759236 | -10154.9 | 1691.501 | 6.146163 | 2.578622 | 264.828 |
| 3 | 0.736002 | -10074.6 | 1455.051 | 6.019844 | 2.501712 | 263.6537 |
| 4 | 0.733924 | -9783.52 | 1465.102 | 6.008892 | 2.501683 | 259.9429 |
| 5 | 0.513567 | -4867.99 | 2366.097 | 6 | 2.5 | 185 |
| 6 | 0.697944 | -7678.31 | 1687.452 | 6.017303 | 2.50273 | 231.2056 |
| 7 | 0.658756 | -6810.18 | 1827.784 | 6.001343 | 2.500155 | 218.0972 |
| 8 | 0.713432 | -10113.2 | 2511.002 | 6.41012 | 3.483817 | 264.8217 |
| 9 | 0.729973 | -10120.6 | 3243.036 | 8.93952 | 3.479054 | 264.9441 |
| 10 | 0.648013 | -10151.3 | 3531.143 | 9.93952 | 3.479054 | 264.9441 |
| 11 | 0.759487 | -10153.4 | 1590.787 | 6.190143 | 2.522787 | 264.7811 |
| 12 | 0.692235 | -7146.17 | 1881.27 | 6.066522 | 2.545311 | 223.3866 |
| 13 | 0.620282 | -6133.67 | 1988.289 | 6.000313 | 2.504471 | 207.254 |
| 14 | 0.672849 | -7051.25 | 1809.86 | 6.002743 | 2.514316 | 221.8396 |
| 15 | 0.633896 | -6331.79 | 1938.688 | 6.009298 | 2.501652 | 210.5019 |
| 16 | 0.720069 | -8525.94 | 1576.758 | 6.013718 | 2.503269 | 243.2305 |
| 17 | 0.731777 | -9350.22 | 1501.169 | 6.011509 | 2.504001 | 254.3243 |
| 18 | 0.673551 | -10141.9 | 3460.468 | 9.68952 | 3.478072 | 264.9441 |

Table 4.31 Optimum combination of parameter for best result of deformation

| Response | | Extrusion ratio | ram speed(m/s) | Temperature ℃ |
|---|---|---|---|---|
| Damage | 0.513567 | 6 | 2.5 | 185 |
| Load | 10074.6(N) | 6.019844 | 2.501712 | 263.6537 |
| Effective stress | 1455.051(Mpa) | 6.019844 | 2.501712 | 263.6537 |

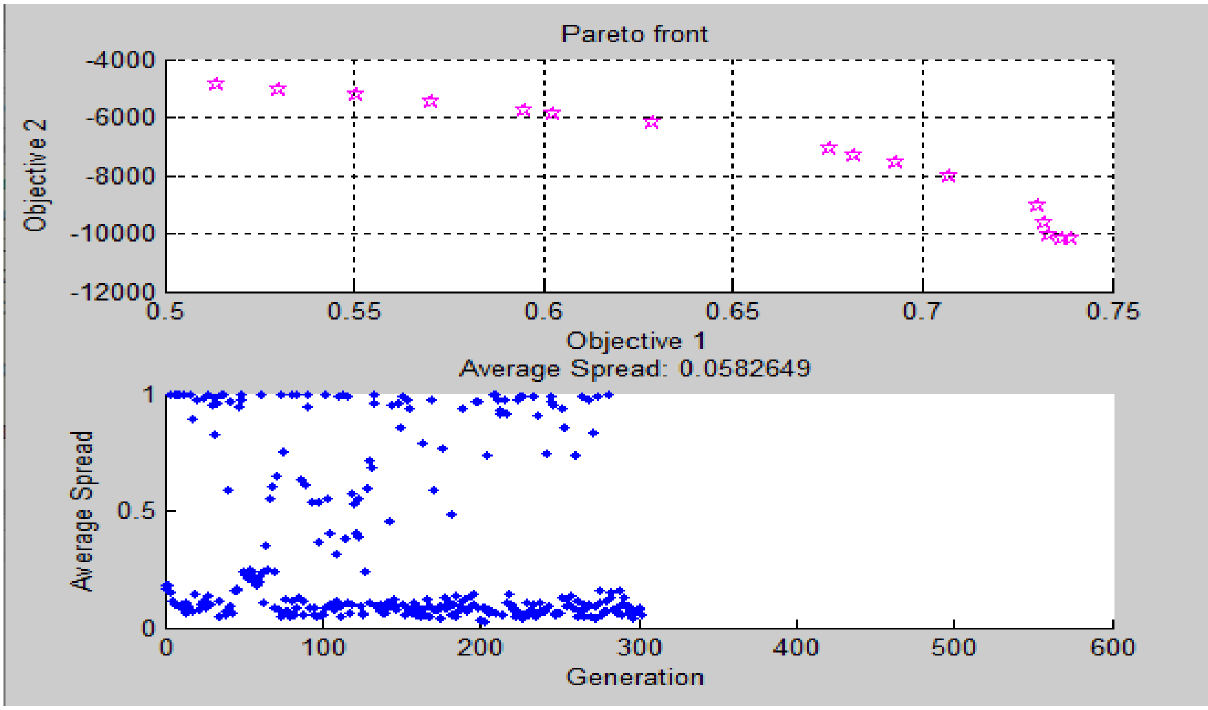


Figure 4.18 Genetic Algorithm for Average spread verses Objective and Generation verses Average spread

### 4.11. Confirmation experiments for the optimization process

To combined to taken optimal value selected as goal of target as based on minimized responses of load, effective stress to obtained from table above and results obtained from pareto optimal solution was compared with confirmation experiment of simulated in Design-Expert software selected optimal value was taken better value for secondary operation cold extrusion process .So closely related both optimal value in Design- Expert software and GA confirmation test was accepted. After decided those combined optimal values was done hot extrusion values and was checked mechanical properties after extrusion process and selected optimal value. The purpose was to obtain the parameter that result in minimum damage, load, and effective stress. So from conformation test, it was note that minimizing the response value was succeeded.

### 4.12. Actual cold extrusion on selected fabricated composite

Cold extrusion is a next secondary operation that was selected to perform forming operation on fabricated composite because it is best in further shape and improve the properties of the material as well dimensional accuracy. Going through all the above process, the cold extrusion was performed on selected stir cast fabricated (81%Al7075+7.5%$CeO_2$+7.5%SiC+4%GO) Composite. Using the cosine die, 6 extrusion ratio, 263.6537℃ Temperature and 2.5m/s ram speed the deformation was perfumed


Figure 4.19 Cold extruded samples

## 4.13. Analysis of results after extrusion process

Density, hardness, and compression strength tests were used to determine how the qualities of the composite samples improved during cold extrusion. The Extrusion process was perfumed with optimal parameter combination obtained for damage percentage, effective stress and extrusion ratio responses obtained using numerical simulation with DEFORM 3D. Selected(81%Al7075+7.5%$CeO_2$+7.5%SiC+4%GO) hybrid composite was extruded with cosine die of 6 extrusion ratios, 2.5mm/s ram speed and at 200.284 ℃ billet temperature. Composite was lubricated with semi-solid grease and solid lubricant graphite as lubricated hot forming is assumed for simulation.

### 4.13.1. Density and hardness test after cold Extrusion

The density and hardness of cold deformed (81%Al7075+7.5%$CeO_2$+7.5%SiC+4%GO) composite was to examine the change in material physical and mechanical properties after deformation operation. The actual density and hardness of casted sample was compared with the actual density and hardness of the same sample after it's deformed as show in table below

Table 4.32 Density and Hardness of extruded sample

| Sample | Casted density ($g/cm^3$ ) | Extruded density ($g/cm^3$ ) | Casted density (HV) | Extruded hardness (HV) | Casted Porosity | Extruded Porosity |
|---|---|---|---|---|---|---|
| (81%Al7075+7.5%$CeO_2$+7.5%SiC+4%GO) | 3.011 | 3.045 | 240.5 | 281.8 (287.2,274.6,283.6) | 0.02584 | 0.01487 |

As shown in table the density of the extruded sample increases to 3.045 ($g/cm^3$ ), when compare to casted sample density 3.011 ($g/cm^3$ ) and decrement in percentage porosity from 2.584% to 1.487% due to cold extrusion. These indicate the significance of the secondary process on density improvement and porosity reduction. The porosity reduction was happen due to plastic deformation, compressive stresses and decreases in the size and space of pores inside the sample while the material pass through the die during cold extrusion process. Improved density and reduction in porosity percentage shows the improvement in mechanical and physical properties of extruded composite sample.

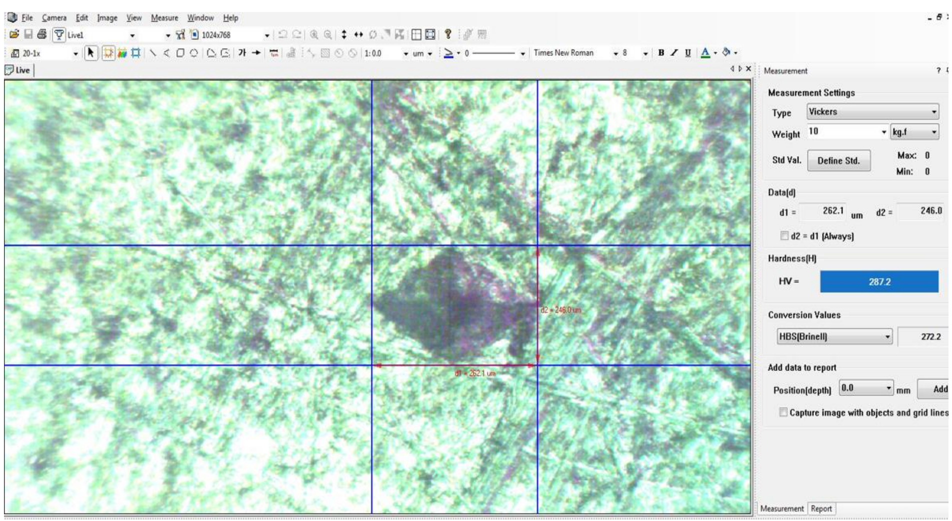


Figure 4.20 The hardness of extruded sample for trial 1.

As shown in table above the hardness of the extruded sample increases to 281.8 HV when compare to casted sample hardness 240.5HV. This improvement in hardness happen due to the change in microstructure especially grain structure in material due to stress occur caused by compressive pressure during cold extrusion. Another reason for the improvement is more uniformly reinforcement particles distortion and dispersion throughout the material, the change in grain size, and higher dislocation density in material occur due to deformation. The all the above reason result in improvement in hardness of the extruded material.

### 4.13.2. Microstructures characterization for extruded sample

The microstructure examination was on stir cast fabricated and cold extruded (81%Al7075+7.5%$CeO_2$+7.5%SiC+4%GO) to analysis the change in microstructure during the deformation process. The result showed the refined and homogeneous morpholog, as well the reduction in grain size was observed due to several plastic deformation experienced by sample during cold extrusion. Deformation and elongation of grain was observed into the direction of extrusion. The distribution of the grains was also more uniform in the extruded samples, indicating a more consistent deformation behavior throughout the cross-section. Presence of the secondary phase precipitates dispersed throughout the matrix was also observed.

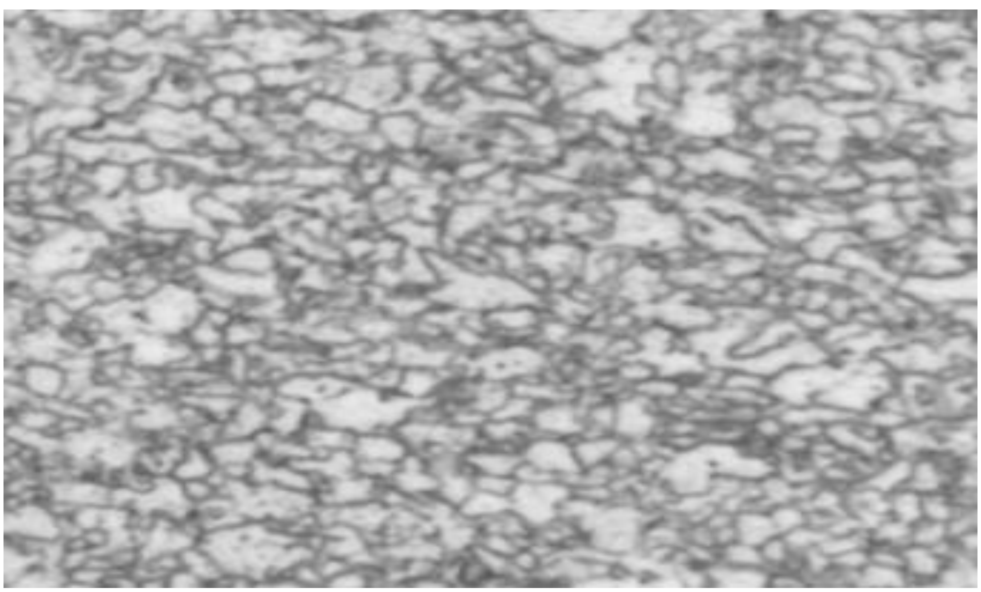

Figure 4.21 Microstructure analyses after extrusion

### 4.13.3. Compression strength of extruded sample

The extruded material (81%Al7075+7.5%$CeO_2$+7.5%SiC+4%GO) density improved, porosity percentage reduced as well the hardness was increase after deformation due to cold extrusion. This implies that the material mechanical properties enhanced. To test the strength of the extrude sample compression strength test was perfumed on universal compression strength tester machine in ASTU and the data obtain was recorded and interpolated using excel. The result showed that the compression strength of the material was improved from 490Mpa to 526Mpa. This implies the extrusion process have a significance on the compression strength fabricated material. The sample surface roughness was reduced but the hardness as well strength was increased due to cold extrusion. Enhancement in bond between the reinforcement and matrix as well orientated and aligned of the reinforced particles in the direction of extrusion during cold extrusion result in improved compressive strength (81%Al7075+7.5%$CeO_2$+7.5%SiC+4%GO) in that direction. This finer grain structure may result in greater mechanical strength.

### 4.13.4. Corrosion resistance of extruded sample

The electrochemical test was perfumed in immersed in 3% NaCl solution for 30 minutes to analyze the corrosion behavior of (81%Al7075+7.5%$CeO_2$+7.5%SiC+4%GO)extruded sample. Tafel curves were produced by adjusting potential volt range of -250mV catholically and +250Mv anodically verses corrosion potential (Ecorr) at scan rate of 1mV/s to test the long-term performance and reliability of the sample. Then the result was compare with extruded sample. The extruded (81%Al7075+7.5%$CeO_2$+7.5%SiC+4%GO) experience lower corrosion current density and positive corrosion potential compared to the casted samples. The variation in corrosion resistance behavior of sample, before and after deformation was occur due to changes in the microstructure, interfacial properties, residual stresses, reinforcement distribution, and surface integrity during extrusion.

Table 4.33 Corrosion rate value for extruded sample

| Sample | $I_{corr}$(mA/cm$^2$) | $E_{corr}$(V) | CR (mm/year) |
|---|---|---|---|
| (81%Al7075+7.5%$CeO_2$+7.5%SiC+4%GO) | -0.907608696, | -0.772 | 0.000341 |

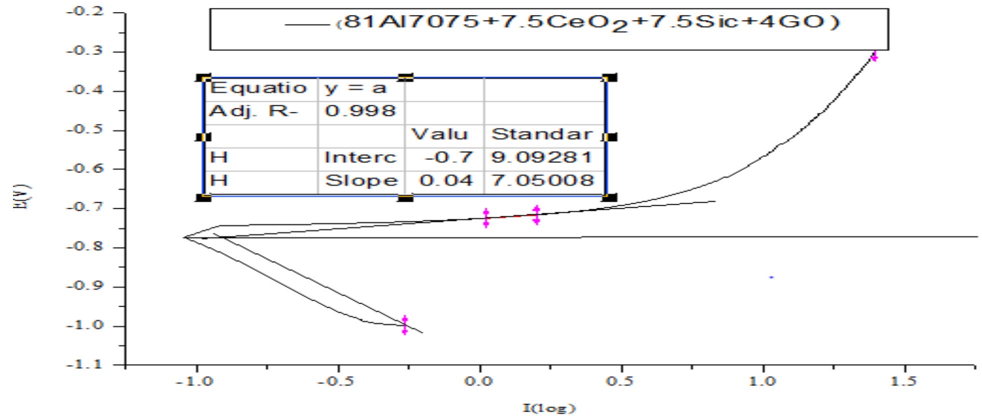


Figure 4.22 corrosion resistance behavior of extruded sample

## CHAPTER

## CONCLUSIONS AND RECOMMADETIONS

### 5.1. Conclusions

The studies was performed on fabrication and deforming of SiC, CeO2and GO –reinforced 7075 Al hybrid composite material through stir casting and cold extrusion. The primary operation, stir casting fabrication was performed to accomplish the uniform distribution of the reinforcement in the 7075 Al matrix to improve the properties while the secondary operation, cold extrusion was performed to further improve the microstructure and mechanical behavior of the fabricated hybrid composite. In first operation stir casting, the important parameters were selected to a get homogenous distribution of the reinforcement. The melting temperature of 71.469g 7075 Al matrix was regulated to be 700°C, and the furnace, the ball milled reinforcement, and the mold were made to pre heated to a 350°C,400°C,350°C temperature respectively. Stirring was performed with speed of 650 rpm for 10 second.

The(81%Al7075+10%$CeO_2$+5%SiC+4%GO),(81%Al7075+7.5%$CeO_2$+7.5%SiC+4%GO), 81%Al7075+5%$CeO_2$+10%SiC+4%GO weight percentage combination sample was fabricated .The mechanical, triabological properties of the fabricated sample was studied and the result was concluded as follow.

- ✓ The formation of new phase, and intense and sharp peak was observed in XRD fabricated composite specially in81%Al7075+7.5%$CeO_2$+7.5%SiC+4%GO sample. These indicate the reduction in crystallite size, higher degree of crystallinity, improvement in the material's hardness and strength.
- ✓ Uniform distribution of reinforcement and the reduction in average grain size was seen.
- ✓ Sample81%Al7075+10%$CeO_2$+5%SiC+4%GO,81%Al7075+7.5%$CeO_2$+7.5%SiC +4%GO,81%Al7075+5%$CeO_2$+10%SiC+4%GO hybrid composite show a hardness of 228.37HV,240.5HV,232.13HV,representing a 57.86%,66.25%,and 60.46% ,percent of improvement ,respectively when compare to the hardness of pure alloy 144.44HV.

- ✓ Sample81%Al7075+10%$CeO_2$+5%SiC+4%GO,81%Al7075+7.5%$CeO_2$+7.5%SiC +4%GO,81%Al7075+5%$CeO_2$+10%SiC+4%GO hybrid composite show an improved in compress strength 490Mpa of ultimate strength verses 150Mpa yield strength( 81%Al7075+7.5%$CeO_2$+7.5%SiC+4%GO).
- ✓ The wear resistance test reviled that the decrement in wear rate and coefficient of friction was observed due to addition of reinforcement.
- ✓ The corrosion resistance of the fabricated composites was also increased. The corrosion rate value of 0.00079,0.00055,and 0.00086 were recorded for 81%Al7075+10%$CeO_2$+5%SiC+4%GO,81%Al7075+7.5%$CeO_2$+7.5%SiC+4%GO,81%Al7075+5%$CeO_2$+10%SiC+4%GO composite ,respectively, the second combination were the best because it has less wear rate value.

To perform the secondary operation the simulation and optimization was performed on fabricated composite using 3D deform software, Design of expert and ANOVA table and genetic algorithm respectively. For these purpose the best sample was selected using used S/N ratio process. From S/N ratio, the 81%Al7075+7.5%$CeO_2$+7.5% SiC+4%GO composite was ranked number one.

- ✓ ANOVA results analysis by Design-Expert software indicated that extrusion ration is significant and extrusion parameters have effect on the response load, damage and effective stress. From the three input extrusion parameter extrusion ration have more effect on the response
- ✓ Multi-objective optimization of extrusion parameters by using GA in MATLAB software was performed and the effect of extrusion parameters on responses is analyzed before optimizing the individual values.
- ✓ At the end the extrusion parameters of 6, 2.5m/s and 263.6537℃ with damage, load, and effective stress of 0.513567, 10.0746KN and 1455.051 Mpa, respectively were select and the actual operation was performed.

By adjusting the extrusion parameters, the really actual cold extrusion was performed on selected samples. The result obtains show that the reduction in grain size and the improvement in density from 3.011g/cm3to 3.045 g/cm3to, hardness from 240.5 HVto281.81HV and, compression strength from 490Mpa to 525Mpa were observed. The corrosion resistance of material was also increased that shoe more reaction anode region.

### 5.2.Recommendations

Based on results of test and values obtained from results to it are recommended for other research work as follow:

- ✓ Ultrasonic Stir casting can be done to avoid agglomeration during stir casting operation.
- ✓ Fabrication of samples can be done as per some experimental design.
- ✓ Numerical Simulation of Stir casting can be carried out to explore the fabrication process in detail.
- ✓ More testing of materials like Fatigue, Creep and Flexural can be done to understand the material behavior more.

## SPECIAL ACKNOWLEDGMENT

This research work is founded by Adama Science and Technology University under the grant number ASTU/SM-R/906/23

## REFERENCES

Abbas, A., Rajagopal, V., & Huang, S.-J. (2021). Magnesium metal matrix composites and their applications. *Magnesium Alloys Structure and Properties*.

Abebe Emiru, A., Sinha, D. K., Kumar, A., & Yadav, A. (2022). Fabrication and Characterization of Hybrid Aluminium (Al6061) Metal Matrix Composite Reinforced with SiC, B4C and MoS2 via Stir Casting. *International Journal of Metalcasting*, 1-12.

Adak, D., Sreeramagiri, P., Roy, S., & Balasubramanian, G. (2023). Advances and Challenges in Predictive Modeling for Additive Manufacturing of Dissimilar Metals and Complex Alloys. *Materials*, *16*(16), 5680.

Aherwar, A., Patnaik, A., & Pruncu, C. I. (2020). Effect of B4C and waste porcelain ceramic particulate reinforcements on mechanical and tribological characteristics of high strength AA7075 based hybrid composite. *Journal of materials research and technology*, *9*(5), 9882-9894.

Akbar, H. I., Surojo, E., Ariawan, D., Putra, G. A., & Wibowo, R. T. (2020). Effect of reinforcement material on properties of manufactured aluminum matrix composite using stir casting route. *Procedia Structural Integrity*, *27*, 62-68.

Alaneme, K. K., & Odoni, B. U. (2016). Mechanical properties, wear and corrosion behavior of copper matrix composites reinforced with steel machining chips. *Engineering science and technology, an international journal*, *19*(3), 1593-1599.

Ali, M. (2020). Review of stir casting technique and technical challenges for ceramic reinforcement particulate and aluminium matrix composites. *Epitoanyag-Journal of Silicate Based & Composite Materials*, *72*(6).

Ashokkumar, S., Sathiyaraj, S., Kumar, N., Muzammil, S., & Kumar, D. R. (2020). Feasibility Study on Aluminium 7075 Metal Matrix Composite Using Graphene Oxide. IOP Conference Series: Materials Science and Engineering,

Balokhonov, R., Romanova, V., Buyakova, S., Kulkov, A., Bakeev, R., Evtushenko, E., & Zemlyanov, A. (2022). Deformation and Fracture Behavior of Particle-Reinforced Metal Matrix Composites and Coatings. *Physical Mesomechanics*, *25*(6), 492-504.

Bansal, P., & Upadhyay, L. (2016). Effect of turning parameters on tool wear, surface roughness and metal removal rate of alumina reinforced aluminum composite. *Procedia Technology*, *23*, 304-310.

Bhowmik, A., Chakraborty, D., Dey, D., & Biswas, A. (2020). Investigation on wear behaviour of Al7075-SiC metal matrix composites prepared by stir casting. *Materials Today: Proceedings*, *26*, 2992-2995.

Callister Jr, W. D., & Rethwisch, D. G. (2020). *Fundamentals of materials science and engineering: an integrated approach*. John Wiley & Sons.

Chiu, C.-H., Huang, C.-H., Nurhadi, D., Rizki, V., & Murdanto, P. (2020). The effect of stirring time varieties in stir casting on the tensile strength and hardness of Al-Cu alloys with alumina reinforcement. In *Innovation in Design, Communication and Engineering* (pp. 17-22). CRC Press.

Dasari, Brabazon, & Naher. (2019). Prediction of Mechanical Properties of Graphene Oxide Reinforced Aluminum Composites. *Metals*, *9*(10). https://doi.org/10.3390/met9101077

Donati, L., Reggiani, B., Pelaccia, R., Negozio, M., & Di Donato, S. (2022). Advancements in extrusion and drawing: a review of the contributes by the ESAFORM community. *International Journal of Material Forming*, *15*(3), 41.

Dwivedi, S. P., Srivastava, A. K., Maurya, N. K., & Sahu, R. (2020). Microstructure and Mechanical Behaviour of Al/SiC/Agro-Waste RHA Hybrid Metal Matrix Composite. *Journal of Composite & Advanced Materials/Revue des Composites et des Matériaux Avancés*, *30*(1).

Gatea, S., Jwad, T., Chen, F., & Ou, H. (2023). Micromechanical modeling of the deformation and damage behavior of al6092/sic particle metal matrix composites. *Journal of Materials Engineering and Performance*, *32*(23), 10680-10701.

Ghanaraja, S., Kumar, K. V., Ravikumar, K., & Madhusudan, B. (2017). Mechanical properties of Al2O3 reinforced cast and hot extruded Al based metal matrix composites. *Materials Today: Proceedings*, *4*(2), 2771-2776.

Gosavi, S. V., & , M. D. J. (2020). Microstructural studies on aluminium metal matrix composite

(Al7075-SiC) fabricated through stir casting process. https://doi.org/10.1016/j.matpr.2020.05.094

Gosavi, S. V., & Jaybhaye, M. (2021). Microstructural studies on aluminium metal matrix composite (Al7075-SiC) fabricated through stir casting process. *Materials Today: Proceedings*, *39*, 1412-1416.

Gowrishankar, M., Hiremath, P., Shettar, M., Sharma, S., & Rao, S. (2020). Experimental validity on the casting characteristics of stir cast aluminium composites. *Journal of materials research and technology*, *9*(3), 3340-3347.

Gukendran, R., Sambathkumar, M., Sasikumar, K., & Karupannasamy, D. (2022). Effect of silicon carbide and alumina reinforcement of different volume fraction on wear characteristics of AL 7075 hybrid composites using response surface methodology. *Materials Research*, *25*, e20220204.

Hamed Basuny, F., & El-Sayed, M. (2020). The effect of holding time before solidification on the properties of aluminium castings. *Journal of the Southern African Institute of Mining and Metallurgy*, *120*(8), 461-466.

Hammar Ilham Akbar, E. S., Dody Ariawan, Galang Ariyanto Putra,, & Wibowo, R. T. (2020). Effect of Reinforcement Material on Properties of Manufactured

Aluminum Matrix Composite Using Stir Casting Route.

Han, J. Y., Femi, O. E., Kilicaslan, F., Jeong, C. U., Baeg, C. H., Hong, S. J., & Koo, J. M. (2017). Improved Mechanical Properties of Al-Si Alloys by Adding an Extrusion Process to Conventional Processing Method. *Archives of Metallurgy and Materials*, *62*(2), 1179-1183. https://doi.org/10.1515/amm-2017-0173

Hao, Z., Ji, F., Fan, Y., Lin, J., Liu, X., & Gao, S. (2017). Flow characteristics and constitutive equations of flow stress in high speed cutting Alloy 718. *Journal of Alloys and Compounds*, *728*, 854-862.

Himabindu, B., Devi, N. L., & Kanth, B. R. (2021). Microstructural parameters from X-ray peak profile analysis by Williamson-Hall models; A review. *Materials Today: Proceedings*, *47*, 4891-4896.

Huang, S., Wu, Y., Xia, X., Zhao, Z., Chen, Q., & Shu, D. (2019). Assessment of Cold Extrusion Effect on Stress–Strain Curves of Pure Copper Arc Parts Based on the Cosine Velocity Model. *Strength of Materials*, *51*(4), 569-577.

Imran, M., & Khan, A. A. (2019). Characterization of Al-7075 metal matrix composites: a review. *Journal of Materials Research and Technology*, *8*(3), 3347-3356.

Jain, R., Pal, S. K., & Singh, S. B. (2017). Finite element simulation of temperature and strain distribution during friction stir welding of AA2024 aluminum alloy. *Journal of The Institution of Engineers (India): Series C*, *98*, 37-43.

Karibeeran, S. S., Sathishkumar, D., Muthaih, B., & Palanivelu, S. (2015). Effect of reinforcement type and extrusion on the microstructure and mechanical behavior of al alloy composites. ASME International Mechanical Engineering Congress and Exposition,

Klemens, A., Sariman, F., & Syahid, M. (2019). Study on effect of temperature smelting and pouring to mechanical properties Aluminum 7075. IOP Conference Series: Earth and Environmental Science,

Kothasiri, A. F., & Chalamalasetti, S. R. (2022). Investigation of Cold Extrusion of Aluminum AA 2024 Alloy using Finite Element Analysis. *INCAS Bulletin*, *14*(3), 157-171.

Kumar, A., Singh, V. P., Singh, R., Chaudhary, R., Kumar, D., & Mourad, A.-H. I. (2024). A review of aluminum metal matrix composites: fabrication route, reinforcements, microstructural, mechanical, and corrosion properties. *Journal of Materials Science*, 1-68.

Kumar, A. V., Ratnam, C., Rao, V. K., & Kumar, C. R. (2019). Study on influence of die angle in cold extrusion on properties of nano sic reinforced 6061 aluminum alloy. *Materials Today: Proceedings*, *18*, 4366-4373.

Kumar, D., Angra, S., & Singh, S. (2022). Mechanical properties and wear behaviour of stir cast aluminum metal matrix composite: a review. *International Journal of Engineering*, *35*(4), 794-801.

Kumar, D., Singh, S., & Angra, S. (2023). Synergistic corrosion protection of stir-cast hybrid aluminum composites reinforcing CeO2 and GNPs nano-particulates. *Aircraft Engineering and Aerospace Technology*, *95*(10), 1706-1715.

Kumar, H., & Shiva, S. (2022). Experimental investigation on stir casting of a metal matrix composite material. *Journal of Micromanufacturing*, *5*(2), 101-106.

Kumar, R. V., Harichandran, R., Vignesh, U., Thangavel, M., & Chandrasekhar, S. (2021). Influence of hot extrusion on strain hardening behaviour of graphene platelets dispersed aluminium composites. *Journal of Alloys and Compounds*, *855*, 157448.

Li, S., Luo, T., Chao, Z., Jiang, L., Han, H., Han, B., Du, S., & Liu, M. (2024). A Review of Dynamic Mechanical Behavior and the Constitutive Models of Aluminum Matrix Composites. *Materials*, *17*(8), 1879.

Loh, P.-R., Danecek, P., Palamara, P. F., Fuchsberger, C., A Reshef, Y., K Finucane, H., Schoenherr, S., Forer, L., McCarthy, S., & Abecasis, G. R. (2016). Reference-based phasing using the Haplotype Reference Consortium panel. *Nature genetics*, *48*(11), 1443-1448.

Lokesh, K., Chetan, I., & Thomas, P. (2017). Influence of graphene on hardness number of Aluminium-7075 based metal matrix composites. *Int. J. Innov. Sci. Res. Technol*, *2*.

Lorella Ceschini, Arne Dahle, Manoj Gupta, Anders Eric Wollmar Jarfors, S. J., Alessandro Morri, Fabio Rotundo, Stefania Toschi, & Singh, R. A. (2017). Aluminum and Magnesium Metal Matrix Nanocomposites. *Engineering Materials*, 264

Lupulescu, A., Henry, S., Marken, K., & Lampman, S. (2016). Science of Casting and Solidification: ASM Handbook Contributions—Honoring Professor Doru Michael Stefanescu. Advances in the Science and Engineering of Casting Solidification: An MPMD Symposium Honoring Doru Michael Stefanescu,

Mehta, V. R., & Sutaria, M. P. (2021). Investigation on the effect of stirring process parameters on the dispersion of SiC particles inside melting crucible. *Metals and Materials International*, *27*, 2989-3002.

Mohal, S. (2017). Microstructural investigation of aluminium-silicon carbide particulate metal matrix composite fabricated by stir casting. *International Journal for Innovative Research in Science & Technology*, *3*(11), 26-30.

Mohanachari, J., Babu, A., & Prasad, B. D. (2018). A review on fabrication, mechanical characterization of aluminium metal matrix composites. *Int. J. Curr. Eng. Sci. Res*, *5*, 75-79.

Mukesh, Y., Bharathesh, T., Saravanan, R., & Keshavamurthy, R. (2019). Effect of hot extrusion on mechanical behaviour of boron nitride reinforced aluminium 6061-based metal matrix composites. *International Journal of Materials Engineering Innovation*, *10*(2), 135-151.

Mukesh, Y., Naik, P. K., Vishwanatha, N., Prema, N., Girish, H., Laxmana, N. L., & Madhusudan, P. (2021). Impact of heat treatment on the mechanical performance of hot extruded Al6061-BN reinforced metal matrix composites. *Bulletin of the Polish Academy of Sciences. Technical Sciences*, *69*(3).

N S, S., & AS, B. (2019). Optimization Of Process Parameters For Drilling Frp And Analyzing Cracks In Drilled Laminates. *International Journal of Mechanical and Production Engineering Research and Development, 9*(5), 1129-1140.

Narwate, M. M., & Mohandas, K. (2016). A Study on Mechanical and Tribological Properties of Aluminum Metal Matrix Composite Reinforced With TiO2 and Graphene Oxide. *International Journal*, *4*(4), 729-732.

Ngo, T.-D. (2020). Introduction to composite materials. *Composite and Nanocomposite Materials—From Knowledge to Industrial Applications*.

Niteesh Kumar, S., Keshavamurthy, R., Haseebuddin, M., & Koppad, P. G. (2017). Mechanical properties of aluminium-graphene composite synthesized by powder metallurgy and hot extrusion. *Transactions of the Indian Institute of Metals*, *70*(3), 605-613.

Nturanabo, F., Masu, L., & Kirabira, J. B. (2019). Novel applications of aluminium metal matrix composites. *Aluminium alloys and composites*.

Olani, M., Kumar, D., & Asrat, G. (2023). Mechanical and corrosion properties of Fe–SiC–ZrO2 hybrid composite fabricated through powder metallurgy process. *Results in Engineering*, *17*, 100866.

Pakdel, A., Witecka, A., Rydzek, G., Shri, D. N. A., & Nicolosi, V. (2018). A comprehensive analysis of extrusion behavior, microstructural evolution, and mechanical properties of 6063 Al–B4C composites produced by semisolid stir casting. *Materials Science and Engineering: A*, *721*, 28-37.

Panwar, N., & Chauhan, A. (2018). Fabrication methods of particulate reinforced Aluminium metal matrix composite-A review. *Materials Today: Proceedings*, *5*(2), 5933-5939.

Patel, M., Pardhi, B., Pal, M., & Singh, M. K. (2019). SiC particulate reinforced aluminium metal matrix composite. *Advanced journal of graduate research*, *5*(1), 8-15.

Rai, A., Rai, P., Kumar, A., Chaturvedi, R. K., & Singh, V. K. (2023). Study of Mechanical Characteristics of Silicon Carbide Reinforced Zn-Mg Based Metal-Ceramic Composite. *Silicon*, 1-12.

Rajasekaran, A., & Pugazhenthi, R. (2020). Study of mechanical properties of stir casted Al7075/SiCp composites after thermomechanical treatment. *Materials Today: Proceedings*, *22*, 766-771.

Ramanathan, A., Krishnan, P. K., & Muraliraja, R. (2019). A review on the production of metal matrix composites through stir casting–Furnace design, properties, challenges, and research opportunities. *Journal of Manufacturing Processes*, *42*, 213-245.

Ramesh, M., Palanikumar, K., & Reddy, K. H. (2017). Plant fibre based bio-composites: Sustainable and renewable green materials. *Renewable and Sustainable Energy Reviews*, *79*, 558-584.

Ramnath, B. V., Parswajinan, C., Dharmaseelan, R., Thileepan, K., & Krishna, K. N. (2021). A review on aluminium metal matrix composites. *Materials Today: Proceedings*, *46*, 4341-4343.

Reddy, M. P., Manakari, V., Parande, G., Shakoor, R., Mohamed, A., & Gupta, M. (2019). Structural, mechanical and thermal characteristics of Al-Cu-Li particle reinforced Al-matrix composites synthesized by microwave sintering and hot extrusion. *Composites Part B: Engineering*, *164*, 485-492.

Ruys, A. J. (2023). *Silicon Carbide Ceramics: Structure, Properties and Manufacturing*. Elsevier.

S. Senthil, M. Raguraman, & Manalan, D. T. (2020). Manufacturing processes & recent applications of aluminium metal

matrix composite materials: A review. https://doi.org/10.1016/j.matpr.2020.08.792

Sahoo, A. K., & Panigrahi, M. R. (2021). A study on strain and density in graphene-induced Bi2O3 thin film. *Bulletin of Materials Science*, *44*(3), 232.

Samal, P., Vundavilli, P. R., Meher, A., & Mahapatra, M. M. (2020). Recent progress in aluminum metal matrix composites: A review on processing, mechanical and wear properties. *Journal of Manufacturing Processes*, *59*, 131-152.

Sambathkumar, M., Navaneethakrishnan, P., Ponappa, K., & Sasikumar, K. (2017). Mechanical and corrosion behavior of Al7075 (hybrid) metal matrix composites by two step stir casting process. *Latin american journal of solids and structures*, *14*, 243-255.

Sathishkumar, D., Sivakumar, P., Sundaram, K. S., & Anand, S. (2017). Finite Element Analysis and Experimental Study on the Effect of Extrusion Ratio during Hot Extrusion Process of Aluminium Matrix Composites. *Defence Science Journal*, *67*(4).

Senapati, A. K., Panda, S. S., Dutta, B. K., & Mishra, S. (2020). Effect of Stirring Speed During Casting on Mechanical Properties of Al–Si Based MMCs. Intelligent Manufacturing and Energy Sustainability: Proceedings of ICIMES 2019,

Shao, P., Chen, G., Ju, B., Yang, W., Zhang, Q., Wang, Z., Tan, X., Pei, Y., Zhong, S., & Hussain, M. (2020). Effect of hot extrusion temperature on graphene nanoplatelets reinforced Al6061 composite fabricated by pressure infiltration method. *Carbon*, *162*, 455-464.

Sharma, D. K., Mahant, D., & Upadhyay, G. (2020). Manufacturing of metal matrix composites: A state of review. *Materials Today: Proceedings*, *26*, 506-519. https://doi.org/10.1016/j.matpr.2019.12.128

Sifakis, E., & Barbič, J. (2022). *Finite element method simulation of 3d deformable solids*. Springer Nature.

Singh, H., Brar, G. S., Kumarand, H., & Aggarwal, V. (2020). Characterization and sustainability of boron carbide reinforced 7075 aluminum metal matrix composites. *J. Green Eng.*, *10*, 7857-7868.

Singh, K., Singh, H., Vardhan, S., & Mohan, S. (2021). Mechanical study of Al 7050 and Al 7075 based metal matrix composites: a review. *Materials Today: Proceedings*, *43*, 673-677.

Sowrabh, B., Gurumurthy, B., Shivaprakash, Y., & Sharma, S. S. (2023). Characterization Studies on 7075 Aluminium Alloy Under As-Cast and in Multiple Step T6 Conditions. *Journal of The Institution of Engineers (India): Series C*, *104*(1), 69-92.

Sun, W., Zhan, K., Yang, Z., Zhao, R., Wang, T., Zhao, B., Ya, Y., & Yang, J. (2020). Facile fabrication of GO/Al composites with improved dispersion of graphene and enhanced mechanical properties by Cu doping and powder metallurgy. *Journal of Alloys and Compounds*, *815*, 152465.

Suresh, S., Gowd, G. H., & Deva Kumar, M. (2019). Tribological behavior of Al 7075/SiC metal matrix nano-composite by stir casting method. *Journal of The Institution of Engineers (India): Series D*, *100*(1), 97-103.

Suresh, S., Gowd, G. H., & Kumar, M. D. (2019). Mechanical and wear behavior of Al 7075/Al 2 O 3/SiC/mg metal matrix nanocomposite by liquid state process. *Advanced Composites and Hybrid Materials*, *2*, 530-539.

Surya, M. S., & Gugulothu, S. (2022). Fabrication, mechanical and wear characterization of silicon carbide reinforced Aluminium 7075 metal matrix composite. *Silicon*, *14*(5), 2023-2032.

Syahid, M., Arma, L. H., Arsyad, H., & Suwardi, Z. A. (2020). Effect of pouring temperature on mechanical properties and microstructures of aluminium matrix composite strengthened by CNT with stir casting method. Materials Science Forum,

Thangaraju, T., Ravikumar, T., & Kanthasamy, S. (2021). Infuence of Pouring Temperature on Stir Casting of Al/SiC/Mg/Cu Composite.

Venkatesan, S., & Xavior, M. A. (2017). Mechanical behaviour of Aluminium metal matrix composite reinforced with graphene particulate by stir casting method. *Journal of chemical and pharmaceutical sciences*, *10*(1), 55-59.

Venugopal, S., & Karikalan, L. (2021). Microstructure and physical properties of hybrid metal matrix composites AA6061-TiO2-SiC via stir casting techniques. *Materials Today: Proceedings*, *37*, 1289-1294. https://doi.org/10.1016/j.matpr.2020.06.462

Vijay Kumar, A., Ratnam, C. H., Kesava Rao, V. V. S., & Rohini Kumar, C. (2019). Study on influence of Die Angle in Cold Extrusion on Properties of Nano Sic Reinforced 6061 Aluminum Alloy. *Materials Today: Proceedings*, *18*, 4366-4373. https://doi.org/10.1016/j.matpr.2019.07.400

Yadav, B. N., Verma, G., Muchhala, D., Kumar, R., & Mondal, D. (2018). Effect of MWCNTs addition on the wear and compressive deformation behavior of LM13-SiC-MWCNTs hybrid composites. *Tribology International*, *128*, 21-33.

Yılmaz, T. (2019). *Development of functionally graded aluminum matrix composite materials for defense industry applications* Middle East Technical University].

Zaiemyekeh, Z., Liaghat, G., Ahmadi, H., Khan, M., & Razmkhah, O. (2019). Effect of strain rate on deformation behavior of aluminum matrix composites with Al2O3 nanoparticles. *Materials Science and Engineering: A*, *753*, 276-284.

Zhang, P., Zhang, J., Li, J., Liu, G., Wu, K., Wang, Y., & Sun, J. (2014). Microstructural evolution, mechanical properties and deformation mechanisms of nanocrystalline Cu thin films alloyed with Zr. *Acta materialia*, *76*, 221-237.

# APPDEX

## Appedex one

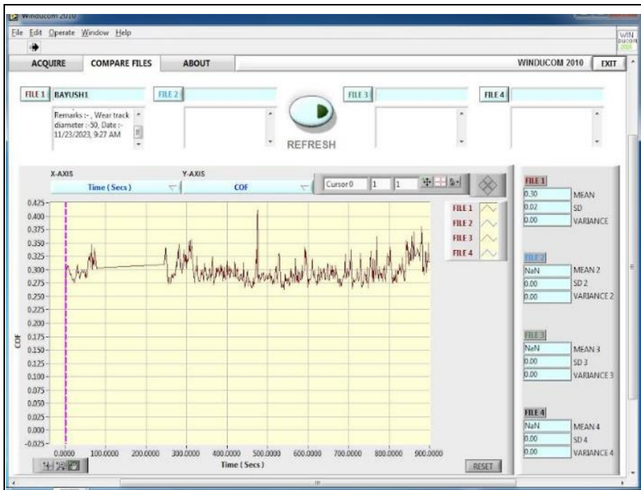


COF of sample 1

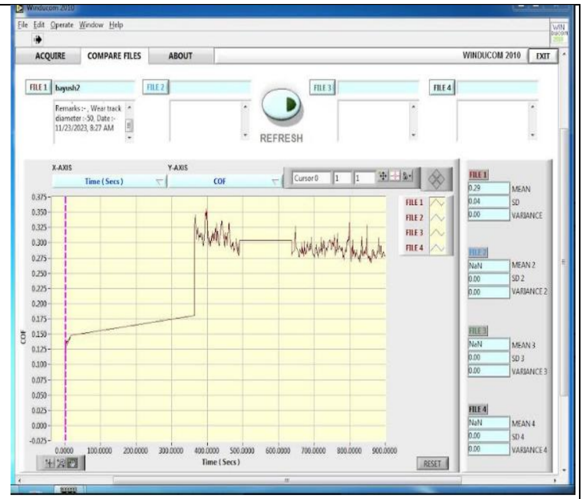


COF of sample 1


COF of sample 3

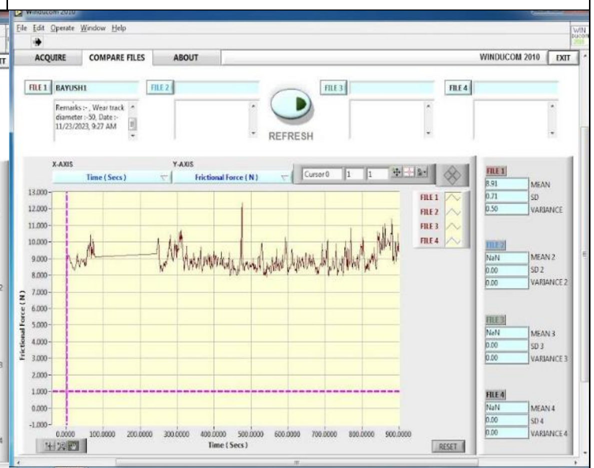


Friction  force verses time for sample 1

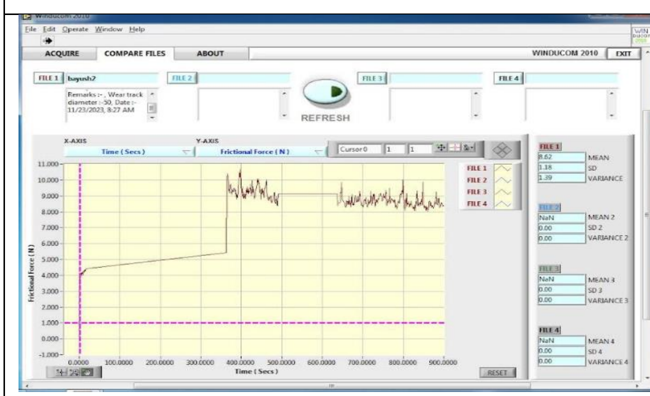


Friction  force verses time for sample two


Friction  force verses ime for sample three

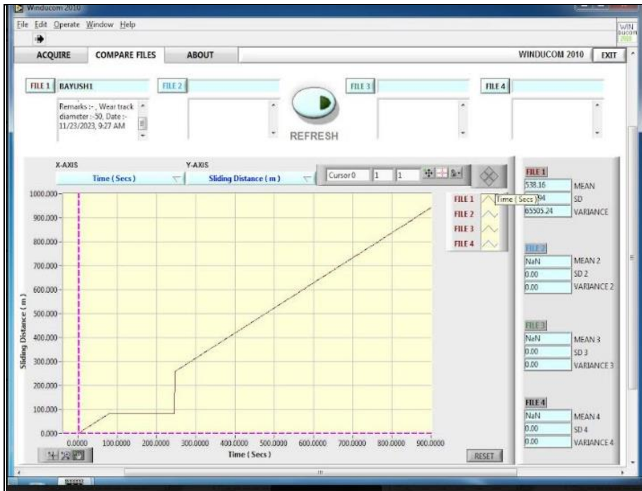

Sliding distance verses time of sample one

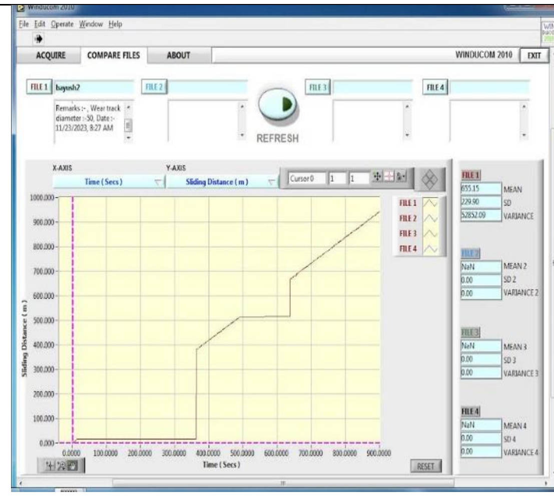

Sliding distance verses time of sample two

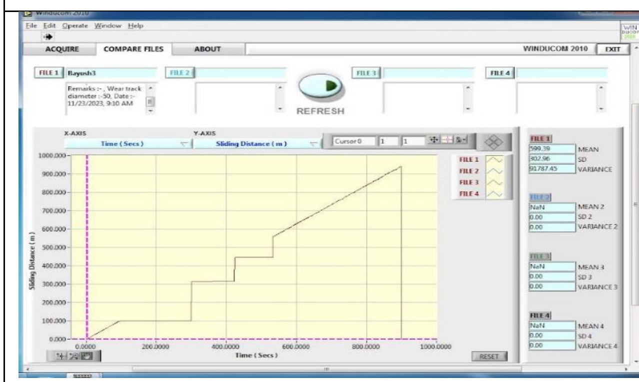

Sliding distance verses time of sample three

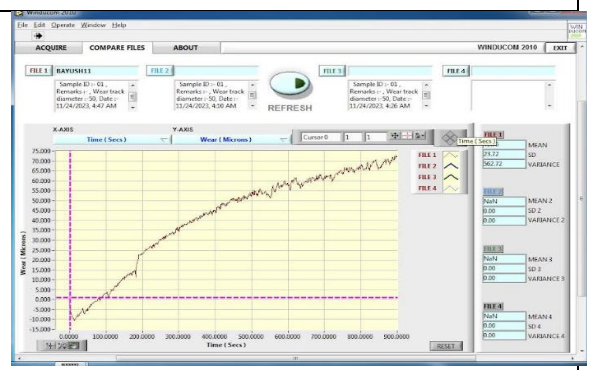

Wear verses time for sample one

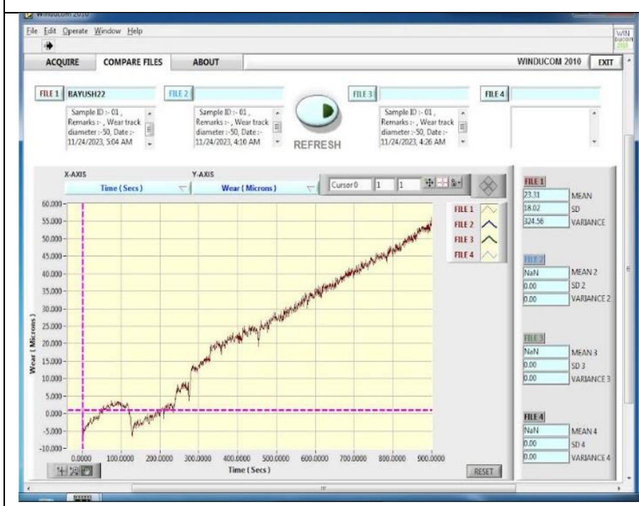

Wear verses time for sample two

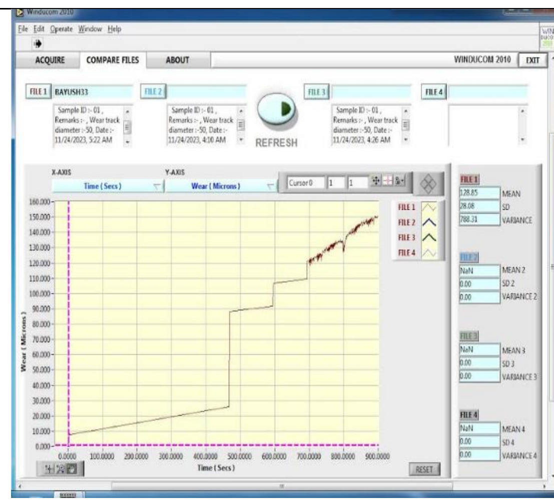

Wear verses time for sample three

# Appedex Two